

Report
Post
Rec'd

GEORGIA INSTITUTE OF TECHNOLOGY
OFFICE OF RESEARCH ADMINISTRATION

RESEARCH PROJECT INITIATION

Date: 17 July 1973

Project Title: "Effects of Crustal Features on the Gravity Field and Isostatic Compensation"

Project No: G-35-608

Principal Investigator Dr. L. T. Long

Sponsor: U. S. Army Research Office - Durham

Agreement Period: From July 1, 1973 Until June 30, 1974

Type Agreement: Grant No. DAHC04-74-G-0003 (continuation of EES

DA-ARO-D-31-124-71-G117) A-183

Amount: \$13,627 ARO-D
718 GIT (G-35-315)

\$14,345 Total

Reports Required:

Progress Reports

Technical Report

Final Report - 30 days after termination or by July 31, 1974

Sponsor Contact Person(s):

Technical

Army Research Office
Scientific Division, Environmental
Sciences
Box CM, Duke Station
Durham, North Carolina 27706

Administrative

Chief, Procurement Officer
Army Research Office - Durham
Box CM, Duke Station
Durham, North Carolina 27706

Assigned to: Geophysical Sciences

COPIES TO:

Principal Investigator

Library

School Director

Rich Electronic Computer Center

Dean of the College

Photographic Laboratory

Director, Research Administration

Project File

Director, Financial Affairs (2)

Security-Reports-Property Office

Patent Coordinator

Other

V
2
4/3
m

GEORGIA INSTITUTE OF TECHNOLOGY
OFFICE OF RESEARCH ADMINISTRATION
RESEARCH PROJECT TERMINATION

P.S.
C.H.

Date: March 7, 1975

Project Title Effects of Crustal Features on the Gravity Field & Isostatic Compensation

Project No: G-35-603

Principal Investigator: Dr. L. T. Long

Sponsor: U. S. Army Research Office - Durham

Effective Termination Date: 3-30-75 (Grant Expiration)

Clearance of Accounting Charges: 10-31-74 (Final Technical Report Due Date)

Grant/Contract Closeout Actions Remaining: Submission of Closing Documents
Submission of Final Fiscal Report
Final Report of Inventions

Assigned to School of Geophysical Sciences

COPIES TO:

Principal Investigator Library, Technical Reports Section

School Director Computer Sciences

Dean of the College Photographic Laboratory

Director of Research Administration Terminated Project File No. _____

Office of Financial Affairs (2) Other _____

Security - Reports - Property Office _____

Patent and Inventions Coordinator _____

PROGRESS REPORT

1. ARO PROPOSAL NUMBER: P-9110-EN
2. PERIOD COVERED BY REPORT: April 1, 1973 to September 30, 1973
3. TITLE OF PROPOSAL: Effects of Crustal Features on the Gravity Field and Isostatic Compensation
4. CONTRACT OR GRANT NUMBER: DA-ARO-D-31-124-71-G117
5. NAME OF INSTITUTION: Georgia Institute of Technology
6. AUTHOR(S) OF REPORT: Leland Timothy Long
7. LIST OF MANUSCRIPTS SUBMITTED OR PUBLISHED UNDER ARO SPONSORSHIP DURING THIS PERIOD, INCLUDING JOURNAL REFERENCES:

L. T. Long and R. P. Lowell (1973) Thermal Model for Some Continental Margin Sedimentary Basins and Uplift Zones, Geology Vol. 1, No. 2, Pg. 87-88.
8. SCIENTIFIC PERSONNEL SUPPORTED BY THIS PROJECT AND DEGREES AWARDED DURING THIS REPORTING PERIOD:

Leland Timothy Long	J. W. Dees *
G. H. Rothe	C. V. Nutt*
S. R. Bridges	Madeline Waller *
J. W. Champion	
H. E. Denman +	* non-technical support personnn
J. H. McKee + (M.S. Geophysics)	+ supported as part-time field
W. W. Patzewitsch +	assistants

BRIEF OUTLINE OF RESEARCH FINDINGS

The primary goal of the work has been to utilize the Dorman and Lewis technique to obtain an isostatic response function for the Southeastern United States. Secondary goals were directed toward improving data coverage and isolating the major geologic features. Modifications of the Dorman-Lewis technique were required to allow application in the Southeastern U.S. since local geological features extend across the entire area and constitute an important factor in the isostatic response function. The final data set based on significant recent data acquisitions is now complete. It was derived from 10463 data points of Elevation & Bouguer anomalies. Surface densities interpreted from available geologic maps have been included in the data set. Profiles perpendicular and parallel to the regional structure have been generated using a weighted average and distance weighted average technique. These will be analyzed for two-dimensional response functions. The response function is not expected to be the same for crustal movements perpendicular or parallel to the regional structure and this analysis should give some indication of the asymmetry of the isostatic response function.

The data for a detailed (0.5 to 1.0 km interval) line perpendicular to the structure is now ready for analysis. The data includes gravity, elevation, density, magnetic intensity and geologic formation. Total length of the line is over 200 kilometers.

Additional gravity data is currently being obtained in South Carolina in cooperation with the South Carolina Division of Geology and Pradeep Talwani at the University of South Carolina. The objective of this cooperative work is to allow publication (planned in July 1974) of a Bouguer Gravity Map of South Carolina similar to the Georgia Bouguer Gravity Map.

PROGRESS REPORT

1. ARO PROPOSAL NUMBER: P-9110-EN
2. PERIOD COVERED BY REPORT: October 1, 1973 to March 30, 1974
3. TITLE OF PROPOSAL: Effects of Crustal Features on the Gravity Field and Isostatic Compensation
4. CONTRACT OR GRANT NUMBER: DA-ARO-D-31-124-71-G117
5. NAME OF INSTITUTION: Georgia Institute of Technology
6. AUTHOR(S) OF REPORT: Dr. Leland Timothy Long
7. LIST OF MANUSCRIPTS SUBMITTED OR PUBLISHED UNDER ARO SPONSORSHIP DURING THIS PERIOD, INCLUDING JOURNAL REFERENCES:

George H. Rothe, III (1973) Geophysical Investigation of a Diabase Dike, Masters Thesis, Georgia Institute of Technology, Atlanta, Georgia.

Long, Leland Timothy (1974) Bouguer Gravity Anomalies of Georgia, in Proceeding of the Symposium on the Petroleum Geology of the Georgia Coastal Plain, (expected June 1974) Georgia Geological Survey.
8. SCIENTIFIC PERSONNEL SUPPORTED BY THIS PROJECT AND DEGREES AWARDED DURING THIS REPORTING PERIOD:

S. R. Bridges
J. W. Champion
H. E. Denman
J. Butler
L. Evans

Dr. L. T. Long
Georgia Institute of Technology
Atlanta, Georgia 30332

9110-EN

BRIEF OUTLINE OF RESEARCH FINDINGS

The primary goal of the work has been to utilize the Dorman and Lewis technique to obtain an isostatic response function for the southeastern United States. Secondary goals were directed toward improving gravity data coverage and understanding the anomalies from major geologic features. The 64 x 64 grid of gravity, elevation and density data with a separation of 8 km has been examined. Preliminary descriptions of this data are similar to the explanation with the Simple Bouguer Map of Georgia and will be presented in more detail in the Symposium Volume. Preliminary results from trend and correlation distance analyses indicate that crustal structures NE of a line which extends NW-SE through central Georgia differ significantly from the structures to the SW. Profiles obtained NE and SW of this line also give significantly different isostatic response functions. On the SW side smoothed free air anomalies which approximate isostatic anomalies correlate, where negative, with uplift zones in recent releveling data. While a different response was expected for profiles parallel and perpendicular to the structure, the strong variation along strike was not expected.

A 200 km NW-SE detailed profile in North Georgia indicates significant topography in the intermediate crustal layer as well as a deepening of the Moho to 45 km near Atlanta.

The data accumulation phase of preparation for a Simple Bouguer Map of South Carolina is now essentially complete. The map is expected to be ready for publication by June, 1974. This work is being performed in cooperation with the South Carolina Division of Geology and the University of South Carolina.

BRIEF OUTLINE OF RESEARCH FINDINGS

A talk presented at the "Symposium on the Petroleum Geology of the Georgia Coastal Plain" - to be published in the Proceedings.

ABSTRACT

On a broad scale, the Bouguer gravity anomalies in Georgia show patterns which correlate with the major geologic subdivisions. The Paleozoic rocks of the Valley and Ridge Province of northwest Georgia are characterized by -20 to -40 milligal anomalies. Their smoothness is a consequence of the sedimentary rocks at the surface which generally show only slight lateral variations in density. The Piedmont and Blue Ridge crystalline rocks of central and northeast Georgia are characterized by the most negative Bouguer anomalies in Georgia. The negative values are a consequence of the elevation and total crustal thickness of these predominantly granitic rocks. Detailed gravity data obtained over crystalline rocks strongly reflect the near surface density variations and structural features. South of the fall line the Bouguer anomalies average about zero. The anomalies are related to density variations in pre-Cretaceous and crystalline basement rocks underlying the younger coastal plain sediments. The positive Bouguer anomalies are most likely due to the occurrence of dense basic rock types (like diabase, gabbro or hornblende gneiss). The negative anomalies are most likely due either to granitic rock or to increased thicknesses of sedimentary rock of pre-Cretaceous age. Detailed gravity data in the Georgia Coastal Plain can be used to delineate the boundaries of the larger structures of the pre-Cretaceous or crystalline basement rocks. Also, correlation of Bouguer anomalies with elevation often give an anomalous (e.g. 3.0 gm/cm^3) reduction density indicating continued tectonic activity of the sediments and pre-Cretaceous crustal rocks.

GEOPHYSICAL INVESTIGATION
OF A DIABASE DIKE

A THESIS

Presented to,

The Faculty of the Division of Graduate
Studies and Research

by

George Henry Rothe, III

In Partial Fulfillment
of the Requirements for the Degree
Master of Science in Geophysical Sciences

Georgia Institute of Technology

November, 1973

GEOPHYSICAL INVESTIGATION OF A DIABASE DIKE

PROGRESS REPORT

Approved:

Chairman

Date approved by Chairman:

11-28-73

ACKNOWLEDGEMENTS

The author wishes to express his gratitude to Dr. L. Timothy Long for his guidance in this study and to Drs. G. Lafayette Maynard and J. Marion Wampler for their suggestions and for reviewing this manuscript. Thanks to Dr. Robert Bentley for his helpful discussions concerning the geology of the Georgia Piedmont. Thanks to Mr. Doyle Watts of the Ohio State University for supplying the paleomagnetic data for the Meriwether dike.

During my tenure as a graduate student I received support in part through a research assistantship made possible by grant #DA-ARO-D-31-124-71-G117 from the Army Research Office - Durham. Also, my thesis research was supported in part by this grant. This support is appreciated.

The School of Geophysical Sciences provided the computer time for the analysis of the data.

Special thanks to Mr. Roland Schenck who assisted in collecting the data. And special thanks to my wife, Donna, for her assistance in the collecting of data, and for editing and typing this manuscript.

GEORGIA TECH LIBRARY

TABLE OF CONTENTS

	Page
ACKNOWLEDGEMENTS	ii
LIST OF TABLES	v
LIST OF FIGURES	vi
SUMMARY	viii
Chapter	
I. INTRODUCTION	1
II. GEOLOGIC SETTING AND REGIONAL GEOPHYSICS	6
Geologic Setting	
Regional Gravity	
Regional Magnetics	
III. PHYSICAL PROPERTIES OF THE MERIWETHER DIKE	16
Density	
Magnetic Susceptibility	
IV. DETERMINATION OF DIP ANGLE FROM GRAVITY AND MAGNETIC ANOMALIES	18
Theoretical Models	
Detailed Gravity Profiles	
V. GROUND-LEVEL MAGNETICS AND THE ROLE OF NATURAL REMANENT MAGNETIZATION IN THE OBSERVED ANOMALIES	30
Ground-Level Magnetics	
Natural Remanent Magnetization of the Meriwether Dike	
Theoretical Anomalies and the Determination of the Koenigsberger Ratio, Q	
VI. DISCUSSION AND CONCLUSIONS	35
APPENDICES	37
I. Gravity Surveys and Data Reduction	
II. Ground-Level Magnetic Surveys and Data Reduction	

Table of Contents (Concluded)

	Page
III. Computer Programs for Gravity and Magnetic Modeling	
IV. Paleomagnetic Data Collection and Reduction	
BIBLIOGRAPHY	75

GEORGIA TECH LIBRARY

LIST OF TABLES

Table	Page
1. Gravity Base Stations Used in this Study.	39
2. Instrumental Drift for Worden Gravimeter	39
3. Gravity Data	42
4. Ground-Level Magnetics Data	51
5. Two-Dimensional Gravity Modeling Program	61
6. Two-Dimensional Magnetics Modeling Program	63
7. Natural Remanent Moments of Cores Taken from the Meriwether Dike	74

LIST OF FIGURES

Figure	Page
1. Map of Diabase Dikes in Eastern North America, West Africa, and Northeastern South America with the Continents Restored to Their Relative Position in the Triassic	2
2. Geology of the Inner Piedmont of West Georgia	5
3. Geology of the Inner Piedmont of West Georgia	7
4. Simple Bouguer Gravity Map of Detail Study Area	8
5. Index Map of Georgia Showing Location of Detail Study Area and Existing Aeromagnetic Maps	10
6. Portion of North-Central Georgia Aeromagnetic Map Covering Area of Detail Study	11
7. Index Map Showing Locations of Detailed Ground-Level Magnetic Surveys and Existing Aeromagnetic Flight Lines	13
8. Ground-Level Magnetic Profiles	14
9. Aeromagnetic Map of the Study Area Recontoured Assuming the Meriwether Dike to be a Continuous Magnetic Feature	15
10. Calculated Curves Showing Effect of Dip Angle on Vertical Gravity Anomaly	19
11. Calculated Curves Showing Effect of Dip Angle on Total Field Anomaly Due to Induction Magnetization Only	20
12. Detailed Gravity Profile A-A'	22
13. Detailed Gravity Profile B-B'	23
14. Detailed Gravity Profile C-C'	24
15. Detailed Gravity Profile D-D'	25
16. Detailed Gravity Profile E-E'	26

List of Figures (Concluded)

Figure	Page
17. Stereographic Projection of Measured Natural Remanent Moments for the Meriwether Dike	32
18. Calculated Curves Showing the Effect of Natural Remanent Magnetism on the Observed Total Field Anomaly	33
19. Standard Department of Defense Gravity Coding Form . . .	41
20. Magnetogram for May 5, 1973	49
21. Magnetogram for May 6, 1973	50

GEORGIA TECH LIBRARIES

SUMMARY

Analysis of gravity, aeromagnetic, ground-level magnetic, paleomagnetic, and high altitude infrared data has revealed a complex injection zone of diabase in central Meriwether County, Georgia. This zone, which previously was considered to be a single large (30-40 meters wide) diabase dike, has been found in places to reach a width of one kilometer.

A simple Bouguer gravity map of the area shows the dikes, which compose the injection zone, to be responsible for an anomaly in the regional gravity trend of about one to two milligals. Combined results from five gravity and three total-field magnetic traverses has suggested the dikes to dip at about 70° toward N 70° E. The mean of the observed ground-level magnetic anomalies for the dikes is a 1000 γ positive anomaly (total field).

On the basis of observed paleomagnetic data and computed bulk susceptibilities the ratio of the remanent to induced magnetizations (Koenigsberger's ratio, Q) has been calculated to be between 0.25 and 0.5. However, the shapes of the observed ground-level magnetic anomalies suggests a Q value of 1.0 or slightly higher for the Meriwether dike.

The total-field magnetic map based on already existing aeromagnetic data has been recontoured under the assumption that the Meriwether dike is continuous, as suggested by ground-level data taken during this investigation.

On the recontoured map the dike is the most prominent magnetic

feature of the area which suggests that the spacing and direction of the aeromagnetic flight lines is inappropriate for correlating dike caused anomalies of limited extent, even though the dike anomalies are large in magnitude.

High altitude infrared photographs show a change in intensity of reflected infrared radiation from vegetation growing on diabase derived soils suggesting that such pictures can be used to map the outcrop pattern of the dike in heavily wooded, highly weathered, and other inaccessible areas. It is suggested that this technique be applied to other areas of eastern North America to determine outcrop patterns of the dikes in areas not yet geologically mapped.

RECORDED FROM MICROFILM

CHAPTER I

INTRODUCTION

A system of diabase dike swarms outcrops throughout eastern North America from Alabama to Nova Scotia (Cohee, et al., 1962), (Stockwell, et al., 1969). Southward along the Appalachian belt from Nova Scotia through New England and into the southern Piedmont, a gradual systematic change in strike is evident (Figure 1). King (1961) commented that the pattern of diabase dikes in eastern North America is probably the result of deep-seated stresses, but that the cause of the stresses is not apparent. May (1971) noted that the systematic pattern of the dikes in eastern North America is actually part of a larger, radial, pattern of diabase dikes surrounding the North Atlantic (Figure 1) and suggested that this pattern is a result of the stress field associated with the onset of North Atlantic sea-floor spreading in Late Triassic or Early Jurassic time.

The age of the dikes in eastern North America is currently in dispute. On the basis of fossil pole positions, de Boer (1967) suggested a Jurassic age for the dikes. On the other hand, Armstrong and Besancon (1970) found whole rock K-Ar ages to fall into two clusters: one at about 200 million years (Middle Triassic) and another smaller one between 225 and 230 million years (Early Triassic). Armstrong and Besancon (1970) suggested that the older dates may represent the actual time of emplacement, while the younger group may be indicative of "burial"

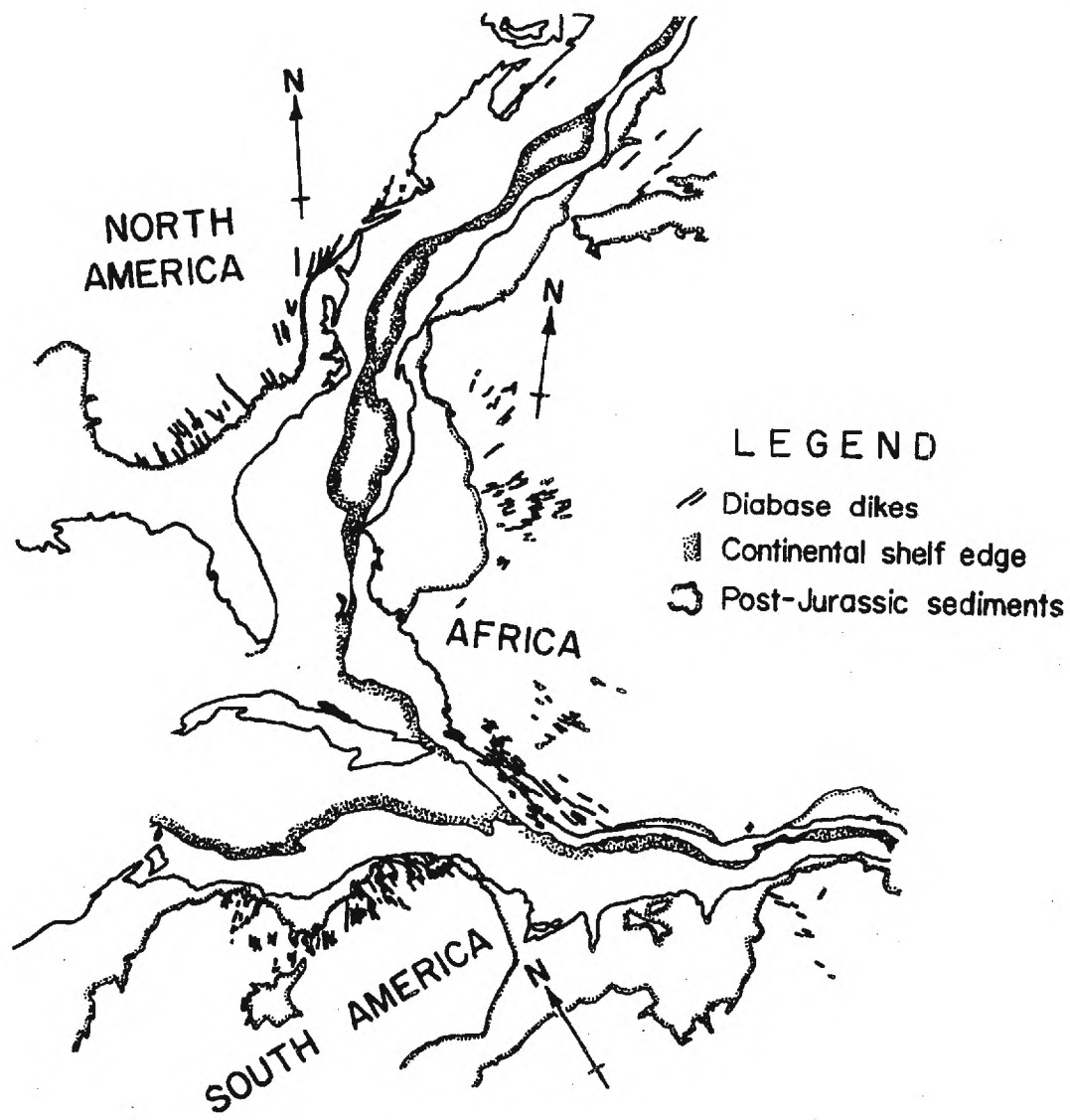


Figure 1. Map of Diabase Dikes in Eastern North America, West Africa, and Northeastern South America with the Continents Restored to Their Relative Position in the Triassic (after May, 1971). (North arrows indicate present geographic direction for each continent.)

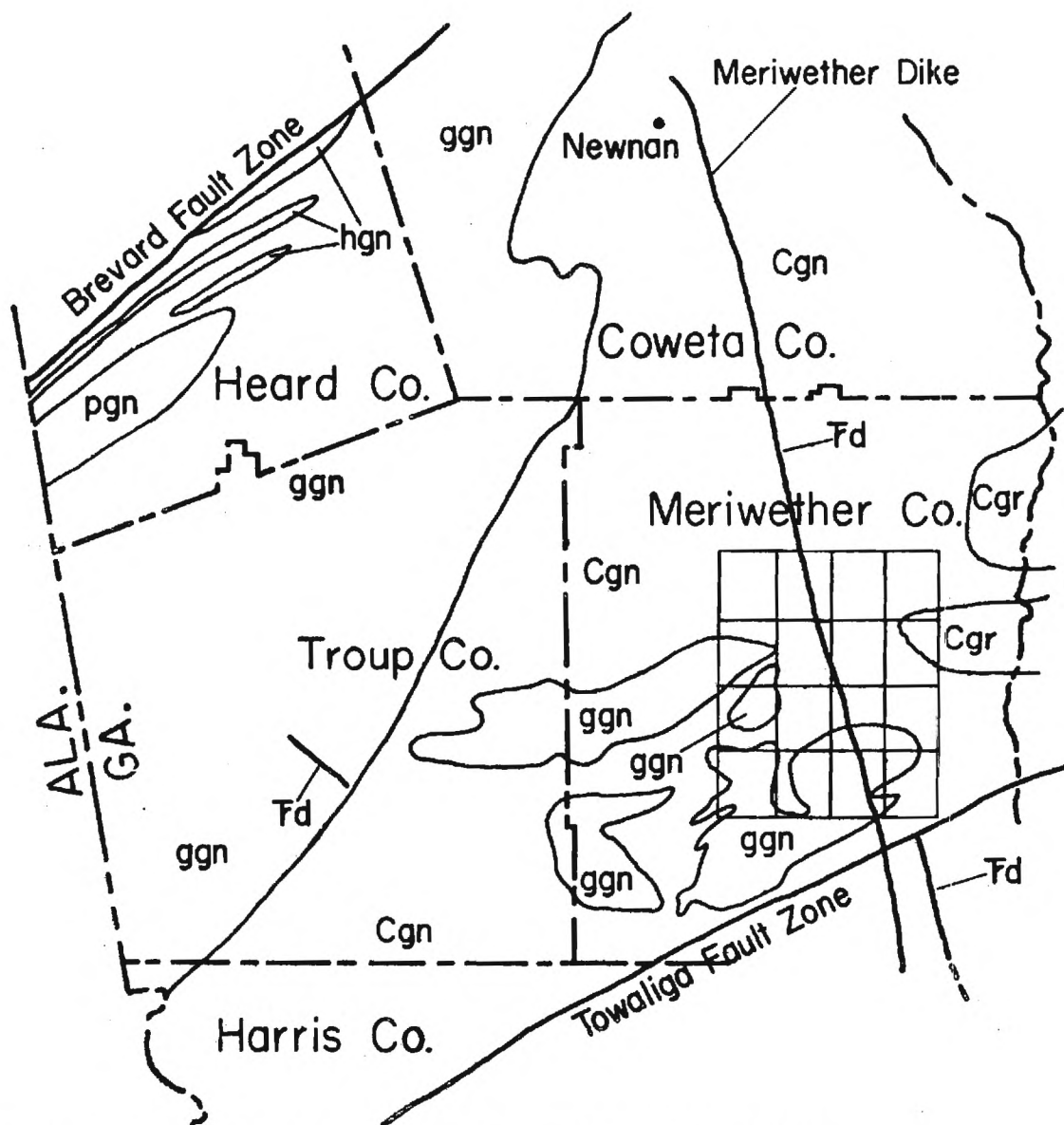
metamorphism.

The chemistry of the diabase dikes, previously thought to be uniform (Lester and Allen, 1950) has been shown by Weigand and Ragland (1970) to vary in both major and trace element assemblages. Weigand and Ragland (1970) divided the dikes of eastern North America into several provinces based on the occurrence of three main chemical types: (1) olivine-normative, (2) high-TiO₂, quartz-normative and (3) low-TiO₂, quartz-normative.

The tracing of individual dikes along strike and the determination of thickness and dip by the usual geological field methods is inhibited in most areas of Southeastern North America by intense chemical weathering and dense vegetation. However, Johnson and Watkins (1963) noted a coincidence of dike outcrops and low-amplitude (less than 20 γ at an altitude of 800 feet above ground level), positive magnetic anomalies along aeromagnetic flight lines in north-central Virginia. On the basis of linear trends in the occurrence of some of these magnetic highs, Johnson and Watkins (1963) inferred the extension of dikes into areas where no outcrops are known. The success of Johnson and Watkins (1963) suggests that geophysical methods at closer range, i.e. aeromagnetics at 500 feet, ground-level magnetics and detailed gravity, could yield detailed structural information as well as outcrop patterns. The purpose of this study was to apply these geophysical methods to a study of the structure of a diabase dike.

A portion of the long dike in central Meriwether County in west-central Georgia (hereinafter referred to as the Meriwether dike) was selected for study. The dike extends southward from an area north-east

of Newnan in Coweta County, to an area south of the Towliga fault in southern Meriwether county (Figure 2). This area of study was selected because of minimal secondary geophysical disturbances, such as gravity and magnetic anomalies associated with fault zones and basic intrusives other than the diabase dike. In addition, the roads in this area traverse the Meriwether dike at almost right angles and are spaced at approximately two miles, affording good access for a geophysical study.



- | | | | |
|------------|----------------------------|------------|---|
| hgn | hornblende gneiss | Cgn | Carolina gneiss
Biotite gneiss and schist |
| pgn | porphyritic granite gneiss | Cgr | Carolina granite
Biotite and muscovite granite |
| ggn | granite gneiss | Fd | Triassic diabase dike |

Figure 2. Geology of the Inner Piedmont of West Georgia (after the 1939 Geologic Map of Georgia). (Hatched square grid shows area of detail study.)

CHAPTER II

GEOLOGICAL SETTING AND REGIONAL GEOPHYSICS

Geologic Setting

According to the Geologic Map of the State of Georgia (Georgia Department of Mines, Mining and Geology, 1939) the geologic formations of the study area consist of granites intermingled with both biotite and granite gneisses (Figure 2). Recent reconnaissance mapping by R. D. Bentley (personal communications) has revealed the geology of the Inner Piedmont (between the Brevard and Towliga Fault Zones) to be more complicated than suggested by the 1939 Georgia Geology Map. Bentley and Neathery (1970) renamed the rocks of the southeastern portion of the Inner Piedmont the Opelika Complex and divided it into two stratigraphic units, the Loachapoka Schist and the Auburn Gneiss-schist (Figure 3). These units were interpreted by Bentley (Bentley and Neathery, 1970) as metamorphosed sediments which are extensively intermingled with granites. The Meriwether dike strikes about N20°W through the area and intersects the rocks of the Opelika Complex at about 60°.

Regional Gravity

Based on measurements taken at 195 stations, a simple Bouguer gravity map of the area under investigation was constructed (Figure 4). The procedures used for the reduction of the data and estimating errors in the final values are given in Appendix I. Estimated error in the regional data is ± 0.35 milligals. Isogals trend approximately north-

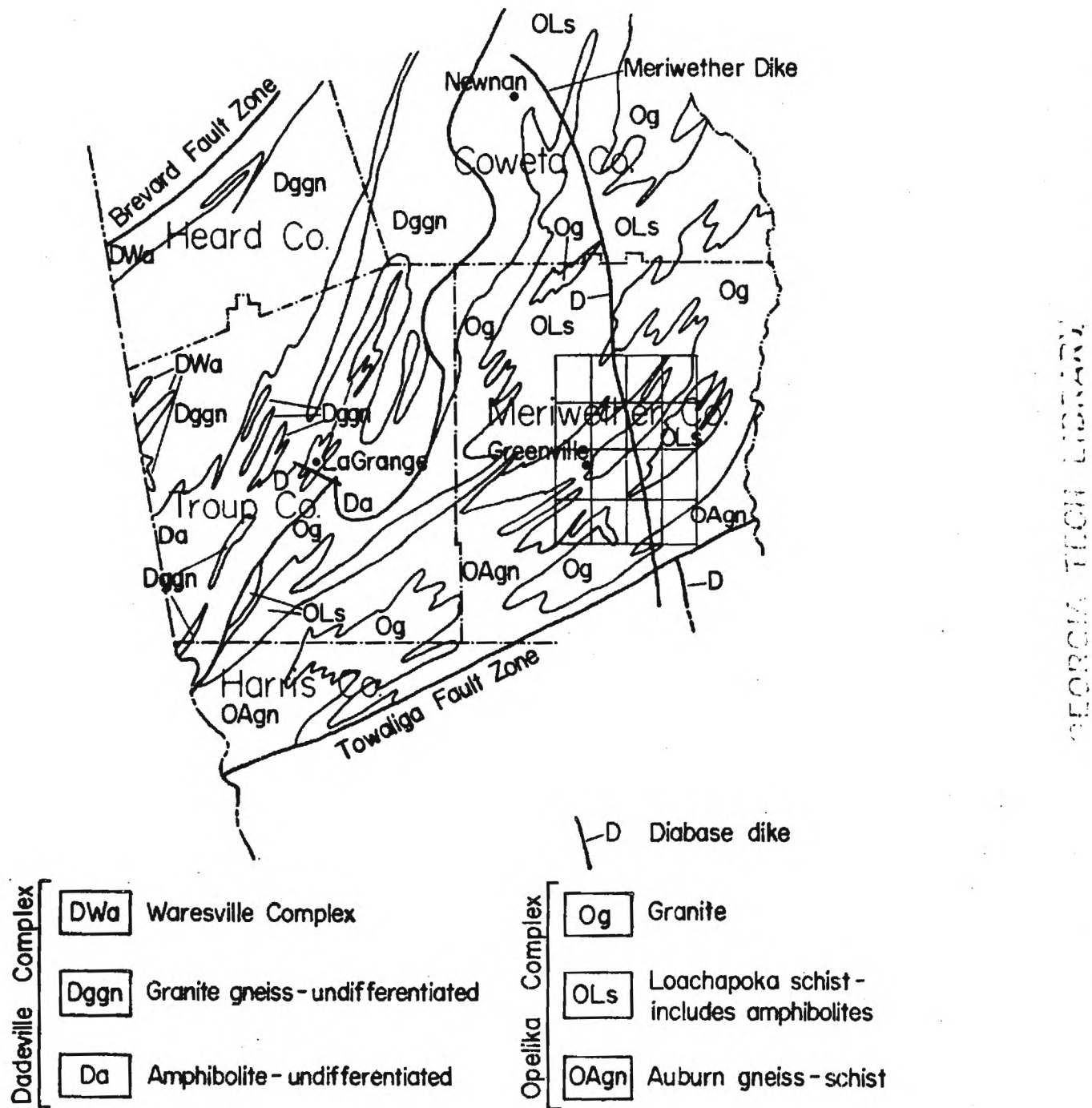


Figure 3. Geology of the Inner Piedmont of West Georgia (after Bentley Neathery, 1970). (Hatched square grid shows area of detail study.)

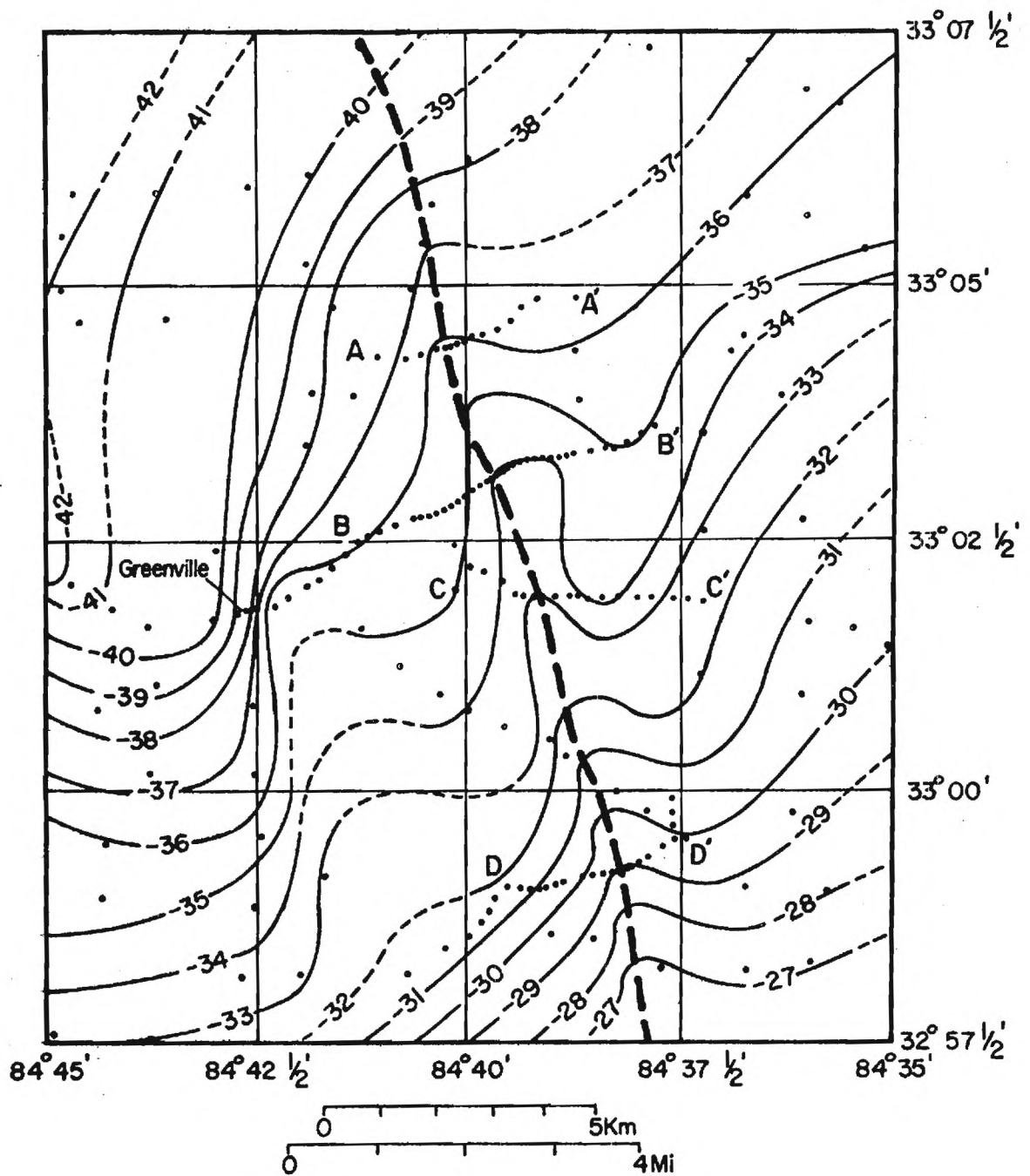


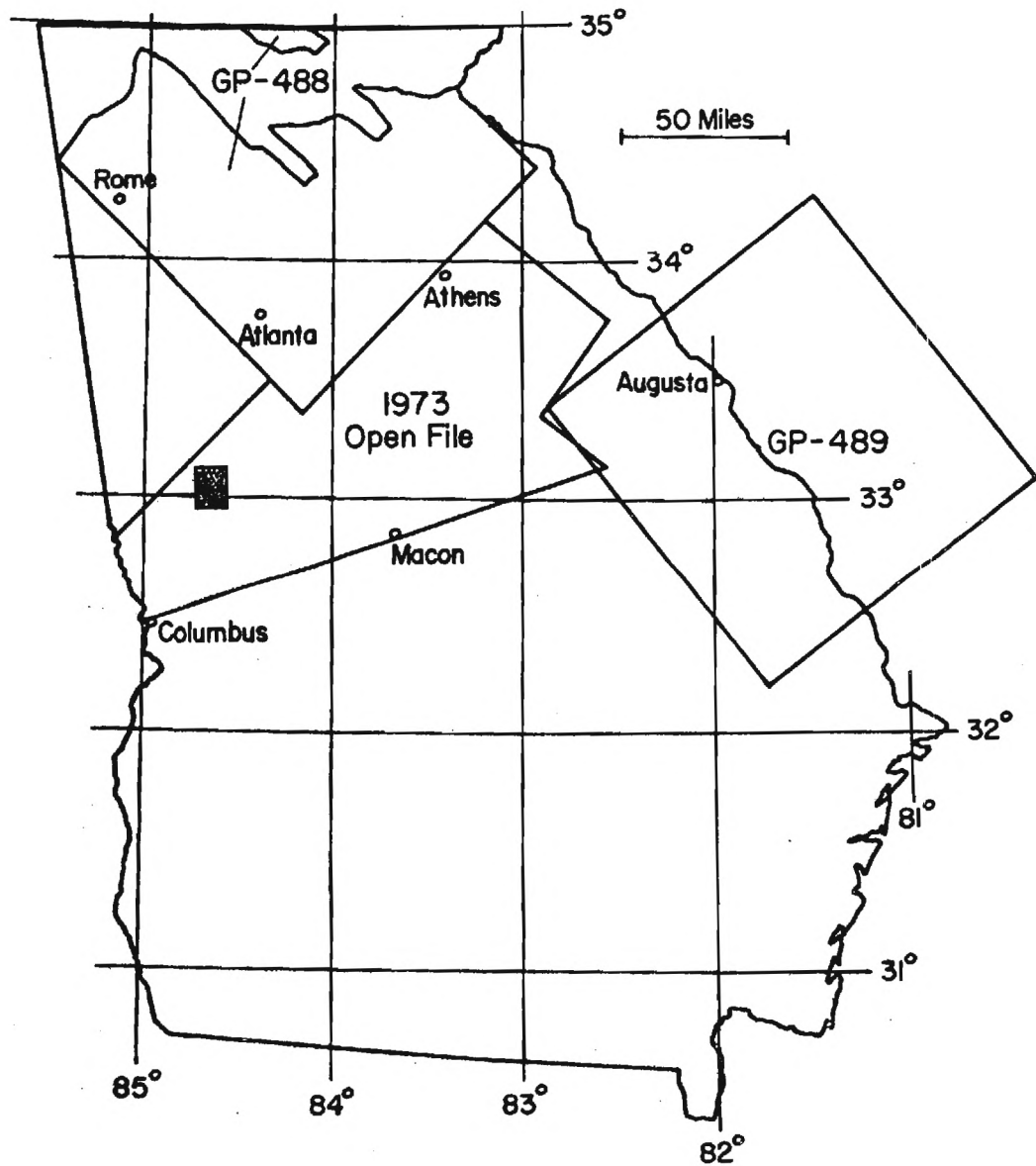
Figure 4. Simple Bouguer Gravity Map of Detail Study Area. (Dashed line gives location of Meriwether dike. Letters designate beginning and end of detailed gravity lines.)

east-southwest, and the regional gradient is about -0.8 milligals/kilometer to the northwest. The prominent features on the simple Bouguer gravity map are the steep gradient in the west-central portion of the study area and an anomaly in the regional trend of one to two milligals beginning in the southeastern part of the study area and continuing northward through the area. The steep gradient is coincidental with the contact between the Loachapoka Schist and granite west of Greenville (Figure 3). The anomaly in the regional trend is largely caused by the existence of the Meriwether dike. Too few gravity stations were taken in the extreme northern portion of the study area to warrant contouring, except by extrapolation. The anomaly probably extends northward out of the study area coincident with the dike.

Regional Magnetics

The North-Central Georgia Aeromagnetics Map (U.S. Geological Survey, open file, 1973) partially fills the gap (Figure 5) between the two previous aeromagnetic surveys of North Georgia Nuclear Laboratory (Philbin, Petrafeso and Long, 1964) and Savannah River Plant (Petty, Petrafeso and Moore, 1965). The area of this investigation (Figure 6) is part of the area covered by this latest work.

Similar to the regional gravity, magnetic features trend NE-SW. Lack of steep gradient immediately east of Greenville suggests that the units responsible for the observed steep gravity gradient in this area have a low contrast in magnetic susceptibility. The most conspicuous feature is the string of localized magnetic highs trending from north to south and having centers located at intersections of the dike and the



REF ID: A6741

Figure 5. Index Map of Georgia Showing Location of Detail Study Area and Existing Aeromagnetic Maps. (Maps GP-488, North Georgia Nuclear Laboratory, and GP-489, Savannah River Plant, have been published by the U. S. Geological Survey. The North-Central Georgia Map is available on open file at the Georgia Geological Survey. Stippled rectangle is area of detail study.)

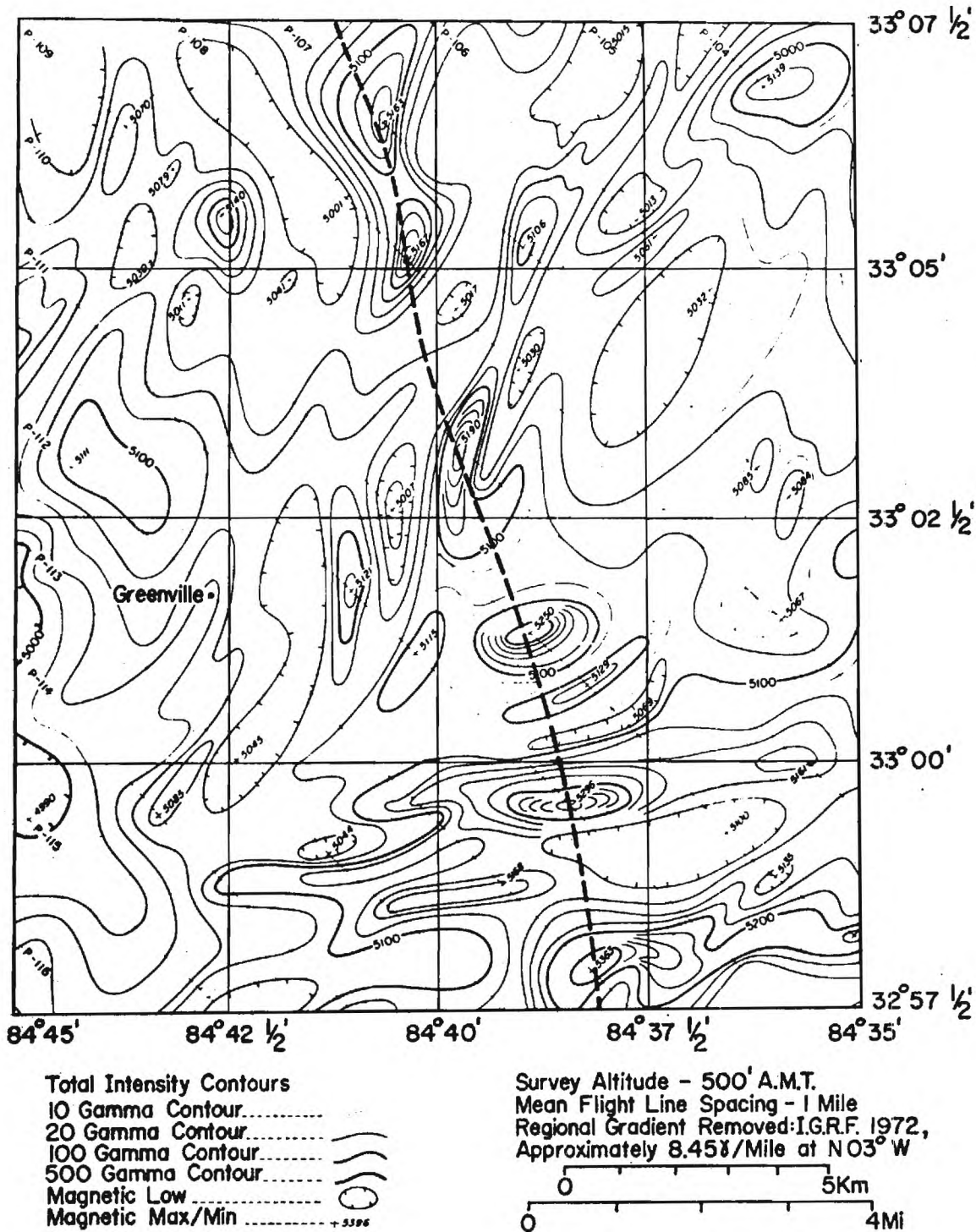


Figure 6. Portion of North-Central Georgia Aeromagnetic Map Covering Area of Detail Study. (U.S.G.S. Open File, 1973) (Dashed line gives location of Meriwether dike. Anomalies are with reference to 50,000' datum.)

flight lines. These magnetic highs are probably a result of the presence of the Meriwether dike.

The Meriwether dike, which outcrops on roads along its entire length, is probably more continuous than suggested by the series of magnetic highs in Figure 6. Detailed ground-level magnetic traverses of the Meriwether dike at points between aeromagnetic flight lines (Figure 7) support this supposition of continuity. Prominent (1000') magnetic highs coinciding with observed dike outcroppings (Figure 8) suggested a recontouring of the aeromagnetic data.

Since the continuous flight line data were not available, all points where flight lines intersect contour lines were assumed to represent true values (the data were extrapolated by computer methods between flight lines). Latitude, longitude, and the total magnetic intensity were determined for each intersection and these points were plotted for recontouring. Under the assumption that the Meriwether dike is continuous along strike, straight lines were drawn connecting points of equal total magnetic intensity on adjacent flight lines in the region where the dike outcrops. In other areas contour lines were assumed to be influenced by the regional geology (after Bentley and Neathery, 1970).

Although no magnetic interpretation is unique, this one (Figure 9) does strongly suggest that the magnetic anomalies associated with the dike can be represented by a continuous linear anomaly. This interpretation is necessary for two-dimensional analysis of the dike by comparison of its observed anomalies with those of easily computed models.

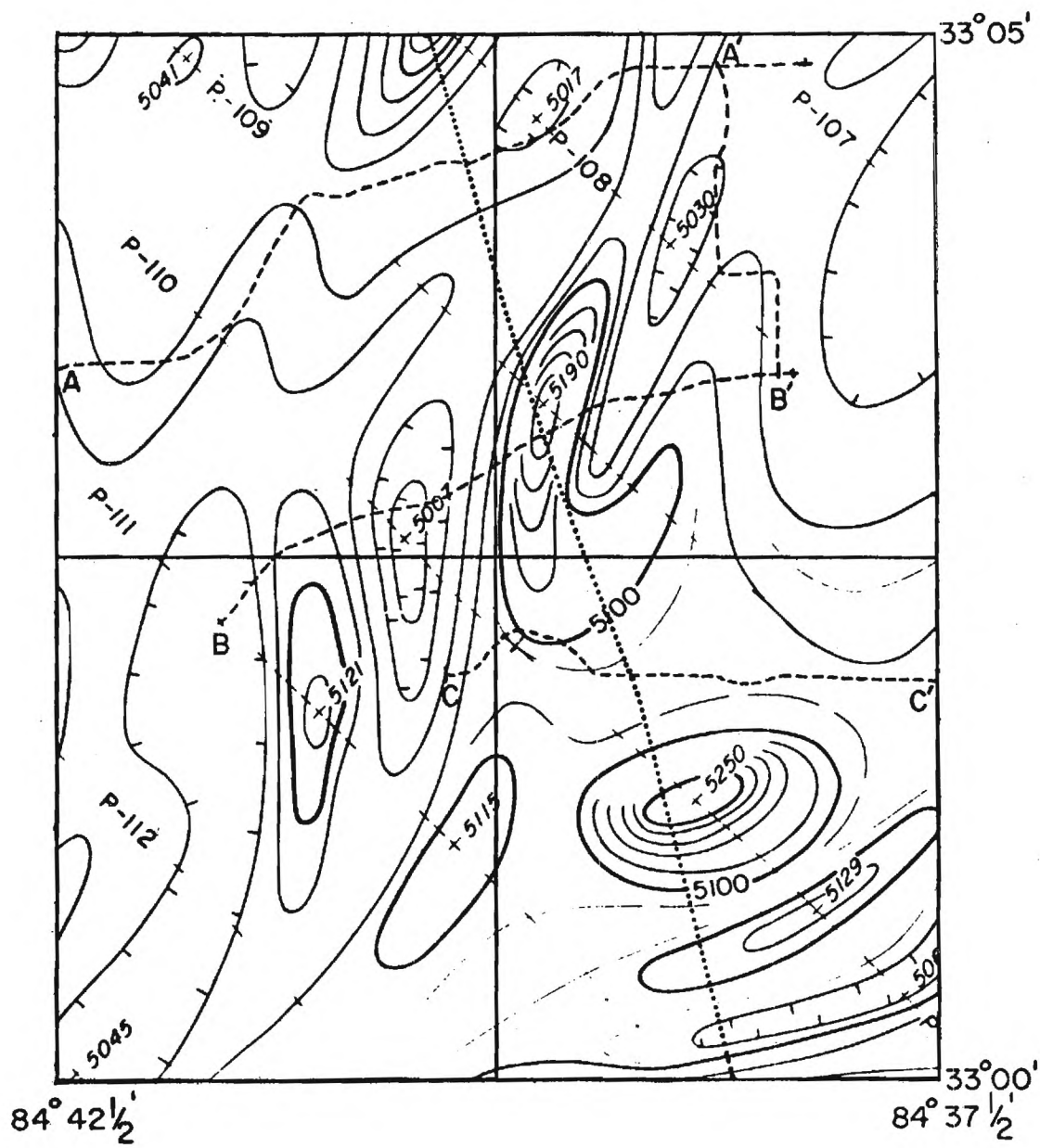


Figure 7. Index Map Showing Locations of Detailed Ground-Level Magnetic Surveys and Existing Aeromagnetic Flight Lines. (Dotted line gives location of Meriwether dike. Anomalies are with reference to 50,000Y datum.)

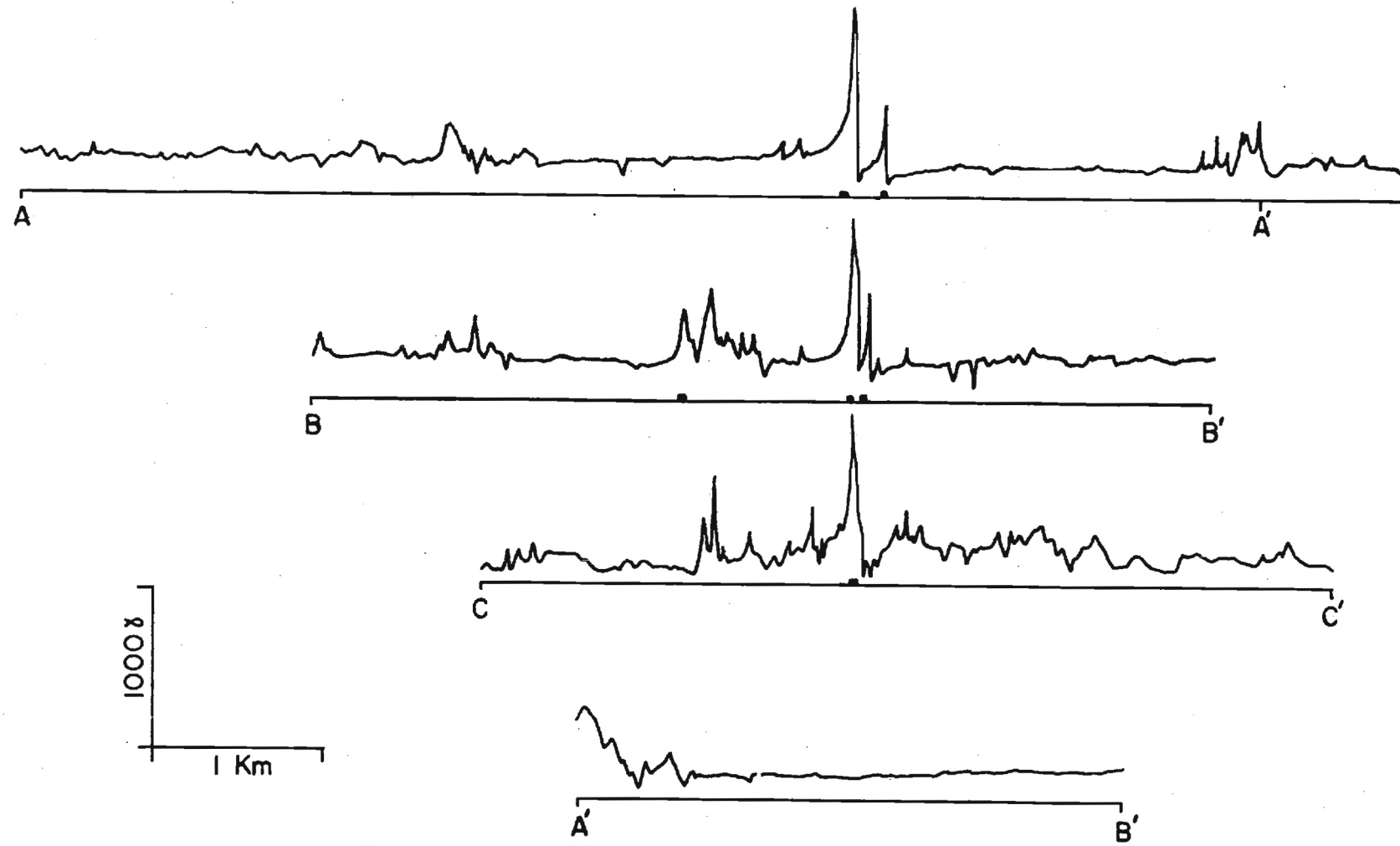


Figure 8. Ground-Level Magnetic Profiles (Total Field). (Heavy bar on profile base indicates diabase outcrop. See Figure 7 for location of profiles.)

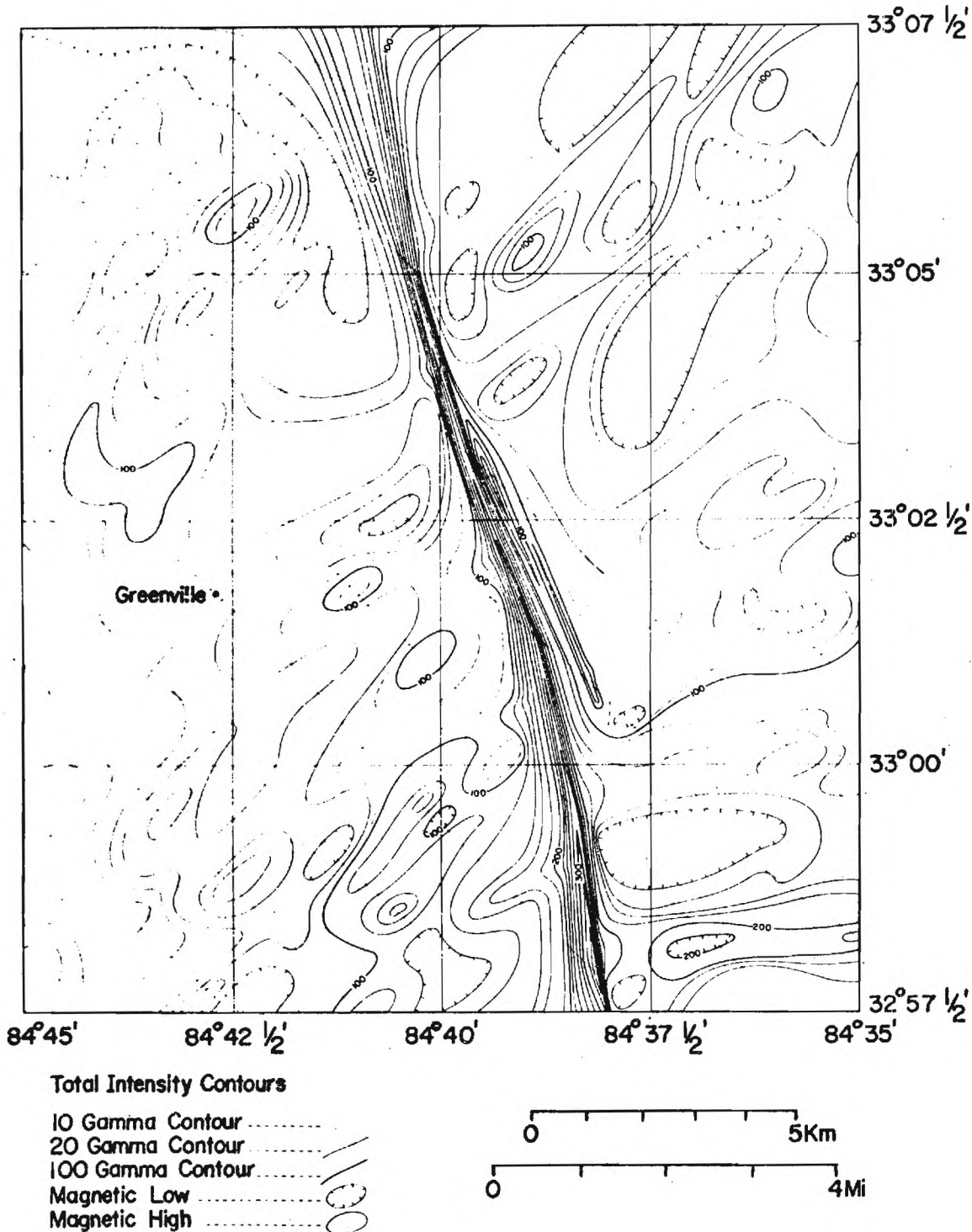


Figure 9. Aeromagnetic Map (Total Field) of the Study Area Recontoured Assuming the Meriwether Dike to be a Continuous Magnetic Feature. (Anomalies are with reference to 55,000Y datum.)

CHAPTER III

PHYSICAL PROPERTIES OF THE MERIWETHER DIKE

Density

Diabase lends itself especially well to geophysical investigation.

The density of the Meriwether diabase is $3.0 \pm 0.05 \text{ gm/cm}^3$ (as determined by gravimetric methods applied to three field samples). Watson (1902) determined the densities of the Loachapoka Schist and local granites to be $2.64 \pm 0.01 \text{ gm/cm}^3$ and $2.70 \pm 0.01 \text{ gm/cm}^3$ respectively. Thus, the density contrast between the diabase of the Meriwether dike and the surrounding rocks (average density $2.67 \pm 0.02 \text{ gm/cm}^3$) is $0.33 \pm 0.07 \text{ gm/cm}^3$. A vertical dike 30 meters wide (average observed outcrop width of the Meriwether dike) with this density contrast should yield a vertical gravity anomaly of approximately 1.5 milligals, an anomaly easily discerned with contemporary instrumentation (see Appendix I).

Magnetic Susceptibility

Several attempts have been made to statistically relate the bulk susceptibility of rocks to petrological parameters. One such attempt was that of Balsey and Buddington (1958) who related the susceptibility of some Adirondack rocks to the fractional volume of all the minerals visually identified as magnetite. This volume would generally include any Fe-Ti oxide minerals of spinel structure. Their empirical formula for the bulk susceptibility (k) in C.G.S. units is

$$k = 2.6 \times 10^{-3} V^{1.11} \quad (1)$$

where V is the volume percentage of all minerals visually identified as magnetite.

Petrographic examination of the Meriwether dike (Lee, 1971) showed that opaque grains (assumed to be Fe-Ti oxides of spinel structure) comprise 2.3 to 4.3 percent of the rock with a higher percentage occurring in the finer-grained zones near its edges. Using the empirical formula of Balsey and Buddington (1958) (Equation 1) and the range of volume percentages of opaques given by Lee (1971), the bulk susceptibility of the diabase composing the Meriwether dike was estimated to be between 0.0066 and 0.0130 cgs.

GEORGE W. TUCK

CHAPTER IV

DETERMINATION OF DIP ANGLE FROM GRAVITY
AND MAGNETIC ANOMALIESTheoretical Models

Theoretical anomalies were calculated for sets of models to examine the effects of dip angle on expected gravity and magnetic anomalies. The method of Talwani, Worzel, and Landisman (1959) was used to compute the gravity anomalies that would be expected for dikes dipping at various angles. Because the observed outcrop width would be fixed for a particular dike, anomalies were computed for models with an outcrop width of 30 meters dipping at 90, 75, 60, and 45° (Figure 10). As would be expected, the gravity anomaly caused by a vertical dike is symmetric about the center of the dike. However, as the dip angle decreases the anomaly becomes asymmetric with the peak shifting toward the direction in which the dike is dipping. The anomaly tails off more slowly on the side toward which the dike dips than the other. Even though there are obvious differences in the anomalies for various values of dip angles, a superimposed regional trend may make determination of the dip more difficult than suggested by Figure 10; in fact, unless the regional trend is simple and well defined, the determination of the dip may be impossible.

Although the dip angle has an obvious effect on the shape and asymmetry of the total-field anomaly (Figure 11), the effects of natural

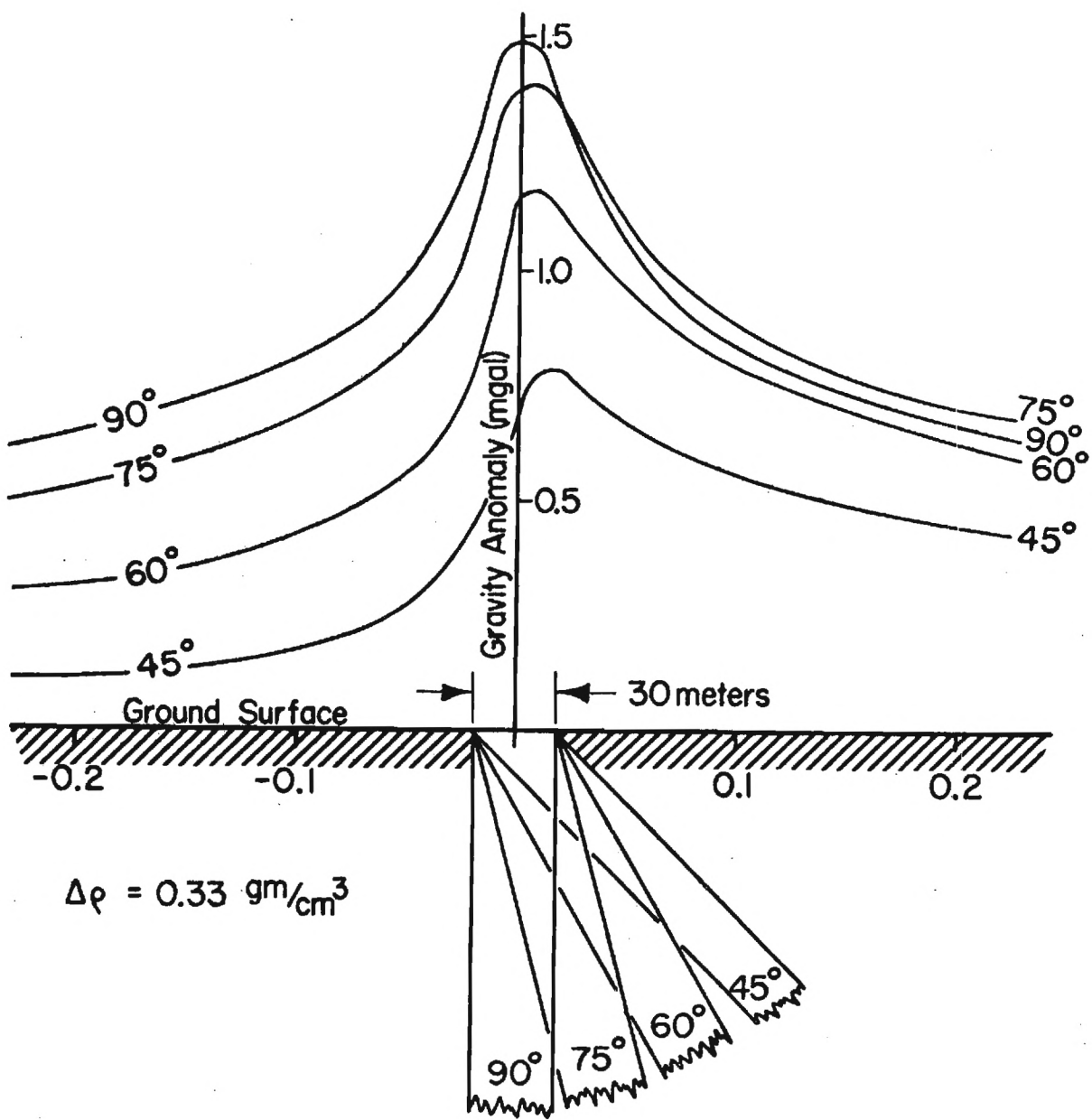


Figure 10. Calculated Curves Showing Effect of Dip Angle on Vertical Gravity Anomaly.

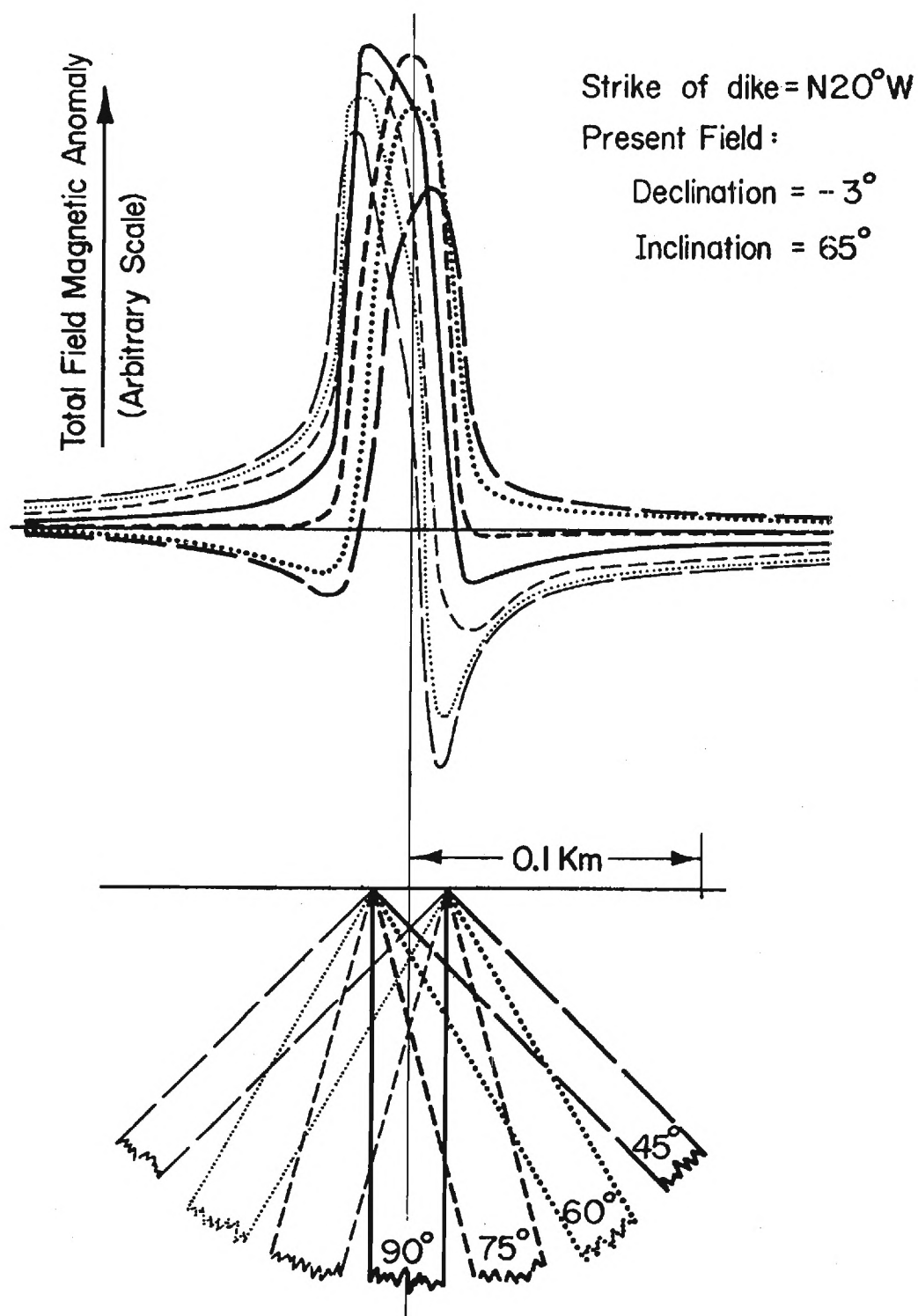


Figure 11. Calculated Curves Showing Effect of Dip Angle on Total Field Anomaly Due to Induction Magnetization Only.

remanent magnetization, when added to the induced magnetization, may complicate the determination of dip angle from the observed anomaly (Hood, 1963). For this reason, the angle of dip was determined using observed gravity anomalies only. The magnetic anomalies, because of their sharpness as compared to the gravity anomalies (Figures 8 and 10), were used only for lateral location of the dike where outcrops were nonexistent.

Detailed Gravity Profiles

Five detailed gravity lines with an average station spacing of 0.15 kilometers and a total length of 20 kilometers were obtained. Station spacing was decreased to about 0.075 kilometers in the immediate proximity of the dike. Four lines traverse the Meriwether dike in the prescribed study area (Figure 4) and the fifth traverses it along Georgia State Highway 16 southeast of Newnan and north of the study area. The observed anomalies (Figures 12 through 16), when smoothed, are about 1.0 kilometer wide at half their maximum value. This width is considerably greater than the computed anomaly width for a vertical dike 30 meters wide, approximately 0.1 kilometers at half its maximum value (Figure 10). Numerous individual peaks superimposed on the broad peaks suggest that a 0.75 kilometer wide swarm of dikes, rather than a single dike, is responsible for the observed anomaly. Such a hypothesis is further supported by the ground-level magnetic profiles, (Figure 8).

Profile A-A'

Gravity line A-A' (Figure 4) was established along a dirt road about 3.0 kilometers north of Georgia State Highway 109. The observed

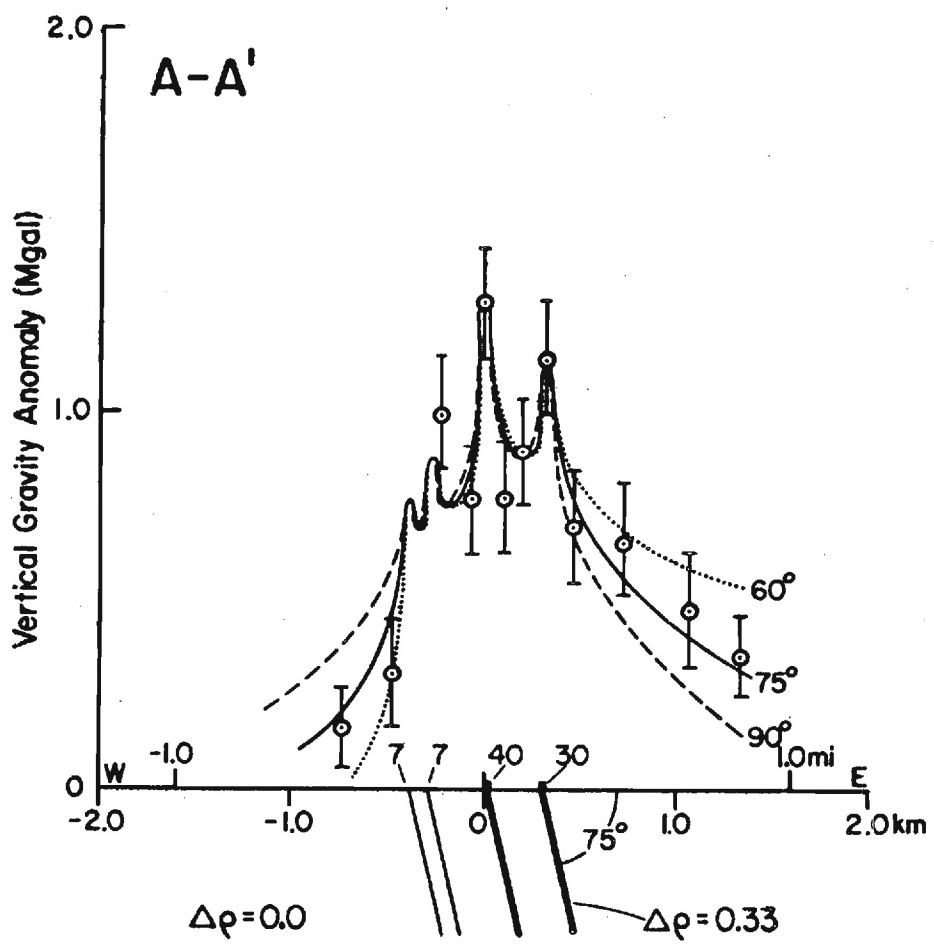


Figure 12. Detailed Gravity Profile A-A'. (Model dikes extend to infinite depth. Thickness of the modeled dike is given by the numeral above the dike. Heavy bar on profile indicates observed dike outcrop.)

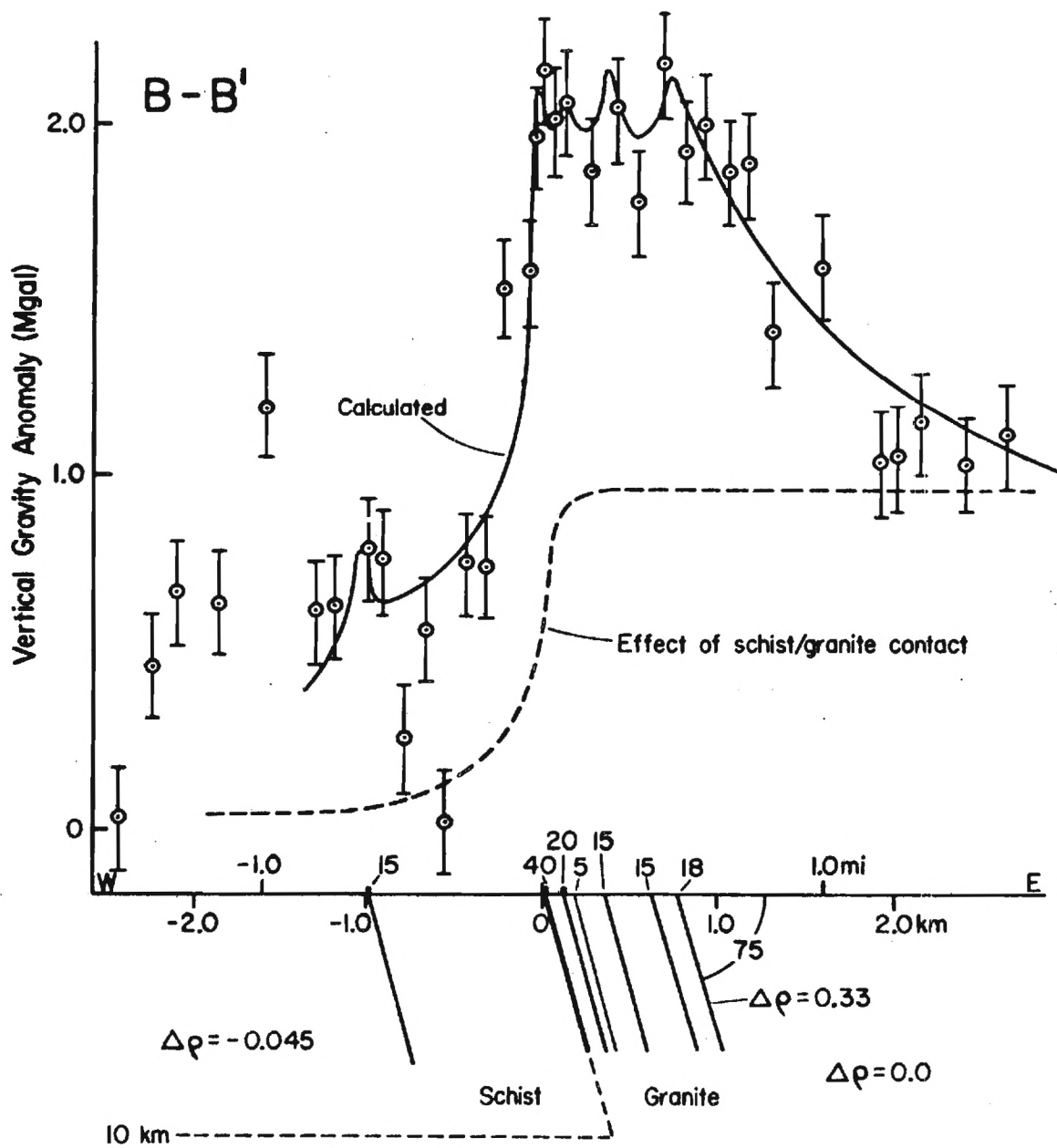


Figure 13. Detailed Gravity Profile B-B'. (Model dikes extend to infinite depth. Thickness of the modeled dike is given by the numeral above the dike. Heavy bar on profile indicates observed dike outcrop.)

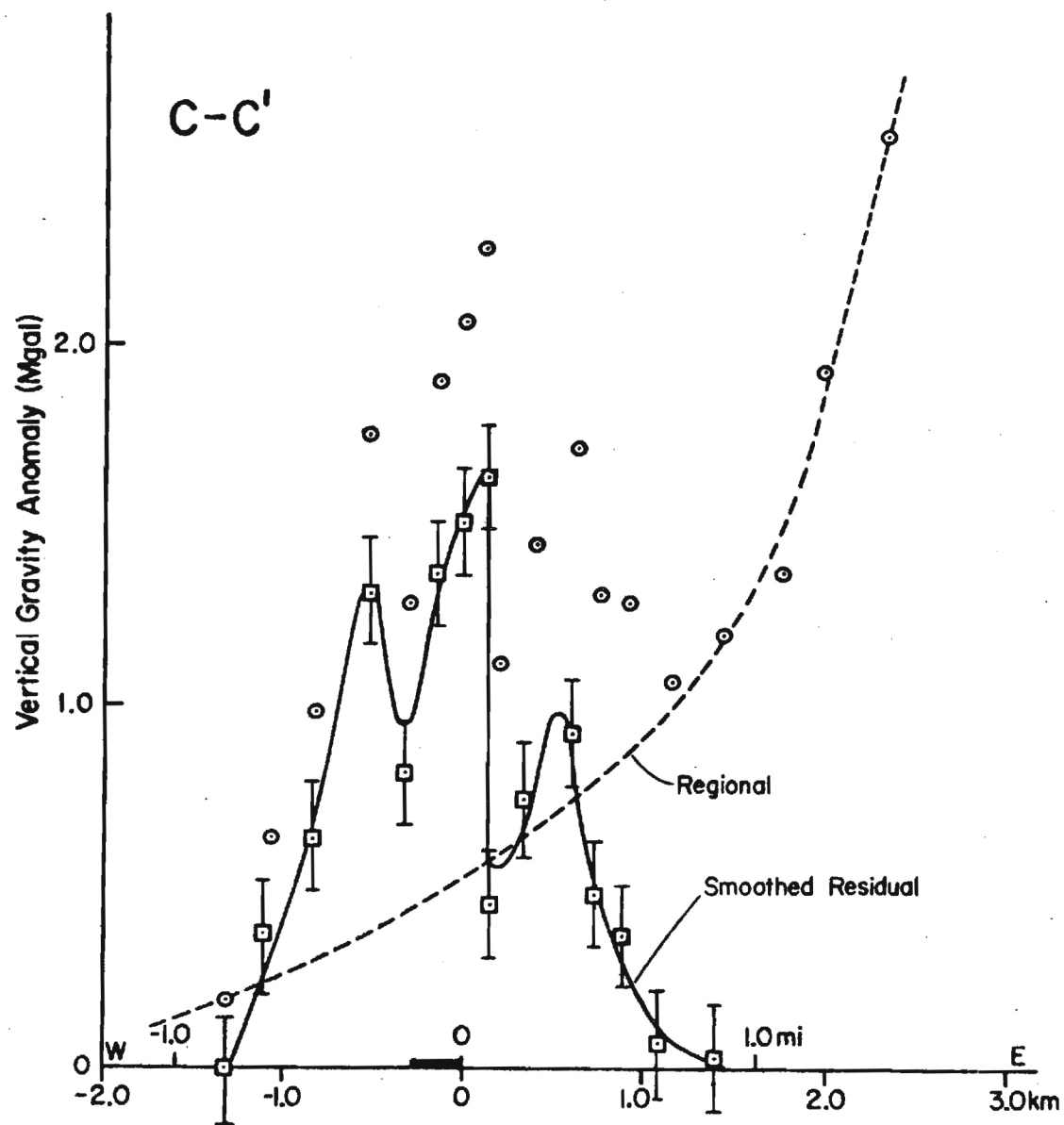


Figure 14. Detailed Gravity Profile C-C'. (Smoothed residual exhibits three definite peaks. Heavy bar on profile indicates observed dike outcrop.)

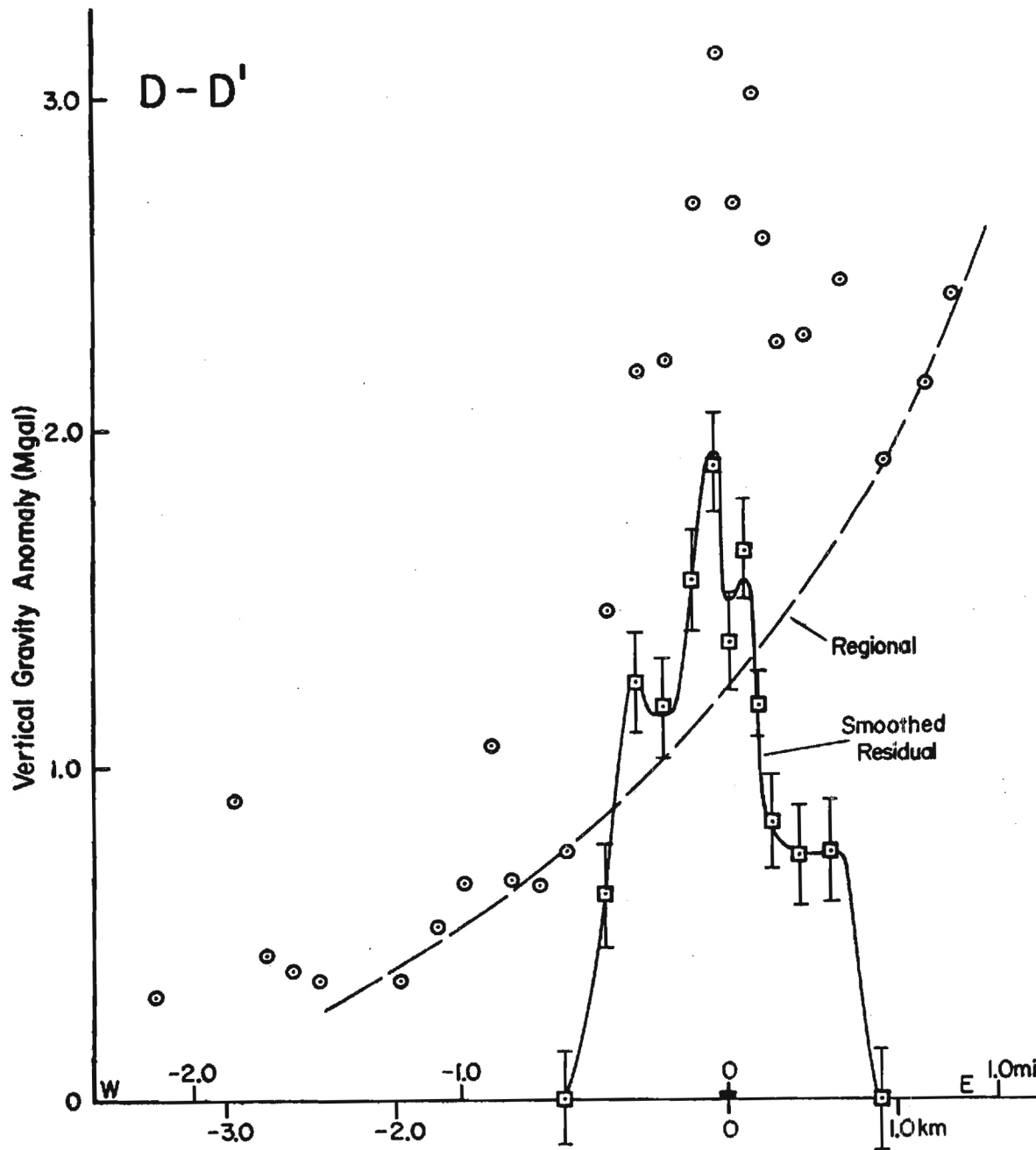


Figure 15. Detailed Gravity Profile D-D'. (Smoothed residual exhibits multiple peaks. Heavy bar on profile indicates observed dike outcrop.)

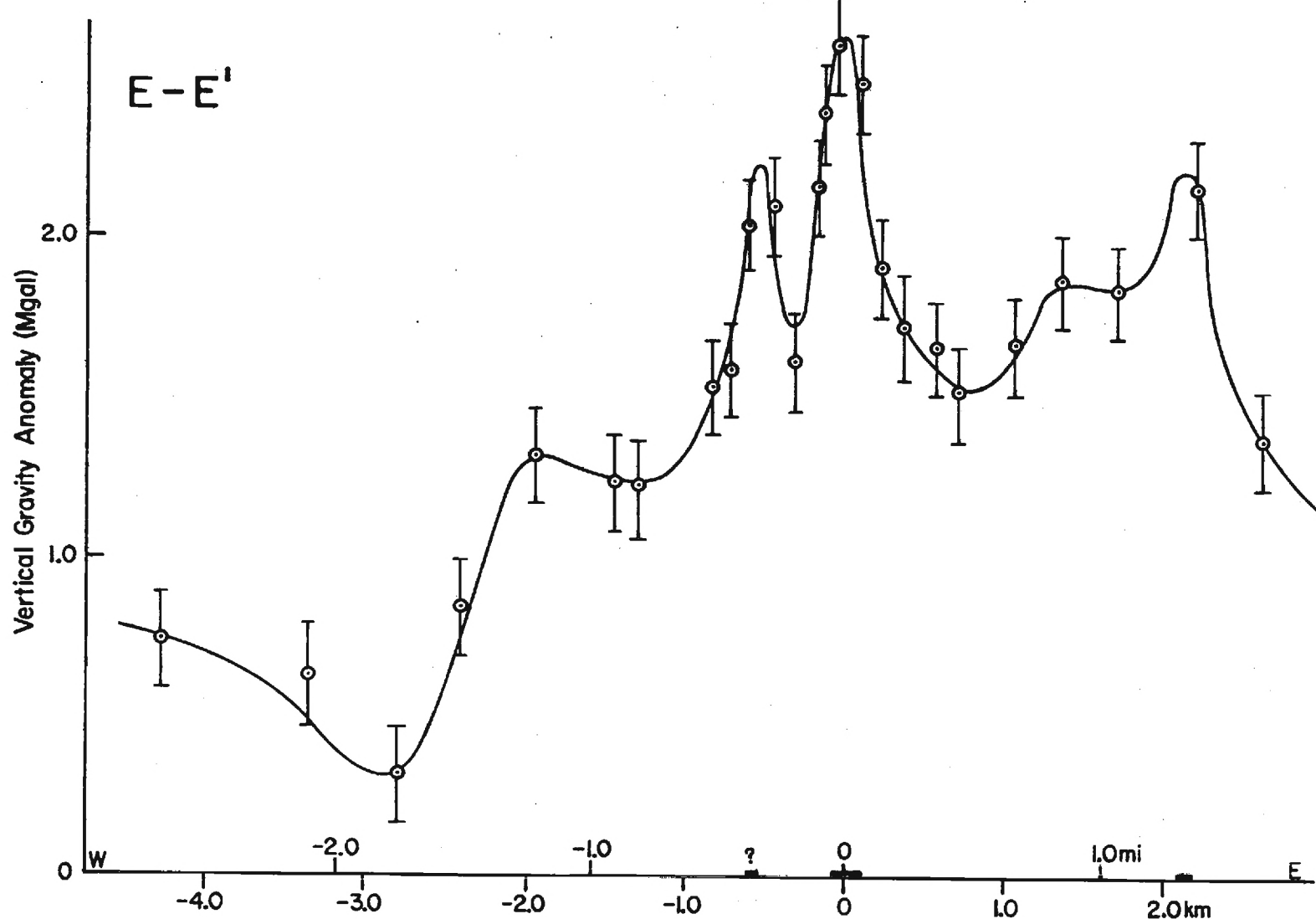


Figure 16. Detailed Gravity Profile E-E'. (Georgia Highway 16, south of Newnan. Heavy bar on profile indicates observed dike outcrops.)

gravity anomaly (Figure 12) consists of three peaks of about one milligal amplitude with the side and less prominent peaks spaced about 0.2 kilometers to either side of the main peak. Because there exist no known density anomalies, with exception of the diabase, along this profile and because the regional isogals are slightly curved in the region of this profile (Figure 4), no regional trend was removed. The three peaks and the asymmetry of the anomaly suggest that three dikes dipping to the east are necessary to account for the observed anomaly. Examination of the ground-level magnetic data for the same profile (Figure 8) suggests that the side dike to the west is actually two thin dikes. Assuming the existence of the four dikes, anomalies were computed using the observed outcrop widths for the main dike (40 meters) and the east dike (30 meters). The west dikes were not found to outcrop and because of the lesser magnitude of the associated gravity anomaly as compared to those of the main dike, they were modeled to be 7.5 meters wide.

Examination of the computed anomalies for dips of 90, 75 and 60° (Figure 12) shows the observed anomaly to fall between the computed curves for 60 and 75 with a dip angle of 70° (by interpolation) probably best satisfying the observed data.

Profile B-B'.

Detailed gravity line B-B' (Figure 4) was established along Georgia State Highway 109 between Greenville and Gay, Georgia. The observed anomaly consists of a "noisy" assymmetric broad peak (Figure 13). Amphibolites were found outcropping to the west of the main dike and could be responsible for the observed scatter in the data west of the dike. Diabase float was also found 1.0 kilometers west of the main

dike indicating that part of the observed scatter in the data may be a result of a side dike. A corresponding magnetic anomaly was encountered during the ground-level magnetic survey of the same profile (Figure 8).

Aside from the scatter in the data to the west of the main dike, there is a difference in the base level of the observed gravity. The east side of the dike is about 1.0 milligal more positive than the west side. This offset can be accounted for by the contact (no fault is visible and the orientation of the contact is unknown) between the Loachapoka Schist to the west and the granite to the east.

After the effect of the contact was removed, the resulting asymmetric residual anomaly could be modeled by a set of six dikes dipping to the east. Only the main dike was observed to outcrop, but the ground-level magnetic data (Figure 8) indicate the existence of the others. Determination of the angle of dip was not attempted because of the uncertainty in the location and orientation of the schist-granite contact.

Profile C-C'.

Profile C-C' (Figure 4) was established along the dirt road about 1.5 kilometers south of Georgia State Highway 109. The strong eastward positive trend of the observed data (Figure 14) is probably caused by granitic rocks which dip westward (Figure 3). Because the exact location and attitude of the granite-schist contact were unknown, a regional trend was estimated (Figure 14). The residual anomaly (Figure 14) consists of a central main peak and two secondary peaks on either side of the main peak. Although the dike was found to outcrop only coincident with the central peak of the gravity anomaly, the secondary peaks of the anomaly are probably due to side dikes. A similar phenomenon was

noted previously for profiles A-A' and B-B' further to the north. Because of the ambiguity created by the removal of the regional gravity trend by smoothing, and the noisy character of the ground-level magnetic data taken for the same profile (Figure 8), no attempt was made to determine the dip angle of the dikes.

Profile D-D'.

Line D-D' (Figure 4) was established along the paved county road about 8.0 kilometers southeast of Greenville and 4.5 kilometers south of detailed gravity line C-C'. As in profile C-C', there is a strong positive regional trend to the east (Figure 15), which was removed. The multiple peaks in the residual anomaly, (Figure 15) although not as well separated as in the previous profiles, again indicates that more than one dike is responsible for the observed anomaly. The only dike found to outcrop was again coincident with the main peak.

Profile E-E'.

Gravity line E-E' lies along Georgia Highway 16, southeast of Newnan. This profile, which is outside the main area of investigation, was obtained for comparison to the four previous profiles which lie within the area of detailed study 20 kilometers to the south. The observed anomaly (Figure 16) consists of three peaks all coincident with observed outcrops of dikes with the central peak corresponding to the widest outcrop. Whereas the side dikes in profiles to the south are located no more than 1.0 kilometers to the side of the main dike, the east dike on profile E-E' is located 2.1 kilometers from the main dike.

CHAPTER V

GROUND-LEVEL MAGNETICS AND THE ROLE OF NATURAL REMANENT
MAGNETIZATION IN THE OBSERVED ANOMALIESGround-Level Magnetics

Four detailed ground-level magnetic (total field) profiles were obtained in order to examine the structure of the Meriwether dike and to provide additional data for the purpose of recontouring the aeromagnetic data previously described. Three of the profiles were obtained along the same roads as detailed gravity profiles A-A', B-B', and C-C'. The fourth was a closure profile connecting A-A' and B-B' (Figure 7). The data was obtained and reduced by standard techniques and are listed in Appendix II.

The reduced data (Figure 8) showed the main dike to be represented by an asymmetric anomaly for all three profiles. However, the calculated anomaly due to induction magnetization for a dike dipping 70° toward $N70^{\circ}E$ is a symmetric positive peak (Figure 11). This suggests that induction magnetization is not the only cause for the observed anomaly and that natural remanent magnetization (NRM) must also be considered in the analysis of magnetic anomalies (Hood, 1963).

Natural Remanent Magnetization of the Meriwether Dike

Samples from a single outcrop of the Meriwether dike were collected and analyzed for NRM by Doyle Watts (personal communications). Intensities and directions for the NRM's are given in Appendix IV. A

Schmidt stereographic projection of the NRM directions (Figure 17) shows the NRM directions to be different from today's magnetic field. Samples from the center of the dike constitute one set of directions and those from the chilled margins another set. Because it is not known what proportion of the dike has which magnetization, an average of the directions (Figure 17) and magnitudes were used for computing the anomaly due to remanent magnetization. The average direction has a declination of 28° and an inclination of 30° . The average magnitude of the NRM is 0.00175 cgs.

Theoretical Anomalies and the Determination
of the Koenigsberger Ratio, Q

The ratio of remanent magnetization to induced magnetization, the Koenigsberger ratio, Q is commonly cited in paleomagnetic studies as an indication of whether or not samples have been subjected to lightning strikes. It has more recently been construed (Green, 1960) as a measure of the importance of remanent magnetization in the analysis of magnetic anomalies. Using the calculated bulk susceptibility for the diabase of the Meriwether dike and the average intensity of NRM, the probable range of Q is 0.25 to 0.50. The range of Q's is a result of the uncertainty in the bulk susceptibility.

To examine the effects of Q on the observed anomalies, several models were computed using the method of Talwani and Heirtzler (1965). For a Q of 0.25 and bulk susceptibility of 0.013 cgs, the remanent magnetization causes the anomaly to become slightly asymmetric (Figure 18) with a peak to trough ratio of about 15 to 1. For bulk suscepti-

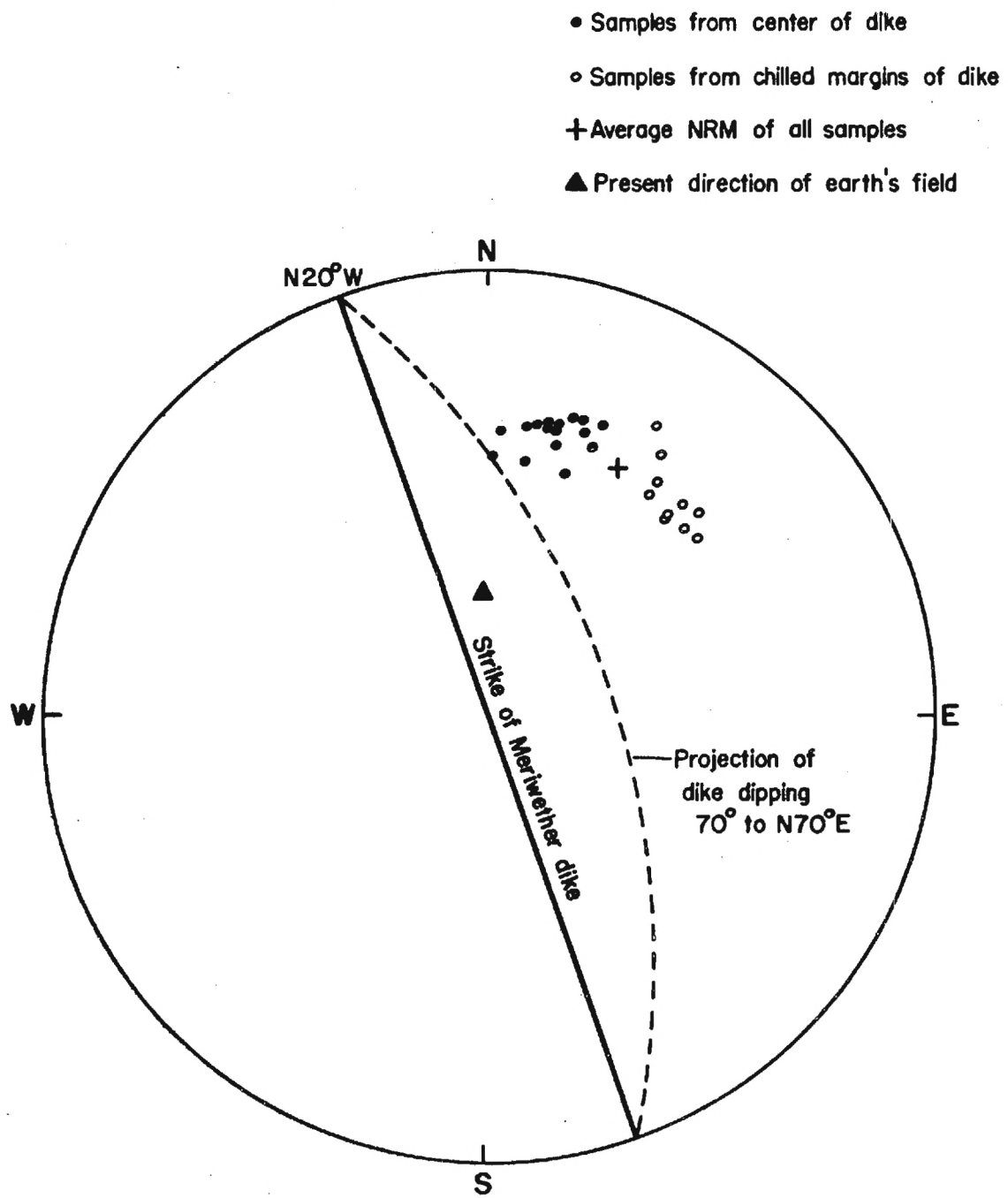


Figure 17. Stereographic Projection (Schmidt net) of Measured Natural Remanent Moments (NRM) for the Meriwether Dike.

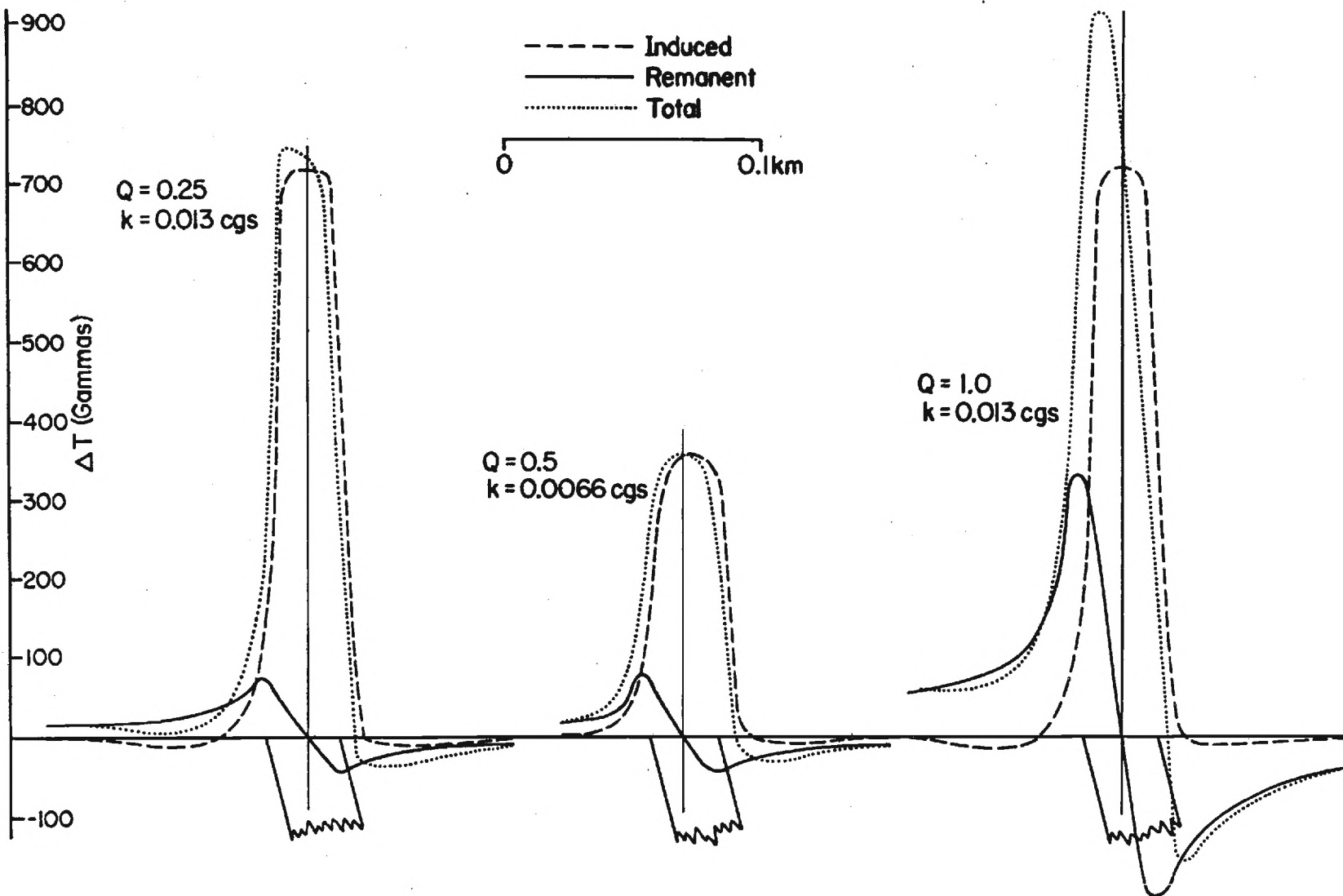


Figure 18. Calculated Curves Showing the Effect of Natural Remanent Magnetism on the Total Field Anomaly. (Dike is 30 meters wide and dips at 75°.)

bility 0.0066 cgs and corresponding Q of 0.5 the anomaly is found to be more asymmetric with a peak to trough ratio of 10 to 1.

The observed anomalies (Figure 8) however, exhibit an average peak to trough ratio of only 6. Further, the amplitude of the observed anomalies is greater than that calculated for the given range of susceptibilities and corresponding magnetizations. An increase in Q to 1.0 at a susceptibility of 0.013 cgs produced an asymmetric anomaly with a peak to trough ratio of about 6 to 1, (Figure 18) indicating that the bulk remanent magnetization was probably greater than that suggested by the surface samples.

Strangway (1965), who sampled a diabase dike at both the surface and at depth in a mine, found the ratio of remanent to induced magnetization to be greater for the underground samples. As a possible cause of this phenomenon Strangway (1965) suggests that temperature fluctuation at the surface, which was probably exposed for a considerable length of time, has accelerated the decay of the remanent magnetization. The same type of process may have occurred in the Meriwether dike and hence, the effective Q, which includes the effect of sub-surface portions of the dike, is probably closer to 1.0.

It should be noted that even if the dike actually dips as much as 80° , the magnetic anomaly due to induction would still be a symmetric peak (Figure 11), and hence the calculated Q of 1.0 would not be seriously affected.

CHAPTER VI

DISCUSSION AND CONCLUSIONS

Examination of the Meriwether dike by means of detailed gravity and magnetic profiles shows the dike to consist of an injection zone of dikes. Because the gravity anomalies of the component dikes are only partially separated, determination of whether or not the side dikes were branches of the main dike was not possible. On the basis of theoretical curves for the dike system dipping at various angles, the Meriwether dike (system) was estimated to dip at 70° toward N 70° E.

The 70° dip is not as steep as noted by Lester and Allen (1950), who found several of the larger dikes in Georgia to have a constant dip toward the east of 75 to 90° and Privett (1966) who found the diabase dikes in central South Carolina to dip 80 to 90° to the NE. It is possible, however, that the Meriwether dike may actually have a dip greater than 70° , but due to the ambiguity of the regional trend it is not possible to resolve how much greater.

A simple Bouguer gravity map compiled for central Meriwether County shows the Meriwether dike to be responsible for an anomaly of one to two milligals in the regional trend. After recontouring of the available aeromagnetic data, the Meriwether dike(s) proved to be the most prominent magnetic feature of the area, and this suggests that the sharpness of the anomaly and the flight line spacing suppressed the dike(s) in previous contouring. It is possible that in other areas of

eastern North America covered by aeromagnetic maps, other occurrences of diabase dikes may be similarly suppressed, thus reducing the probability of locating such dikes by their magnetic anomalies in areas not yet geologically mapped. Locating other dikes by this method may also be hampered by the effects of remanent magnetization.

Although not studied in detail, examination of high altitude infrared photographs (N.A.S.A., 1970) of central Meriwether County, revealed the existence of a linear anomaly coinciding with the Meriwether dike at known outcrops in the northern third of the study area. The anomaly is probably due to a change of intensity of reflected infrared radiation from the vegetation growing in the soil derived from the diabase. It is suggested that this technique might be applied to other areas of eastern North America to determine outcrop patterns of the dikes in areas not yet geologically mapped.

Many problems currently exist concerning the diabase dikes which surround the North Atlantic Ocean such as dating, distribution and chemistry. It is hoped that more economic and efficient methods such as those suggested in this study will lead to the location of unmapped dikes, thus presenting a more complete picture of the distribution and role of these dikes in the history of the opening of the North Atlantic Ocean.

APPENDICES

APPENDIX I

GRAVITY SURVEYS AND DATA REDUCTION

Gravity data were collected and reduced by standard techniques (Dobrin, 1960). The data consist of 242 points in total including base stations - 201 gravity observations are along five detailed lines and 41 gravity observations are regional data.

The gravimeter used was the Worden Educator, Model 113. The reading precision of this meter, when read by a single operator, is approximately ± 0.1 milligals. Instrumental drift for the Worden gravimeter for an eight hour period is typically 0.2 milligals, but can be as high as 0.5 milligals for the same period. The gravimeter was stored in the field vehicle each night preceding a survey to minimize the instrumental drift due to temperature change. The uncertainty in drift and reading precision combined give a gravity precision of ± 0.2 milligals. In all, three different base stations (Dorman and Ziegler, in preparation, Georgia Department of Mines, Mining and Geology) were used to correct for instrumental drift. Pertinent data concerning these base stations are given in Table 1.

The observed drifts are given in Table 2.

Table 1. Gravity Base Stations Used in this Study

Name	Base Number	Location	Gravity Value	Estimated Precision
Atlanta D	4	Georgia Tech	979527.37	± 0.023
LaGrange	33	City Hall	979484.42	± 0.014
Greenville	63	Meriwether County Court House	979489.58	± 0.05

Table 2. Instrumental Drift for Worden Gravimeter

Station Nos.	Georgia Tech Gravity Survey No.	Drift (Mgals/hr)	Time Between Base Stations
1 - 49	36	-0.074	6.1 hours
1 - 33	46	-0.018	9.8
1 - 48	51	0.000	7.4
48 - 72	51	-0.109	3.9
72 - 95	51	0.016	2.3
4 - 20	52	-0.053	2.8
20 - 41	52	-0.121	3.8

The gravity data were corrected for latitude effect by using the international gravity formula of 1930 (as given in Dobrin, 1960, page 187) and drift corrections for the meter by assuming linear meter drift between subsequent occupations of the base station. The standard Bouguer reduction density of 2.67 gm/cm^3 was used to compute the Bouguer anomalies.

Elevation and location control were obtained from the following U. S. Geological Survey, $7\frac{1}{2}$ minute topographic maps: Greenville (1971), Gay (1971), Warm Springs (1971), and Woodbury (1971). Where possible bench marks (± 1 foot) or intersection elevations (assumed ± 5 feet) were used. Elevations of stations for which bench marks or intersections were not available were obtained by interpolating between contour lines (20 foot contour interval) and confirming those interpolations with barometric altimetry data. Elevations obtained by this technique were estimated to be plus or minus five feet. The resulting uncertainty in the reduced gravity values is thus ± 0.35 milligals. Because of the relatively shorter distance between stations along detail lines, and hence shorter times between gravity and barometric readings errors in drift for these measurements were considered less. This results in an estimated precision of ± 0.2 milligals for the reduced gravity values for stations along detail lines.

The data, in the standard Department of Defense computer card format, are listed by individual surveys in Table 3 (Figure 19).

SOURCE NO		TITLE				CODED BY		DATE CODED																					
SECURITY CLASS GEOGRAPHIC UNITS SIGN + = N - = S	LATITUDE	SIGN E W	LONGITUDE	TYPE UNITS SIGN	ELEVATION	ELEVATION	SUPPLEMENTAL ELEVATION	+9750000 OBSERVED GRAVITY	FREE AIR ANOMALY	SIGN BOUGUER ANOMALY (DENSITY 2.67)	ISO. OR T.C. SIGN	SOURCE	BASE REFERENCE STATION BASE REF SITE	SEQUENCE	FILE MAINTENANCE	FST STD. DEV. FREE AIR	EST STD. DEV. BOUGUER												
0 0 0 0 0 0 0 0 0 0 0	0 0 0 0 0 0 0 0 0 0	0 0 0 0 0 0 0 0 0 0	0 0 0 0 0 0 0 0 0 0	0 0 0 0 0 0 0 0 0 0	0 0 0 0 0 0 0 0 0 0	0 0 0 0 0 0 0 0 0 0	0 0 0 0 0 0 0 0 0 0	0 0 0 0 0 0 0 0 0 0	0 0 0 0 0 0 0 0 0 0	0 0 0 0 0 0 0 0 0 0	0 0 0 0 0 0 0 0 0 0	0 0 0 0 0 0 0 0 0 0	0 0 0 0 0 0 0 0 0 0	0 0 0 0 0 0 0 0 0 0	0 0 0 0 0 0 0 0 0 0	0 0 0 0 0 0 0 0 0 0	0 0 0 0 0 0 0 0 0 0												
1 2 3 4 5 6 7 8 9 10	11 12 13 14 15 16 17 18 19	20 21 22 23 24 25 26 27 28 29	30 31 32 33 34 35 36 37 38 39	40 41 42 43 44 45 46 47 48 49	50 51 52 53 54 55 56 57 58 59	60 61 62 63 64 65 66 67 68 69	70 71 72 73 74 75 76 77 78 79	80 81 82 83 84 85 86 87 88 89	90 91 92 93 94 95 96 97 98 99	0 0 0 0 0 0 0 0 0 0	0 0 0 0 0 0 0 0 0 0	0 0 0 0 0 0 0 0 0 0	0 0 0 0 0 0 0 0 0 0	0 0 0 0 0 0 0 0 0 0	0 0 0 0 0 0 0 0 0 0	0 0 0 0 0 0 0 0 0 0	0 0 0 0 0 0 0 0 0 0	0 0 0 0 0 0 0 0 0 0											
1 1 1 1 1 1 1 1 1 1	1 1 1 1 1 1 1 1 1 1	1 1 1 1 1 1 1 1 1 1	1 1 1 1 1 1 1 1 1 1	1 1 1 1 1 1 1 1 1 1	1 1 1 1 1 1 1 1 1 1	1 1 1 1 1 1 1 1 1 1	1 1 1 1 1 1 1 1 1 1	1 1 1 1 1 1 1 1 1 1	1 1 1 1 1 1 1 1 1 1	1 1 1 1 1 1 1 1 1 1	1 1 1 1 1 1 1 1 1 1	1 1 1 1 1 1 1 1 1 1	1 1 1 1 1 1 1 1 1 1	1 1 1 1 1 1 1 1 1 1	1 1 1 1 1 1 1 1 1 1	1 1 1 1 1 1 1 1 1 1	1 1 1 1 1 1 1 1 1 1												
2 2 2 2 2 2 2 2 2 2	2 2 2 2 2 2 2 2 2 2	2 2 2 2 2 2 2 2 2 2	2 2 2 2 2 2 2 2 2 2	2 2 2 2 2 2 2 2 2 2	2 2 2 2 2 2 2 2 2 2	2 2 2 2 2 2 2 2 2 2	2 2 2 2 2 2 2 2 2 2	2 2 2 2 2 2 2 2 2 2	2 2 2 2 2 2 2 2 2 2	2 2 2 2 2 2 2 2 2 2	2 2 2 2 2 2 2 2 2 2	2 2 2 2 2 2 2 2 2 2	2 2 2 2 2 2 2 2 2 2	2 2 2 2 2 2 2 2 2 2	2 2 2 2 2 2 2 2 2 2	2 2 2 2 2 2 2 2 2 2	2 2 2 2 2 2 2 2 2 2												
3 3 3 3 3 3 3 3 3 3	3 3 3 3 3 3 3 3 3 3	3 3 3 3 3 3 3 3 3 3	3 3 3 3 3 3 3 3 3 3	3 3 3 3 3 3 3 3 3 3	3 3 3 3 3 3 3 3 3 3	3 3 3 3 3 3 3 3 3 3	3 3 3 3 3 3 3 3 3 3	3 3 3 3 3 3 3 3 3 3	3 3 3 3 3 3 3 3 3 3	3 3 3 3 3 3 3 3 3 3	3 3 3 3 3 3 3 3 3 3	3 3 3 3 3 3 3 3 3 3	3 3 3 3 3 3 3 3 3 3	3 3 3 3 3 3 3 3 3 3	3 3 3 3 3 3 3 3 3 3	3 3 3 3 3 3 3 3 3 3	3 3 3 3 3 3 3 3 3 3												
4 4 4 4 4 4 4 4 4 4	4 4 4 4 4 4 4 4 4 4	4 4 4 4 4 4 4 4 4 4	4 4 4 4 4 4 4 4 4 4	4 4 4 4 4 4 4 4 4 4	4 4 4 4 4 4 4 4 4 4	4 4 4 4 4 4 4 4 4 4	4 4 4 4 4 4 4 4 4 4	4 4 4 4 4 4 4 4 4 4	4 4 4 4 4 4 4 4 4 4	4 4 4 4 4 4 4 4 4 4	4 4 4 4 4 4 4 4 4 4	4 4 4 4 4 4 4 4 4 4	4 4 4 4 4 4 4 4 4 4	4 4 4 4 4 4 4 4 4 4	4 4 4 4 4 4 4 4 4 4	4 4 4 4 4 4 4 4 4 4	4 4 4 4 4 4 4 4 4 4												
5 5 5 5 5 5 5 5 5 5	5 5 5 5 5 5 5 5 5 5	5 5 5 5 5 5 5 5 5 5	5 5 5 5 5 5 5 5 5 5	5 5 5 5 5 5 5 5 5 5	5 5 5 5 5 5 5 5 5 5	5 5 5 5 5 5 5 5 5 5	5 5 5 5 5 5 5 5 5 5	5 5 5 5 5 5 5 5 5 5	5 5 5 5 5 5 5 5 5 5	5 5 5 5 5 5 5 5 5 5	5 5 5 5 5 5 5 5 5 5	5 5 5 5 5 5 5 5 5 5	5 5 5 5 5 5 5 5 5 5	5 5 5 5 5 5 5 5 5 5	5 5 5 5 5 5 5 5 5 5	5 5 5 5 5 5 5 5 5 5	5 5 5 5 5 5 5 5 5 5												
6 6 6 6 6 6 6 6 6 6	6 6 6 6 6 6 6 6 6 6	6 6 6 6 6 6 6 6 6 6	6 6 6 6 6 6 6 6 6 6	6 6 6 6 6 6 6 6 6 6	6 6 6 6 6 6 6 6 6 6	6 6 6 6 6 6 6 6 6 6	6 6 6 6 6 6 6 6 6 6	6 6 6 6 6 6 6 6 6 6	6 6 6 6 6 6 6 6 6 6	6 6 6 6 6 6 6 6 6 6	6 6 6 6 6 6 6 6 6 6	6 6 6 6 6 6 6 6 6 6	6 6 6 6 6 6 6 6 6 6	6 6 6 6 6 6 6 6 6 6	6 6 6 6 6 6 6 6 6 6	6 6 6 6 6 6 6 6 6 6													
7 7 7 7 7 7 7 7 7 7	7 7 7 7 7 7 7 7 7 7	7 7 7 7 7 7 7 7 7 7	7 7 7 7 7 7 7 7 7 7	7 7 7 7 7 7 7 7 7 7	7 7 7 7 7 7 7 7 7 7	7 7 7 7 7 7 7 7 7 7	7 7 7 7 7 7 7 7 7 7	7 7 7 7 7 7 7 7 7 7	7 7 7 7 7 7 7 7 7 7	7 7 7 7 7 7 7 7 7 7	7 7 7 7 7 7 7 7 7 7	7 7 7 7 7 7 7 7 7 7	7 7 7 7 7 7 7 7 7 7	7 7 7 7 7 7 7 7 7 7	7 7 7 7 7 7 7 7 7 7	7 7 7 7 7 7 7 7 7 7													
8 8 8 8 8 8 8 8 8 8	8 8 8 8 8 8 8 8 8 8	8 8 8 8 8 8 8 8 8 8	8 8 8 8 8 8 8 8 8 8	8 8 8 8 8 8 8 8 8 8	8 8 8 8 8 8 8 8 8 8	8 8 8 8 8 8 8 8 8 8	8 8 8 8 8 8 8 8 8 8	8 8 8 8 8 8 8 8 8 8	8 8 8 8 8 8 8 8 8 8	8 8 8 8 8 8 8 8 8 8	8 8 8 8 8 8 8 8 8 8	8 8 8 8 8 8 8 8 8 8	8 8 8 8 8 8 8 8 8 8	8 8 8 8 8 8 8 8 8 8	8 8 8 8 8 8 8 8 8 8	8 8 8 8 8 8 8 8 8 8													
9 9 9 9 9 9 9 9 9 9	9 9 9 9 9 9 9 9 9 9	9 9 9 9 9 9 9 9 9 9	9 9 9 9 9 9 9 9 9 9	9 9 9 9 9 9 9 9 9 9	9 9 9 9 9 9 9 9 9 9	9 9 9 9 9 9 9 9 9 9	9 9 9 9 9 9 9 9 9 9	9 9 9 9 9 9 9 9 9 9	9 9 9 9 9 9 9 9 9 9	9 9 9 9 9 9 9 9 9 9	9 9 9 9 9 9 9 9 9 9	9 9 9 9 9 9 9 9 9 9	9 9 9 9 9 9 9 9 9 9	9 9 9 9 9 9 9 9 9 9	9 9 9 9 9 9 9 9 9 9	9 9 9 9 9 9 9 9 9 9													
1 1 4 5 6 7 8 9 10	11 12 13 14 15 16 17 18 19	20 21 22 23 24 25 26 27 28 29	30 31 32 33 34 35 36 37 38 39	40 41 42 43 44 45 46 47 48 49	50 51 52 53 54 55 56 57 58 59	60 61 62 63 64 65 66 67 68 69	70 71 72 73 74 75 76 77 78 79	80 81 82 83 84 85 86 87 88 89	90 91 92 93 94 95 96 97 98 99	0 0 0 0 0 0 0 0 0 0	0 0 0 0 0 0 0 0 0 0	0 0 0 0 0 0 0 0 0 0	0 0 0 0 0 0 0 0 0 0	0 0 0 0 0 0 0 0 0 0	0 0 0 0 0 0 0 0 0 0	0 0 0 0 0 0 0 0 0 0	0 0 0 0 0 0 0 0 0 0	0 0 0 0 0 0 0 0 0 0											
CODES USED IN ABOVE										TYPE OF ELEVATION (Col. 21)										ELEVATION OF STATION (Col. 23-29)									
SECURITY CLASS (Col. 1)										1 - LAND 2 - SUBSURFACE 3 - OCEAN SURFACE 4 - OCEAN SUBMERGED 5 - OCEAN BOTTOM 6 - LAKE SURFACE (ABOVE SEA LEVEL) 7 - LAKE BOTTOM (ABOVE SEA LEVEL) 8 - LAKE BOTTOM (BELOW SEA LEVEL) 9 - LAKE SURFACE (ABOVE SEA LEVEL) WITH LAKE BOTTOM BELOW SEA LEVEL A - LAKE SURFACE (BELOW SEA LEVEL) B - LAKE BOTTOM (SURFACE BELOW SEA LEVEL) C - ICE CAP (BOTTOM BELOW SEA LEVEL) D - ICE CAP (BOTTOM ABOVE SEA LEVEL) E - TRANSFER DATA GIVEN										NOTE: THIS FIELD WILL CONTAIN DEPTH OF OCEAN (POSITIVE DOWNWARD) IF COL 21 CONTAINS 3, 4, OR 5									
SECURITY CONTROL (Col. 2)										SUPPLEMENTAL ELEVATION (Col. 31-35) DEPTH OF INSTRUMENT, LAKE OR ICE; POSITIVE DOWNWARD FROM SURFACE										BOUGUER ANOMALY (Col. 50-54) SIMPLE BOUGUER ANOMALY WITH A MEAN DENSITY OF 2.67. NO TERRAIN CORRECTION									
U - UNCLASSIFIED MATERIAL F - FOR OFFICIAL USE ONLY C - CONFIDENTIAL S - SECRET										ISO. OR T.C. CODE (Col. 56)										INDICATES IF ISOSTATIC ANOMALY OR TERRAIN CORRECTION IS GIVEN IN DOCUMENT: 0 - NO ISOSTATIC ANOM. OR T.C. IN DOCUMENT 1 - TERRAIN CORRECTION GIVEN IN DOCUMENT 2 - ISOSTATIC ANOMALY GIVEN IN DOCUMENT 3 - BOTH ARE GIVEN IN DOCUMENT									
GEOGRAPHIC UNITS (Col. 3)										ELEVATION UNITS (Col. 22) BLANK OR 0 - DEGREES AND MINUTES TO .01 MINUTE 1 - DEGREES, MINUTES AND SECONDS 2 - DEGREES TO .0001 DEGREE																			

ACIC HQ FORM 0-154
NOV 66

PREVIOUS EDITION OF THIS FORM WILL BE USED UNTIL STOCK IS EXHAUSTED

DoD GR

Figure 19. Standard Department of Defense Gravity Coding Form.

Table 3. Gravity Data

Gravity Survey GT 36 (Includes Data for Profile B-B')

12345678901234567890123456789012345678901234567890123456789012345678901234567890						
334640	- 842370	1	2984	3527367-	2305-	5633
332121	- 844745	1	3064	3510125-	295-	3714
33 240	- 85 180	1	2353	3484422-	2473-	5n97
33 172	- 844278	1	2651	3489586-	944-	3901
33 178	- 844232	1	2426	3498070-	798-	3504
33 184	- 844217	1	2369	3498750-	913-	3556
33 197	- 844195	1	2499	3496398-	763-	3551
33 203	- 844178	1	2606	3494070-	674-	3581
33 214	- 844164	1	2554	3495086-	749-	3598
33 228	- 844147	1	2579	3494789-	721-	3598
33 244	- 844133	1	2569	3495625-	689-	3555
33 253	- 844222	1	2612	3495133-	619-	3533
33 260	- 844105	1	2566	3496102-	673-	3536
33 267	- 844086	1	2600	3496102-	579-	3479
33 272	- 844066	1	2615	3495281-	621-	3538
33 273	- 844057	1	2606	3495492-	630-	3537
33 274	- 844046	1	2591	3495961-	631-	3521
33 277	- 844037	1	2569	3496383-	658-	3524
33 280	- 844028	1	2582	3495664-	696-	3576
33 284	- 844020	1	2597	3495758-	646-	3543
33 289	- 844013	1	2572	3495758-	731-	3599
33 295	- 844004	1	2575	3496531-	653-	3525
33 300	- 843995	1	2573	3496609-	656-	3526
33 304	- 843987	1	2569	3497555-	579-	3445
33 309	- 843978	1	2544	3498188-	601-	3439
33 312	- 843975	1	2556	3498367-	550-	3401
33 314	- 843970	1	2567	3498375-	518-	3382
33 317	- 843965	1	2557	3498461-	544-	3396
33 319	- 843962	1	2545	3498766-	553-	3392
33 323	- 843951	1	2532	3498891-	587-	3411
33 326	- 843942	1	2566	3498438-	530-	3393
33 328	- 843932	1	2557	3498391-	566-	3419
33 330	- 843923	1	2552	3498898-	533-	3380
33 331	- 843913	1	2566	3498391-	542-	3405
33 332	- 843905	1	2571	3498383-	530-	3398
33 333	- 843895	1	2565	3498375-	550-	3412
33 335	- 843886	1	2536	3499016-	579-	3408
33 337	- 843877	1	2512	3499008-	656-	3458
33 339	- 843858	1	2530	3498867-	617-	3439
33 341	- 843833	1	2536	3498219-	666-	3495
33 346	- 843818	1	2472	3499664-	726-	3484
33 356	- 843801	1	2502	3499086-	704-	3496
33 363	- 843784	1	2518	3498961-	678-	3487
33 450	- 843679	1	2286	3505477-	862-	3412
33 563	- 843447	1	2536	3501578-	635-	3464
33 314	- 843970	1	2567	3498273-	527-	3391
33 178	- 844232	1	2426	3497859-	819-	3525
33 172	- 844278	1	2651	3489586-	944-	3901
33 240	- 85 180	1	2353	3484422-	2473-	5n97
33 172	- 844278	1	2651	3489445-	957-	3914
33 240	- 85 180	1	2353	3484422-	2473-	5n97
332121	- 844745	1	3064	3510680-	239-	3658
334640	- 842370	1	2984	3527367-	2305-	5633

12345678901234567890123456789012345678901234567890123456789012345678901234567890

Table 3. (Continued)

Gravity Survey GT 46 (Includes Data for Profile E-E')

12345678901234567890123456789012345678901234567890123456789012345678901234567890
 334640 - 842370 1 2984 3527367- 2305- 5633 GT46 GA 4 1 1
 332248 - 844802 1 3051 3510453- 480- 3883 GT46 GA 4 2 1
 331998 - 844812 1 2950 3511008- 389- 3680 GT46 GA 4 3 1
 331976 - 844685 1 2962 3511320- 292- 3596 GT46 GA 4 4 5
 331984 - 844627 1 2936 3511828- 333- 3608 GT46 GA 4 5 5
 331989 - 844591 1 2819 3513875- 494- 3639 GT46 GA 4 6 5
 331992 - 844566 1 2850 3513836- 407- 3587 GT46 GA 4 7 5
 331998 - 844537 1 2841 3514570- 372- 3540 GT46 GA 4 8 5
 332008 - 844507 1 2743 3516547- 487- 3547 GT46 GA 4 9 3
 332011 - 844498 1 2771 3516047- 458- 3549 GT46 GA 4 10 5
 332016 - 844475 1 2751 3516781- 450- 3519 GT46 GA 4 11 3
 332016 - 844467 1 2733 3517211- 464- 3512 GT46 GA 4 12 3
 332017 - 844458 1 2719 3517945- 436- 3468 GT46 GA 4 13 3
 332017 - 844448 1 2682 3518734- 469- 3461 GT46 GA 4 14 3
 332017 - 844440 1 2643 3519023- 561- 3509 GT46 GA 4 15 5
 332017 - 844431 1 2682 3518773- 465- 3457 GT46 GA 4 16 3
 332017 - 844427 1 2686 3518969- 436- 3431 GT46 GA 4 17 5
 332016 - 844423 1 2640 3520055- 466- 3411 GT46 GA 4 18 3
 332015 - 844413 1 2608 3520563- 513- 3422 GT46 GA 4 19 3
 332013 - 844406 1 2585 3520406- 598- 3481 GT46 GA 4 20 5
 332012 - 844395 1 2560 3520695- 643- 3499 GT46 GA 4 21 5
 332012 - 844383 1 2541 3521008- 671- 3506 GT46 GA 4 22 5
 332012 - 844374 1 2587 3519969- 634- 3520 GT46 GA 4 23 5
 332012 - 844354 1 2621 3520438- 480- 3404 GT46 GA 4 24 3
 332012 - 844343 1 2545 3521133- 646- 3485 GT46 GA 4 25 5
 332007 - 844310 1 2509 3521750- 690- 3488 GT46 GA 4 26 5
 332001 - 844277 1 2414 3523875- 762- 3455 GT46 GA 4 27 5
 331996 - 844252 1 2399 3523305- 858- 3534 GT46 GA 4 28 5
 331992 - 844152 1 2649 3517711- 641- 3596 GT46 GA 4 29 5
 332036 - 844107 1 2682 3519266- 443- 3435 GT46 GA 4 30 3
 332013 - 844406 1 2585 3520094- 629- 3512 GT46 GA 4 31 5
 332248 - 844802 1 3051 3510063- 518- 3921 GT46 GA 4 32 1
 334640 - 842370 1 2984 3527367- 2305- 5633 GT46 GA 4 33 1
 12345678901234567890123456789012345678901234567890123456789012345678901234567890

Table 3. (Continued)

Gravity Survey GT 51 (Continued)

12345678901234567890123456789012345678901234567890123456789012345678901234567890												
33	390	-	843870	1	2509	3499047-	736-	3534	GT51	GA63	66	3
33	437	-	843877	1	2243	3504266-	1097-	3600	GT51	GA63	67	3
33	488	-	843875	1	2533	3499258-	773-	3599	GT51	GA63	68	3
33	488	-	843921	1	2505	3499273-	857-	3651	GT51	GA63	69	3
33	428	-	844073	1	2566	3497359-	778-	3641	GT51	GA63	70	3
33	344	-	844192	1	2643	3492906-	873-	3821	GT51	GA63	71	5
33	172	-	844278	1	2651	3489578-	944-	3901	GT51	GA63	72	1
33	272	-	844065	1	2615	3495016-	647-	3564	GT51	GA63	73	3
33	243	-	844018	1	2566	3495898-	670-	3533	GT51	GA63	74	3
33	194	-	844018	1	2502	3496789-	711-	3503	GT51	GA63	75	5
33	213	-	844000	1	2612	3495320-	545-	3459	GT51	GA63	76	5
33	216	-	843983	1	2573	3496477-	556-	3425	GT51	GA63	77	3
33	206	-	843961	1	2594	3496703-	453-	3347	GT51	GA63	78	5
33	194	-	843947	1	2539	3497164-	561-	3393	GT51	GA63	79	5
33	193	-	843936	1	2521	3498125-	520-	3331	GT51	GA63	80	5
33	193	-	843926	1	2493	3498859-	531-	3312	GT51	GA63	81	5
33	193	-	843917	1	2463	3499633-	547-	3294	GT51	GA63	82	5
33	193	-	843913	1	2454	3498625-	676-	3413	GT51	GA63	83	5
33	193	-	843900	1	2454	3499008-	638-	3375	GT51	GA63	84	5
33	193	-	843882	1	2463	3499086-	602-	3349	GT51	GA63	85	5
33	192	-	843872	1	2441	3499086-	667-	3390	GT51	GA63	86	5
33	189	-	843862	1	2441	3499008-	670-	3393	GT51	GA63	87	5
33	192	-	843846	1	2402	3499617-	735-	3414	GT51	GA63	88	5
33	192	-	843826	1	2323	3501313-	811-	3402	GT51	GA63	89	5
33	192	-	843803	1	2292	3502086-	827-	3384	GT51	GA63	90	5
33	192	-	843788	1	2335	3501813-	722-	3327	GT51	GA63	91	5
33	192	-	843762	1	2246	3504242-	753-	3259	GT51	GA63	92	5
33	191	-	843743	1	2164	3506484-	780-	3194	GT51	GA63	93	5
33	186	-	844214	1	2341	3498609-	1016-	3627	GT51	GA63	94	5
33	172	-	844278	1	2651	3489578-	944-	3901	GT51	GA63	95	1
33	233	-	844301	1	2618	3489883-	1098-	4018	GT51	GA63	96	3
33	393	-	844134	1	2627	3496133-	665-	3595	GT51	GA63	97	5
33	428	-	844073	1	2566	3497055-	808-	3671	GT51	GA63	98	3
33	433	-	844054	1	2560	3497398-	800-	3656	GT51	GA63	99	5
33	438	-	844035	1	2551	3498328-	741-	3587	GT51	GA63	100	3
33	440	-	844023	1	2573	3497711-	740-	3610	GT51	GA63	101	5
33	440	-	844019	1	2597	3497750-	662-	3559	GT51	GA63	102	5
33	442	-	844010	1	2560	3497977-	754-	3610	GT51	GA63	103	5
33	444	-	844005	1	2545	3498438-	759-	3598	GT51	GA63	104	5
33	449	-	843995	1	2545	3498750-	734-	3573	GT51	GA63	105	5
33	452	-	843985	1	2493	3499367-	836-	3618	GT51	GA63	106	5
33	458	-	843967	1	2542	3498438-	787-	3622	GT51	GA63	107	5
33	469	-	843951	1	2542	3497664-	879-	3714	GT51	GA63	108	5
33	481	-	843939	1	2548	3498664-	776-	3619	GT51	GA63	109	5
33	427	-	844106	1	2563	3496039-	918-	3777	GT51	GA63	110	5
33	497	-	844063	1	2390	3501133-	1041-	3706	GT51	GA63	111	5
33	540	-	844052	1	2280	3503750-	1177-	3720	GT51	GA63	112	5
33	579	-	844039	1	2481	3500125-	972-	3740	GT51	GA63	113	3
33	623	-	843998	1	2265	3504367-	1277-	3803	GT51	GA63	114	5
334640	-	842370	1	2984	3527367-	2305-	5633	GT51	GA63	115	1	

1234567890123456789012345678901234567890123456789012345678901234567890

Table 3. (Concluded)

Gravity Survey GT 52 (Regional Data)

APPENDIX II

GROUND LEVEL MAGNETIC SURVEYS AND DATA REDUCTION

Measurements of the magnitude of the geomagnetic field were made using a Geometrics Model G-816 proton-precession magnetometer. The digital display has a resolution of ± 1 gamma. The sensing element of the magnetometer is held at the end of an eight foot aluminum staff to suppress the magnetic effects of iron debris, e.g., beverage cans, small underground pipes, etc.

The data were reduced using standard techniques (Dobrin, 1960). The data consist of three detailed lines along graded dirt roads and a fourth along a two lane asphalt highway (Georgia State Highway 109). Approximately 0.016 kilometer was paced off between stations. Division of the actual length of the profile line by the number of station intervals yielded the actual station spacing. Times, needed for drift corrections, were recorded every ten minutes and the stations between time readings were assigned a time by assuming a linear sampling rate.

The variation in the main field over the area of investigation has been removed by approximating a gradient of $8.45\text{y}/\text{mile}$ at $N3^{\circ}\text{W}$ (Garland, 1971, Figure 17.2) by a simple latitude correction of $9.56\text{y}/\text{minute}$. Corrections for the diurnal variation were made using magneto-grams of the Geomagnetic Observatory in Fredericksburg, Virginia (Figures 20 and 21) which were obtained from the World Data Center A of the National Oceanographic and Atmospheric Administration in

Boulder, Colorado.

These records were digitized and the vertical and horizontal components were added vectorily to give the magnitude of the total field. The difference between the computed total field and the value for the base line was taken to be the diurnal variation in the total field at Fredericksburg. Since the diurnal drift at any one place on the earth has been shown to be directly related to the hour angle of the sun (Matshusita and Campbell, 1965, Chapter 3) a shift of twenty-eight minutes was made in the drift curve so that it could be applied to the area of investigation. The variation of the diurnal drift with respect to latitude is negligible for the difference between Fredericksburg, Virginia and Greenville, Georgia (see Matshusita and Campbell, 1965, Figure 8, pages 321-323).

The computed latitude and longitude, time (Eastern Daylight Savings), raw magnetic value and corrected total magnetic field for each station occupied are given in Table 4.

NOAA
FREDERICKSBURG, VA.
MAY 5 1973

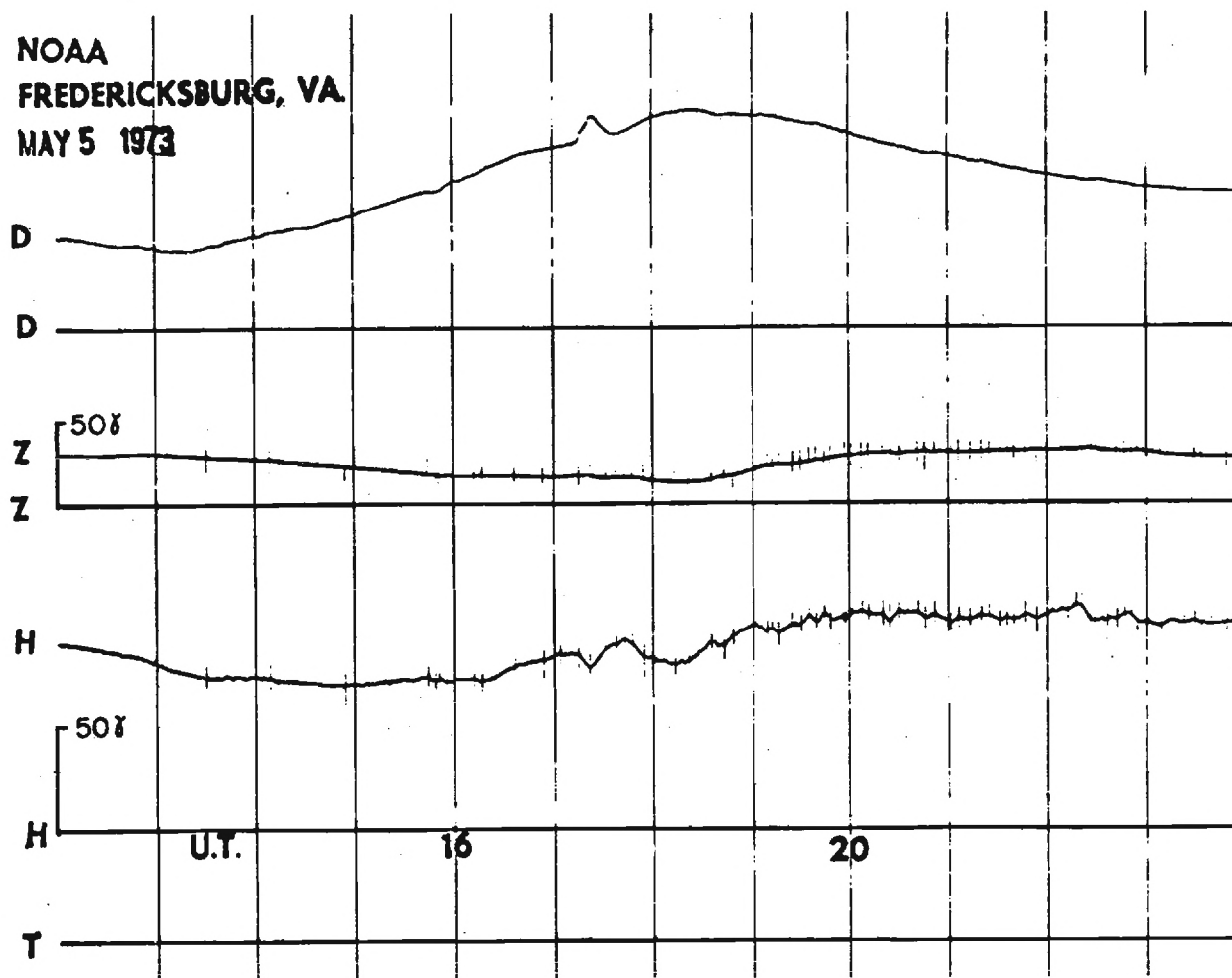


Figure 20. Magnetogram for May 5, 1973. (Courtesy National Oceanographic and Atmospheric Administration.

NOAA
FREDERICKSBURG, VA.

MAY 6 1973

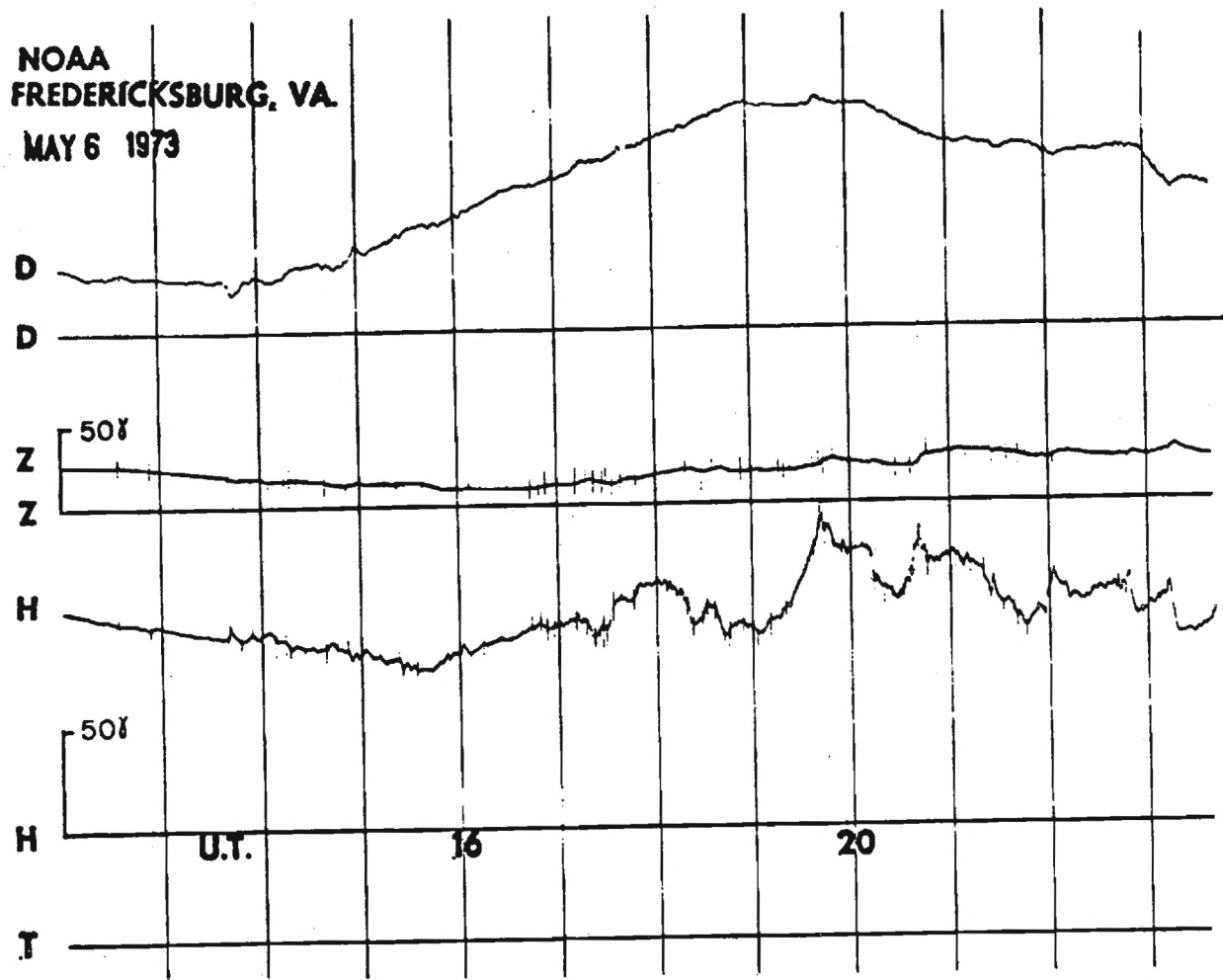


Figure 21. Magnetogram for May 6, 1973. (Courtesy National Oceanographic and Atmospheric Administration.

Table 4. Ground-Level Magnetics

Profile A-A', May 5, 1973

LATITUDE	LONGITUDE	TIME	RAW	REDUCED	LATITUDE	LONGITUDE	TIME	RAW	REDUCED
12345678901234567890123456789012345678901234567890	12345678901234567890123456789012345678901234567890				12345678901234567890123456789012345678901234567890	12345678901234567890123456789012345678901234567890			
33 3.030	84 42.670	15.483	53594	53631	33 3.477	84 41.493	16.345	53605	53644
33 3.078	84 42.673	15.495	53586	53622	33 3.488	84 41.481	16.357	53605	53645
33 3.126	84 42.676	15.507	53584	53620	33 3.500	84 41.468	16.368	53617	53657
33 3.174	84 42.680	15.518	53590	53625	33 3.511	84 41.456	16.380	53593	53633
33 3.222	84 42.683	15.530	53598	53633	33 3.523	84 41.444	16.392	53533	53573
33 3.270	84 42.686	15.542	53584	53623	33 3.534	84 41.432	16.403	53617	53657
33 3.318	84 42.689	15.553	53609	53643	33 3.546	84 41.420	16.415	53622	53662
33 3.366	84 42.693	15.565	53603	53637	33 3.558	84 41.408	16.427	53625	53665
33 3.414	84 42.696	15.577	53618	53651	33 3.569	84 41.395	16.438	53627	53667
33 3.461	84 42.699	15.588	53625	53658	33 3.581	84 41.383	16.450	53609	53649
33 3.509	84 42.702	15.600	53632	53665	33 3.592	84 41.371	16.462	53622	53662
33 3.557	84 42.706	15.613	53630	53662	33 3.604	84 41.359	16.473	53702	53743
33 3.605	84 42.709	15.627	53636	53668	33 3.610	84 41.353	16.479	53721	53762
33 3.653	84 42.712	15.640	53640	53671	33 3.615	84 41.347	16.485	53709	53750
33 3.701	84 42.715	15.653	53586	53617	33 3.621	84 41.340	16.491	53705	53746
33 3.749	84 42.719	15.667	53616	53647	33 3.627	84 41.334	16.497	53699	53740
33 3.797	84 42.722	15.680	53617	53647	33 3.638	84 41.322	16.508	53667	53708
33 3.845	84 42.725	15.693	53571	53601	33 3.650	84 41.310	16.520	53581	53622
33 3.891	84 42.706	15.707	53594	53624	33 3.657	84 41.310	16.526	53647	53687
33 3.757	84 42.686	15.720	53569	53599	33 3.665	84 41.310	16.532	53629	53669
33 3.713	84 42.667	15.733	53595	53626	33 3.680	84 41.309	16.543	53616	53656
33 3.669	84 42.647	15.747	53604	53635	33 3.694	84 41.309	16.555	53601	53641
33 3.625	84 42.628	15.761	53606	53637	33 3.709	84 41.308	16.567	53589	53629
33 3.603	84 42.618	15.768	53607	53639	33 3.724	84 41.308	16.576	53583	53623
33 3.581	84 42.608	15.775	53802	53834	33 3.739	84 41.307	16.586	53587	53627
33 3.559	84 42.598	15.782	53604	53636	33 3.753	84 41.307	16.595	53579	53619
33 3.537	84 42.589	15.789	53612	53644	33 3.768	84 41.306	16.605	53584	53623
33 3.493	84 42.569	15.803	53613	53645	33 3.783	84 41.306	16.614	53602	53641
33 3.449	84 42.550	15.817	53635	53668	33 3.798	84 41.305	16.624	53593	53632
33 3.405	84 42.530	15.833	53612	53645	33 3.812	84 41.305	16.633	53620	53659
33 3.407	84 42.500	15.850	53618	53651	33 3.827	84 41.305	16.647	53656	53695
33 3.409	84 42.470	15.867	53617	53650	33 3.835	84 41.304	16.653	53741	53779
33 3.410	84 42.440	15.883	53617	53650	33 3.842	84 41.304	16.660	53821	53859
33 3.412	84 42.409	15.900	53615	53648	33 3.849	84 41.304	16.667	53825	53863
33 3.414	84 42.379	15.917	53624	53658	33 3.857	84 41.304	16.673	53840	53878
33 3.416	84 42.349	15.926	53605	53639	33 3.864	84 41.303	16.680	53786	53824
33 3.417	84 42.319	15.935	53608	53643	33 3.872	84 41.303	16.687	53760	53798
33 3.419	84 42.289	15.944	53600	53635	33 3.879	84 41.303	16.693	53710	53748
33 3.421	84 42.259	15.953	53605	53640	33 3.886	84 41.303	16.700	53633	53671
33 3.423	84 42.229	15.962	53590	53626	33 3.894	84 41.303	16.707	53679	53717
33 3.424	84 42.198	15.971	53608	53644	33 3.901	84 41.302	16.714	53594	53632
33 3.426	84 42.168	15.979	53600	53636	33 3.909	84 41.302	16.722	53644	53681
33 3.428	84 42.138	15.988	53593	53629	33 3.916	84 41.302	16.729	53640	53677
33 3.430	84 42.108	15.997	53615	53652	33 3.923	84 41.302	16.736	53574	53611
33 3.431	84 42.078	16.006	53607	53644	33 3.931	84 41.301	16.743	53495	53532
33 3.433	84 42.048	16.015	53607	53644	33 3.938	84 41.301	16.750	5358A	53625
33 3.435	84 42.018	16.024	53607	53644	33 3.945	84 41.301	16.758	53635	53672
33 3.437	84 41.987	16.033	53626	53663	33 3.953	84 41.301	16.765	53682	53719
33 3.439	84 41.957	16.053	53636	53674	33 3.960	84 41.300	16.772	53604	53641
33 3.440	84 41.927	16.072	53666	53698	33 3.968	84 41.300	16.779	53603	53640
33 3.441	84 41.912	16.082	53655	53693	33 3.975	84 41.300	16.786	53620	53656
33 3.443	84 41.882	16.101	53655	53694	33 3.982	84 41.294	16.794	53581	53617
33 3.445	84 41.852	16.121	53644	53682	33 3.988	84 41.289	16.801	53587	53623
33 3.446	84 41.837	16.131	53635	53673	33 4.002	84 41.277	16.815	53593	53629
33 3.447	84 41.806	16.150	53629	53667	33 4.015	84 41.266	16.830	53574	53610
33 3.449	84 41.776	16.161	53639	53677	33 4.029	84 41.255	16.844	53633	53668
33 3.451	84 41.746	16.172	53619	53658	33 4.042	84 41.243	16.858	53625	53660
33 3.453	84 41.716	16.183	53694	53733	33 4.055	84 41.232	16.873	53666	53701
33 3.454	84 41.686	16.194	53617	53656	33 4.069	84 41.220	16.887	53637	53672
33 3.455	84 41.656	16.206	53607	53646	33 4.082	84 41.209	16.902	53601	53636
33 3.458	84 41.626	16.217	53603	53642	33 4.096	84 41.198	16.916	53561	53599
33 3.460	84 41.595	16.246	53616	53655	33 4.109	84 41.186	16.930	53563	53601
33 3.461	84 41.565	16.275	53601	53640	33 4.122	84 41.175	16.945	53567	53603
33 3.463	84 41.535	16.304	53587	53626	33 4.136	84 41.164	16.959	53574	53612
33 3.465	84 41.505	16.333	53604	53643	33 4.149	84 41.152	16.973	53343	53379
1234567890123456789012345678901234567890					1234567890123456789012345678901234567890				

Table 4. (Continued)

Profile A-A' (Continued)

LATITUDE LONGITUDE TIME RAW REDUCED
1234567890123456789012345678901234567890
33 4.163 84 41.141 16.988 53597 53633
33 4.176 84 41.130 17.002 53592 53628
33 4.190 84 41.118 17.017 53595 53631
33 4.203 84 41.107 17.029 53591 53627
33 4.216 84 41.095 17.042 53593 53628
33 4.230 84 41.084 17.054 53610 53645
33 4.243 84 41.073 17.067 53589 53624
33 4.257 84 41.061 17.367 53605 53639
33 4.263 84 41.056 17.372 53602 53636
33 4.270 84 41.050 17.378 53604 53638
33 4.268 84 41.030 17.389 53593 53627
33 4.266 84 41.010 17.401 53585 53619
33 4.264 84 40.990 17.412 53506 53540
33 4.262 84 40.970 17.424 53595 53629
33 4.260 84 40.950 17.435 53594 53632
33 4.258 84 40.930 17.446 53605 53639
33 4.256 84 40.910 17.458 53594 53628
33 4.254 84 40.890 17.469 53605 53639
33 4.252 84 40.870 17.481 53605 53639
33 4.250 84 40.850 17.492 53557 53591
33 4.255 84 40.832 17.504 53589 53623
33 4.260 84 40.814 17.515 53612 53646
33 4.265 84 40.796 17.526 53618 53652
33 4.270 84 40.779 17.538 53621 53655
33 4.275 84 40.761 17.549 53616 53650
33 4.280 84 40.743 17.561 53613 53647
33 4.285 84 40.725 17.572 53614 53647
33 4.290 84 40.706 17.583 53609 53642
33 4.295 84 40.687 17.596 53608 53641
33 4.301 84 40.668 17.608 53615 53648
33 4.306 84 40.649 17.621 53622 53655
33 4.311 84 40.631 17.633 53626 53659
33 4.316 84 40.612 17.646 5362A 53661
33 4.321 84 40.593 17.658 53624 53657
33 4.326 84 40.574 17.671 53629 53662
33 4.332 84 40.555 17.683 53624 53657
33 4.337 84 40.536 17.696 53654 53688
33 4.342 84 40.517 17.708 53651 53685
33 4.347 84 40.498 17.723 53636 53670
33 4.352 84 40.479 17.733 53667 53701
33 4.355 84 40.470 17.741 53695 53729
33 4.357 84 40.460 17.749 53764 53A02
33 4.358 84 40.449 17.757 53631 53665
33 4.360 84 40.439 17.761 53644 53678
33 4.363 84 40.418 17.780 53657 53691
33 4.367 84 40.397 17.796 53689 53723
33 4.368 84 40.387 17.803 53734 53768
33 4.370 84 40.377 17.811 53732 53766
33 4.372 84 40.366 17.819 53650 53684
33 4.373 84 40.356 17.827 53673 53707
33 4.375 84 40.346 17.834 53655 53689
33 4.377 84 40.335 17.842 53659 53693
33 4.378 84 40.325 17.850 53666 53700
33 4.382 84 40.304 17.864 53676 53710
33 4.385 84 40.283 17.877 53707 53741
33 4.388 84 40.263 17.891 53719 53753
33 4.392 84 40.242 17.905 53749 53783
33 4.393 84 40.231 17.912 53784 53A18
33 4.395 84 40.221 17.919 53852 53A86
33 4.397 84 40.211 17.925 53849 53A83
33 4.398 84 40.200 17.932 53922 53956
33 4.400 84 40.190 17.939 53965 53999
33 4.403 84 40.181 17.946 54111 54145
33 4.407 84 40.171 17.953 54592 54626
33 4.410 84 40.162 17.960 54246 54280
1234567890123456789012345678901234567890

LATITUDE LONGITUDE TIME RAW REDUCED
1234567890123456789012345678901234567890
33 4.413 84 40.153 17.967 54096 54130
33 4.416 84 40.144 17.976 53488 53522
33 4.420 84 40.134 17.985 54541 54575
33 4.423 84 40.125 17.994 53550 53584
33 4.426 84 40.116 18.003 53564 53598
33 4.429 84 40.107 18.012 53587 53621
33 4.433 84 40.097 18.021 53599 53633
33 4.436 84 40.088 18.030 53623 53657
33 4.439 84 40.079 18.039 53602 53636
33 4.443 84 40.069 18.048 53637 53671
33 4.446 84 40.060 18.058 53726 53760
33 4.449 84 40.051 18.067 53979 54013
33 4.452 84 40.042 18.072 53453 53487
33 4.456 84 40.032 18.077 53483 53517
33 4.459 84 40.023 18.083 53505 53539
33 4.462 84 40.014 18.088 53511 53545
33 4.465 84 40.005 18.093 53513 53547
33 4.469 84 39.995 18.099 53517 53551
33 4.472 84 39.986 18.104 53515 53549
33 4.479 84 39.967 18.115 53524 53558
33 4.485 84 39.949 18.126 53536 53570
33 4.492 84 39.930 18.136 53540 53574
33 4.498 84 39.912 18.147 53554 53588
33 4.505 84 39.893 18.158 53561 53595
33 4.511 84 39.875 18.168 53554 53588
33 4.518 84 39.856 18.179 5355A 53592
33 4.524 84 39.838 18.190 5355A 53592
33 4.531 84 39.819 18.201 53600 53634
33 4.534 84 39.810 18.206 53561 53595
33 4.541 84 39.791 18.217 53596 53629
33 4.547 84 39.773 18.227 53587 53620
33 4.554 84 39.754 18.238 53581 53614
33 4.560 84 39.736 18.249 53593 53626
33 4.567 84 39.717 18.260 53583 53615
33 4.573 84 39.699 18.270 53584 53616
33 4.580 84 39.680 18.281 53543 53575
33 4.592 84 39.665 18.292 53560 53592
33 4.605 84 39.649 18.302 53574 53605
33 4.617 84 39.634 18.313 53582 53613
33 4.629 84 39.619 18.324 53595 53626
33 4.642 84 39.604 18.335 53587 53618
33 4.654 84 39.588 18.345 53592 53623
33 4.667 84 39.573 18.356 53586 53617
33 4.679 84 39.558 18.367 53584 53615
33 4.691 84 39.543 18.377 53590 53621
33 4.704 84 39.527 18.388 53584 53615
33 4.716 84 39.512 18.399 53581 53612
33 4.728 84 39.497 18.410 5358A 53619
33 4.741 84 39.482 18.420 53591 53622
33 4.753 84 39.466 18.431 53587 53618
33 4.766 84 39.451 18.442 53583 53614
33 4.778 84 39.436 18.452 53589 53620
33 4.790 84 39.421 18.463 53595 53626
33 4.803 84 39.405 18.474 53587 53618
33 4.815 84 39.390 18.485 5358n 53611
33 4.821 84 39.372 18.495 53612 53643
33 4.827 84 39.354 18.506 53589 53620
33 4.833 84 39.336 18.517 53573 53604
33 4.839 84 39.318 18.537 53581 53612
33 4.845 84 39.300 18.557 53577 53608
33 4.851 84 39.282 18.578 53575 53607
33 4.857 84 39.264 18.598 53581 53613
33 4.863 84 39.246 18.619 53582 53614
33 4.869 84 39.228 18.639 53584 53616
33 4.875 84 39.210 18.659 5354A 53580
1234567890123456789012345678901234567890

Table 4. (Continued)

Profile A-A' (Concluded)

LATITUDE	LONGITUDE	TIME	RAW	REDUCED
1234567890123456789012345678901234567890				
33 4.875	84 39.190	18.680	53549	53581
33 4.875	84 39.170	18.700	53564	53596
33 4.875	84 39.150	18.713	53611	53644
33 4.875	84 39.130	18.725	53614	53647
33 4.875	84 39.110	18.738	53583	53616
33 4.875	84 39.090	18.750	53588	53621
33 4.875	84 39.070	18.763	53584	53617
33 4.875	84 39.050	18.776	53594	53627
33 4.875	84 39.030	18.788	53571	53603
33 4.875	84 39.010	18.801	53565	53597
33 4.875	84 38.990	18.813	53557	53589
33 4.875	84 38.980	18.820	53612	53644
33 4.875	84 38.970	18.826	53701	53732
33 4.875	84 38.960	18.832	53587	53618
33 4.875	84 38.940	18.845	53637	53668
33 4.875	84 38.930	18.851	53602	53633
33 4.875	84 38.920	18.857	53822	53853
33 4.875	84 38.910	18.864	53697	53728
33 4.875	84 38.890	18.876	53610	53640
33 4.875	84 38.870	18.889	53716	53746
33 4.875	84 38.850	18.901	53559	53589
33 4.875	84 38.830	18.914	53647	53877
33 4.875	84 38.820	18.920	53770	53800
33 4.875	84 38.810	18.927	53852	53882
33 4.875	84 38.800	18.933	53760	53790
33 4.875	84 38.780	18.946	53698	53728
33 4.875	84 38.760	18.958	5392n	53950
33 4.875	84 38.740	18.971	5368n	53710
33 4.875	84 38.720	18.983	53576	53605
33 4.875	84 38.700	18.994	53548	53577
33 4.875	84 38.680	19.006	53572	53601
33 4.875	84 38.660	19.017	5361n	53639
33 4.875	84 38.640	19.028	5364n	53669
33 4.875	84 38.620	19.039	53624	53653
33 4.875	84 38.600	19.050	53617	53646
33 4.875	84 38.580	19.061	53616	53645
33 4.875	84 38.560	19.072	53635	53664
33 4.875	84 38.540	19.083	53668	53697
33 4.875	84 38.520	19.094	53654	53683
33 4.875	84 38.500	19.106	53594	53623
33 4.875	84 38.480	19.117	53670	53699
33 4.875	84 38.460	19.131	53640	53669
33 4.875	84 38.440	19.144	53628	53657
33 4.875	84 38.420	19.158	53628	53657
33 4.875	84 38.400	19.172	53623	53652
33 4.875	84 38.380	19.186	53645	53674
33 4.875	84 38.360	19.200	53677	53706
33 4.875	84 38.340	19.212	53643	53672
33 4.875	84 38.320	19.224	53608	53637
33 4.875	84 38.300	19.236	53599	53628
33 4.875	84 38.280	19.248	53598	53627
33 4.875	84 38.260	19.260	53605	53634
33 4.875	84 38.240	19.271	53605	53634
33 4.875	84 38.220	19.283	53592	53621
1234567890123456789012345678901234567890				

Table 4. (Continued)

Profile B-B', May 5, 1973

LATITUDE	LONGITUDE	TIME	RAW	REDUCED	LATITUDE	LONGITUDE	TIME	RAW	REDUCED
1234567890123456789012345678901234567890	1234567890123456789012345678901234567890				1234567890123456789012345678901234567890	1234567890123456789012345678901234567890			
33 2.180	84 41.580	9.083	53311	53359	33 2.327	84 40.204	10.133	5357n	53612
33 2.194	84 41.567	9.139	5359n	53638	33 2.378	84 40.231	10.300	53546	53587
33 2.209	84 41.554	9.194	53723	53771	33 2.429	84 40.259	10.317	53565	53605
33 2.223	84 41.541	9.250	53614	53661	33 2.480	84 40.286	10.337	53553	53593
33 2.238	84 41.528	9.267	53614	53661	33 2.531	84 40.313	10.357	5354A	53587
33 2.252	84 41.515	9.283	53565	53612	33 2.582	84 40.340	10.377	53551	53590
33 2.267	84 41.502	9.300	53562	53609	33 2.607	84 40.354	10.387	53526	53564
33 2.281	84 41.489	9.317	53573	53620	33 2.633	84 40.367	10.397	53275	53313
33 2.296	84 41.476	9.333	5358n	53626	33 2.658	84 40.381	10.407	53524	53562
33 2.310	84 41.463	9.378	53575	53621	33 2.684	84 40.394	10.417	53542	53580
33 2.325	84 41.450	9.422	53578	53624	33 2.709	84 40.408	10.428	53542	53579
33 2.339	84 41.437	9.467	53586	53631	33 2.735	84 40.421	10.440	53534	53571
33 2.354	84 41.424	9.478	53584	53629	33 2.760	84 40.435	10.452	53529	53566
33 2.368	84 41.411	9.489	53601	53646	33 2.762	84 40.425	10.464	53532	53569
33 2.383	84 41.398	9.500	53579	53624	33 2.765	84 40.405	10.487	5353n	53567
33 2.397	84 41.385	9.513	53578	53623	33 2.768	84 40.385	10.511	53541	53578
33 2.412	84 41.372	9.527	53576	53620	33 2.772	84 40.365	10.534	53573	53610
33 2.426	84 41.359	9.540	53595	53639	33 2.773	84 40.355	10.546	53572	53608
33 2.441	84 41.346	9.553	53639	53683	33 2.777	84 40.335	10.570	53593	53629
33 2.448	84 41.340	9.560	53581	53625	33 2.780	84 40.315	10.593	53675	53711
33 2.455	84 41.333	9.567	53561	53605	33 2.785	84 40.305	10.605	53787	53423
33 2.470	84 41.320	9.584	53599	53642	33 2.791	84 40.296	10.617	53893	53929
33 2.481	84 41.302	9.602	53561	53604	33 2.796	84 40.286	10.625	53879	53915
33 2.491	84 41.284	9.620	53574	53617	33 2.802	84 40.277	10.633	53694	53730
33 2.502	84 41.266	9.637	5358n	53623	33 2.807	84 40.267	10.642	53695	53731
33 2.513	84 41.248	9.655	53548	53590	33 2.813	84 40.258	10.650	53713	53749
33 2.523	84 41.230	9.673	53626	53668	33 2.818	84 40.248	10.658	5353A	53573
33 2.529	84 41.221	9.681	53616	53658	33 2.824	84 40.239	10.667	5360A	53643
33 2.534	84 41.212	9.690	53642	53684	33 2.829	84 40.229	10.675	53662	53697
33 2.539	84 41.203	9.699	5374n	53786	33 2.835	84 40.220	10.683	53763	53798
33 2.545	84 41.194	9.708	53656	53698	33 2.840	84 40.210	10.692	5388A	53923
33 2.550	84 41.185	9.717	53626	53668	33 2.846	84 40.245	10.700	54061	54096
33 2.544	84 41.165	9.727	53622	53664	33 2.851	84 40.280	10.709	53971	54006
33 2.538	84 41.146	9.737	53611	53653	33 2.857	84 40.314	10.719	53941	53976
33 2.532	84 41.126	9.747	53614	53656	33 2.863	84 40.349	10.728	53696	53731
33 2.519	84 41.087	9.767	53617	53659	33 2.868	84 40.384	10.737	53677	53711
33 2.507	84 41.048	9.783	53619	53661	33 2.874	84 40.419	10.746	53718	53752
33 2.495	84 41.009	9.800	53845	53A87	33 2.880	84 40.453	10.756	53666	53700
33 2.489	84 40.990	9.808	53624	53670	33 2.885	84 40.488	10.765	53770	53804
33 2.483	84 40.970	9.817	53609	53651	33 2.891	84 40.523	10.774	53708	53742
33 2.470	84 40.931	9.833	53591	53633	33 2.897	84 40.558	10.783	53711	53745
33 2.458	84 40.892	9.850	53673	53715	33 2.902	84 40.593	10.791	53621	53655
33 2.446	84 40.853	9.867	53593	53635	33 2.908	84 40.627	10.798	5358A	53622
33 2.433	84 40.814	9.883	53581	53623	33 2.913	84 40.662	10.806	53570	53603
33 2.421	84 40.775	9.900	53502	53544	33 2.919	84 40.697	10.814	53742	53775
33 2.415	84 40.755	9.908	53581	53630	33 2.925	84 40.732	10.821	53659	53692
33 2.409	84 40.736	9.917	53586	53628	33 2.930	84 40.767	10.829	53616	53649
33 2.403	84 40.716	9.925	5356n	53601	33 2.936	84 40.801	10.836	5360n	53633
33 2.397	84 40.697	9.933	53551	53592	33 2.942	84 40.836	10.844	53746	53779
33 2.391	84 40.677	9.940	53550	53592	33 2.947	84 40.871	10.852	53667	53700
33 2.378	84 40.638	9.952	53557	53599	33 2.953	84 40.906	10.859	5362n	53653
33 2.366	84 40.599	9.965	53556	53598	33 2.959	84 40.940	10.867	53635	53667
33 2.354	84 40.560	9.978	5356n	53602	33 2.964	84 40.975	10.874	53544	53576
33 2.342	84 40.521	9.990	53553	53595	33 2.970	84 41.010	10.882	53457	53489
33 2.329	84 40.482	10.003	53552	53594	33 2.975	84 40.979	10.889	53499	53531
33 2.317	84 40.443	10.016	53553	53595	33 2.980	84 40.947	10.897	53539	53571
33 2.305	84 40.404	10.029	53565	53607	33 2.985	84 40.916	10.905	53555	53587
33 2.292	84 40.365	10.041	53576	53618	33 2.990	84 40.884	10.912	53554	53586
33 2.280	84 40.326	10.054	5356n	53606	33 3.001	84 40.821	10.927	53561	53593
33 2.268	84 40.287	10.067	5356n	53602	33 3.011	84 40.758	10.942	53567	53598
33 2.256	84 40.248	10.079	53561	53603	33 3.021	84 40.696	10.958	53554	53585
33 2.243	84 40.209	10.091	53561	53604	33 3.031	84 40.633	10.973	5355A	53589
33 2.231	84 40.170	10.103	53557	53600	33 3.036	84 40.601	10.980	53552	53583
33 2.225	84 40.150	10.109	53556	53599	33 3.042	84 40.570	10.988	53664	53695
33 2.276	84 40.177	10.121	5354A	53590	33 3.047	84 40.538	10.995	53607	53638
1234567890123456789012345678901234567890					1234567890123456789012345678901234567890				

Page 55 is missing.

Table 4. (Continued)

Profile B-B' (Concluded)

LATITUDE	LONGITUDE	TIME	RAW	REDUCED
1234567890123456789012345678901234567890				
33 3.052	84 40.507	11.003	5359n	53621
33 3.057	84 40.475	11.011	53574	53604
33 3.062	84 40.446	11.018	53567	53597
33 3.067	84 40.413	11.026	53574	53604
33 3.072	84 40.381	11.033	53574	53604
33 3.077	84 40.350	11.067	5357A	53608
33 3.082	84 40.318	11.100	53585	53614
33 3.088	84 40.287	11.133	53593	53622
33 3.093	84 40.255	11.167	53603	53632
33 3.098	84 40.224	11.200	53609	53638
33 3.103	84 40.192	11.209	53613	53641
33 3.108	84 40.161	11.219	53617	53645
33 3.113	84 40.130	11.228	5365n	53678
33 3.118	84 40.098	11.237	5367A	53706
33 3.123	84 40.067	11.246	53724	53752
33 3.128	84 40.035	11.256	53751	53779
33 3.134	84 40.004	11.265	53812	53840
33 3.139	84 39.972	11.274	5394	53972
33 3.144	84 39.941	11.283	544n	54467
33 3.149	84 39.909	11.294	54392	54419
33 3.154	84 39.878	11.305	54096	54123
33 3.159	84 39.847	11.315	53502	53529
33 3.164	84 39.815	11.326	53526	53553
33 3.169	84 39.784	11.337	5359n	53623
33 3.174	84 39.752	11.348	53681	53710
33 3.180	84 39.721	11.358	54017	54044
33 3.185	84 39.689	11.369	53415	53441
33 3.190	84 39.658	11.380	5346n	53492
33 3.195	84 39.626	11.390	5352n	53546
33 3.200	84 39.595	11.401	5363n	53656
33 3.203	84 39.587	11.412	5346n	53486
33 3.207	84 39.578	11.423	53495	53521
33 3.210	84 39.570	11.433	53513	53539
33 3.214	84 39.561	11.445	53526	53552
33 3.217	84 39.553	11.456	53529	53555
33 3.221	84 39.544	11.467	5353n	53556
33 3.227	84 39.528	11.490	53534	53560
33 3.231	84 39.519	11.502	53535	53558
33 3.234	84 39.511	11.513	53672	53697
33 3.238	84 39.502	11.524	53539	53564
33 3.241	84 39.494	11.536	5355n	53575
33 3.248	84 39.477	11.559	5355n	53575
33 3.255	84 39.460	11.581	53553	53578
33 3.259	84 39.440	11.604	53544	53569
33 3.264	84 39.420	11.627	53544	53569
33 3.269	84 39.400	11.650	53524	53549
33 3.273	84 39.380	11.672	53562	53586
33 3.274	84 39.360	11.695	53559	53583
33 3.280	84 39.350	11.707	53559	53583
33 3.282	84 39.340	11.718	53436	53460
33 3.284	84 39.330	11.729	53543	53567
33 3.287	84 39.320	11.741	53554	53582
33 3.289	84 39.310	11.752	5355A	53582
33 3.291	84 39.300	11.763	53554	53578
33 3.296	84 39.280	11.786	53563	53587
33 3.298	84 39.270	11.798	5356n	53584
33 3.300	84 39.260	11.809	53424	53450
33 3.301	84 39.249	11.820	53557	53580
33 3.303	84 39.228	11.843	53593	53616
33 3.304	84 39.217	11.854	5360n	53623
33 3.305	84 39.206	11.866	53561	53584
33 3.306	84 39.195	11.877	53559	53582
33 3.308	84 39.174	11.900	53585	53608
33 3.311	84 39.152	11.918	53569	53592
33 3.312	84 39.141	11.927	53576	53599

1234567890123456789012345678901234567890

LATITUDE	LONGITUDE	TIME	RAW	REDUCED
1234567890123456789012345678901234567890				
33 3.313	84 39.131	11.936	53594	53617
33 3.315	84 39.109	11.953	53609	53632
33 3.316	84 39.098	11.962	53574	53597
33 3.317	84 39.087	11.971	53587	53610
33 3.318	84 39.077	11.980	53630	53653
33 3.319	84 39.066	11.989	5356A	53591
33 3.320	84 39.055	11.998	53563	53586
33 3.322	84 39.044	12.007	53613	53636
33 3.324	84 39.034	12.016	53634	53656
33 3.326	84 39.023	12.024	53667	53689
33 3.327	84 39.012	12.033	53655	53677
33 3.329	84 39.002	12.048	53632	53654
33 3.331	84 38.991	12.062	53629	53651
33 3.333	84 38.980	12.076	53633	53655
33 3.335	84 38.970	12.090	53612	53634
33 3.337	84 38.959	12.105	53605	53627
33 3.338	84 38.948	12.119	53602	53624
33 3.340	84 38.938	12.133	53601	53623
33 3.342	84 38.927	12.142	53604	53626
33 3.344	84 38.916	12.150	53612	53634
33 3.346	84 38.906	12.158	53597	53619
33 3.348	84 38.895	12.167	5358A	53610
33 3.349	84 38.884	12.175	53571	53593
33 3.351	84 38.874	12.183	53573	53595
33 3.353	84 38.863	12.192	53573	53594
33 3.355	84 38.853	12.200	53574	53595
33 3.359	84 38.831	12.217	53573	53594
33 3.362	84 38.810	12.231	53583	53604
33 3.366	84 38.789	12.245	53610	53630
33 3.370	84 38.767	12.260	53584	53604
33 3.373	84 38.746	12.274	53607	53627
33 3.377	84 38.725	12.288	53612	53632
33 3.381	84 38.703	12.302	53639	53659
33 3.384	84 38.682	12.317	53554	53574
33 3.388	84 38.661	12.350	53554	53574
33 3.390	84 38.650	12.367	53557	53577
33 3.392	84 38.629	12.389	53043	53063
33 3.393	84 38.608	12.411	53577	53597
33 3.395	84 38.586	12.433	53583	53603
33 3.396	84 38.565	12.456	5359A	53618
33 3.398	84 38.544	12.478	53619	53639
33 3.399	84 38.523	12.500	53596	53616
33 3.401	84 38.501	12.513	5359A	53614
33 3.402	84 38.480	12.527	5360A	53628
33 3.404	84 38.459	12.540	53557	53577
33 3.406	84 38.437	12.553	53571	53591
33 3.407	84 38.416	12.567	53584	53604
33 3.409	84 38.395	12.580	53599	53619
33 3.410	84 38.374	12.593	53594	53614
33 3.411	84 38.363	12.600	53587	53607
33 3.412	84 38.352	12.607	53596	53616
33 3.413	84 38.342	12.613	53594	53614
33 3.413	84 38.331	12.620	5358A	53608
33 3.414	84 38.321	12.627	5358A	53609
33 3.415	84 38.310	12.633	53581	53601

1234567890123456789012345678901234567890

Table 4. (Continued)

Profile C-C', May 6, 1973

LATITUDE LONGITUDE TIME RAW REDUCED
1234567890123456789012345678901234567890
33 1.945 84 40.277 12.050 53593 53624
33 1.944 84 40.259 12.060 53595 53626
33 1.942 84 40.242 12.070 53561 53592
33 1.941 84 40.224 12.080 53548 53578
33 1.940 84 40.206 12.090 53561 53591
33 1.939 84 40.188 12.100 53709 53739
33 1.938 84 40.179 12.109 53535 53565
33 1.937 84 40.171 12.118 53594 53624
33 1.936 84 40.153 12.136 53701 53731
33 1.935 84 40.135 12.154 53620 53650
33 1.949 84 40.125 12.172 53609 53638
33 1.963 84 40.116 12.190 53705 53734
33 1.977 84 40.106 12.208 53595 53624
33 1.991 84 40.096 12.226 53659 53688
33 2.005 84 40.087 12.244 53655 53683
33 2.019 84 40.077 12.262 53669 53697
33 2.032 84 40.068 12.281 53655 53683
33 2.046 84 40.058 12.299 53661 53689
33 2.060 84 40.048 12.317 53661 53689
33 2.074 84 40.039 12.327 53657 53685
33 2.088 84 40.029 12.337 53627 53650
33 2.102 84 40.019 12.347 53637 53660
33 2.116 84 40.010 12.357 53572 53600
33 2.130 84 40.000 12.367 53535 53563
33 2.132 84 39.990 12.377 53537 53565
33 2.134 84 39.980 12.387 53541 53569
33 2.136 84 39.970 12.397 53542 53570
33 2.138 84 39.960 12.407 53554 53582
33 2.142 84 39.940 12.427 53573 53601
33 2.146 84 39.920 12.447 53554 53582
33 2.151 84 39.900 12.467 53615 53644
33 2.155 84 39.880 12.667 53624 53653
33 2.159 84 39.860 12.687 53558 53587
33 2.163 84 39.840 12.708 53614 53643
33 2.165 84 39.830 12.719 53631 53660
33 2.161 84 39.822 12.729 53609 53638
33 2.157 84 39.813 12.740 53588 53617
33 2.153 84 39.805 12.750 53599 53629
33 2.144 84 39.789 12.768 53582 53612
33 2.136 84 39.772 12.787 53585 53615
33 2.128 84 39.756 12.805 53580 53610
33 2.120 84 39.739 12.824 53563 53593
33 2.111 84 39.723 12.842 53591 53620
33 2.103 84 39.706 12.860 53540 53570
33 2.095 84 39.690 12.879 53559 53582
33 2.091 84 39.681 12.888 53545 53576
33 2.087 84 39.673 12.897 53529 53560
33 2.082 84 39.665 12.906 53520 53551
33 2.078 84 39.657 12.916 53533 53564
33 2.074 84 39.648 12.925 53605 53636
33 2.070 84 39.640 12.934 53741 53772
33 2.066 84 39.634 12.943 53826 53857
33 2.060 84 39.627 12.952 53765 53796
33 2.056 84 39.621 12.961 53667 53698
33 2.051 84 39.615 12.971 53944 53975
33 2.046 84 39.609 12.980 5418A 54219
33 2.041 84 39.602 12.989 53664 53700
33 2.036 84 39.596 12.998 53621 53653
33 2.031 84 39.590 13.007 53727 53759
33 2.027 84 39.583 13.017 53600 53641
33 2.022 84 39.577 13.100 53643 53676
33 2.017 84 39.571 13.106 53613 53646
33 2.012 84 39.564 13.111 53624 53657
33 2.007 84 39.558 13.117 5361A 53652
33 1.998 84 39.546 13.128 53626 53660
1234567890123456789012345678901234567890

LATITUDE LONGITUDE TIME RAW REDUCED
1234567890123456789012345678901234567890
33 1.988 84 39.533 13.139 53699 53733
33 1.979 84 39.520 13.150 53809 53A43
33 1.974 84 39.514 13.156 53689 53723
33 1.964 84 39.501 13.167 53680 53715
33 1.954 84 39.489 13.180 53605 53640
33 1.950 84 39.483 13.187 53577 53612
33 1.940 84 39.470 13.200 53627 53662
33 1.940 84 39.452 13.213 5365n 53685
33 1.939 84 39.433 13.227 53585 53620
33 1.939 84 39.424 13.233 53654 53689
33 1.939 84 39.415 13.242 53677 53712
33 1.939 84 39.406 13.250 5374A 53778
33 1.939 84 39.397 13.258 5364A 53683
33 1.939 84 39.388 13.267 53671 53706
33 1.939 84 39.378 13.275 53693 53729
33 1.938 84 39.369 13.283 53710 53746
33 1.938 84 39.360 13.292 5366A 53704
33 1.938 84 39.351 13.300 53694 53730
33 1.938 84 39.342 13.308 53785 53821
33 1.938 84 39.332 13.317 53871 53907
33 1.938 84 39.323 13.325 53991 54027
33 1.938 84 39.314 13.333 53704 53740
33 1.938 84 39.305 13.342 53744 53780
33 1.937 84 39.296 13.350 53641 53677
33 1.937 84 39.287 13.358 53770 53806
33 1.937 84 39.278 13.367 5365n 53686
33 1.937 84 39.268 13.375 53773 53A09
33 1.937 84 39.259 13.383 53781 53A17
33 1.937 84 39.250 13.392 53785 53A21
33 1.937 84 39.241 13.400 53795 53A31
33 1.936 84 39.232 13.408 53844 53880
33 1.936 84 39.223 13.417 53863 53900
33 1.936 84 39.213 13.427 5383A 53A70
33 1.936 84 39.204 13.438 53931 53968
33 1.936 84 39.195 13.448 53947 53984
33 1.936 84 39.186 13.459 54494 54531
33 1.936 84 39.177 13.470 54314 54351
33 1.935 84 39.168 13.480 54259 54296
33 1.935 84 39.158 13.491 53926 53963
33 1.935 84 39.149 13.502 53849 53A86
33 1.935 84 39.140 13.512 53525 53562
33 1.935 84 39.131 13.523 53609 53646
33 1.935 84 39.122 13.533 53626 53663
33 1.935 84 39.113 13.544 53545 53583
33 1.934 84 39.103 13.555 53585 53623
33 1.934 84 39.094 13.565 53635 53673
33 1.934 84 39.085 13.576 5359n 53637
33 1.934 84 39.076 13.586 5360n 53638
33 1.934 84 39.067 13.597 53685 53723
33 1.934 84 39.048 13.618 53729 53767
33 1.933 84 39.030 13.639 53783 53A21
33 1.933 84 39.021 13.650 53831 53A70
33 1.933 84 39.012 13.659 53761 53A00
33 1.933 84 39.003 13.668 53770 53A09
33 1.933 84 38.984 13.686 5395A 53997
33 1.933 84 38.975 13.695 53773 53A12
33 1.932 84 38.966 13.705 53806 53A45
33 1.932 84 38.957 13.714 5374A 53787
33 1.932 84 38.938 13.732 53855 53A95
33 1.932 84 38.920 13.750 53732 53771
33 1.931 84 38.902 13.761 53716 53755
33 1.931 84 38.883 13.773 53707 53745
33 1.931 84 38.865 13.784 53686 53724
33 1.931 84 38.847 13.796 53647 53684
33 1.930 84 38.828 13.807 5376n 53797
1234567890123456789012345678901234567890

Table 4. (Continued)

Profile C-C' (Concluded)

LATITUDE LONGITUDE TIME RAW REDUCED
 1234567890123456789012345678901234567890
 33 1.930 84 38.810 13.819 53735 53772
 33 1.925 84 38.790 13.830 53723 53760
 33 1.921 84 38.770 13.842 53623 53661
 33 1.916 84 38.750 13.853 53712 53750
 33 1.913 84 38.740 13.859 53670 53708
 33 1.909 84 38.720 13.871 53724 53762
 33 1.904 84 38.700 13.882 53729 53767
 33 1.899 84 38.680 13.894 53722 53760
 33 1.894 84 38.660 13.905 53773 53811
 33 1.892 84 38.650 13.911 53823 53A61
 33 1.890 84 38.640 13.917 53791 53A29
 33 1.885 84 38.620 13.937 53660 53698
 33 1.889 84 38.602 13.957 53826 53A64
 33 1.890 84 38.593 13.967 53803 53A42
 33 1.892 84 38.584 13.977 53754 53793
 33 1.894 84 38.575 13.987 53809 53A49
 33 1.896 84 38.566 13.997 53793 53A33
 33 1.899 84 38.548 14.017 53735 53776
 33 1.903 84 38.530 14.027 5380A 53A49
 33 1.906 84 38.512 14.038 5384A 53A89
 33 1.910 84 38.494 14.049 53857 53899
 33 1.913 84 38.476 14.060 53773 53A15
 33 1.917 84 38.458 14.071 53783 53A25
 33 1.920 84 38.440 14.081 53661 53703
 33 1.920 84 38.421 14.092 5370A 53751
 33 1.920 84 38.403 14.103 53609 53652
 33 1.919 84 38.384 14.114 53649 53692
 33 1.919 84 38.365 14.125 53662 53705
 33 1.919 84 38.347 14.135 5373n 53773
 33 1.919 84 38.328 14.146 53720 53764
 33 1.918 84 38.309 14.157 53801 53845
 33 1.918 84 38.291 14.168 53735 53779
 33 1.918 84 38.272 14.178 53702 53746
 33 1.918 84 38.253 14.189 53623 53667
 33 1.918 84 38.235 14.200 53590 53634
 33 1.917 84 38.216 14.210 53586 53631
 33 1.917 84 38.197 14.221 53596 53642
 33 1.917 84 38.179 14.231 53636 53682
 33 1.917 84 38.160 14.241 53653 53700
 33 1.916 84 38.141 14.251 53669 53716
 33 1.916 84 38.123 14.262 53646 53693
 33 1.916 84 38.113 14.267 53593 53640
 33 1.916 84 38.095 14.277 53586 53633
 33 1.916 84 38.076 14.287 53578 53625
 33 1.915 84 38.057 14.297 53578 53625
 33 1.915 84 38.039 14.308 53563 53610
 33 1.915 84 38.020 14.318 53603 53650
 33 1.915 84 38.010 14.323 53593 53640
 33 1.915 84 37.991 14.333 53669 53717
 33 1.915 84 37.972 14.344 53663 53711
 33 1.914 84 37.953 14.355 53683 53731
 33 1.914 84 37.934 14.365 53679 53727
 33 1.914 84 37.915 14.376 53653 53701
 33 1.914 84 37.886 14.392 53616 53664
 33 1.914 84 37.867 14.403 53641 53689
 33 1.914 84 37.847 14.413 53663 53712
 33 1.913 84 37.828 14.424 53661 53710
 33 1.913 84 37.809 14.435 53670 53719
 33 1.913 84 37.790 14.445 53633 53682
 33 1.913 84 37.771 14.456 53633 53682
 33 1.913 84 37.751 14.467 53620 53669
 33 1.913 84 37.732 14.477 53599 53648
 33 1.912 84 37.713 14.488 53632 53681
 33 1.912 84 37.694 14.499 53679 53729
 33 1.912 84 37.675 14.509 53626 53676
 1234567890123456789012345678901234567890

LATITUDE LONGITUDE TIME RAW REDUCED
 1234567890123456789012345678901234567890
 33 1.912 84 37.656 14.520 5363A 53688
 33 1.912 84 37.636 14.531 5371n 53760
 33 1.912 84 37.617 14.541 53676 53726
 33 1.911 84 37.598 14.552 53779 53A29
 33 1.911 84 37.579 14.563 5366A 53718
 33 1.911 84 37.560 14.573 53651 53701
 33 1.911 84 37.540 14.584 53619 53669
 33 1.911 84 37.521 14.595 53614 53663
 33 1.911 84 37.512 14.600 53614 53663
 33 1.910 84 37.493 14.608 53609 53658
 33 1.910 84 37.473 14.617 5361A 53667
 33 1.910 84 37.454 14.625 53614 53663
 33 1.910 84 37.435 14.633 53567 53616
 1234567890123456789012345678901234567890

Table 4. (Concluded)

Profile A'-B', May 6, 1973

LATITUDE	LONGITUDE	TIME	RAW	REDUCED
1234567890123456789012345678901234567890				
33 4.675	84 38.740	10.033	53999	54014
33 4.659	84 38.735	10.045	54025	54040
33 4.643	84 38.731	10.056	54055	54070
33 4.627	84 38.726	10.068	54026	54n41
33 4.611	84 38.721	10.079	5395A	53973
33 4.796	84 38.716	10.090	53807	53822
33 4.780	84 38.712	10.102	53841	53856
33 4.764	84 38.707	10.113	53865	53880
33 4.748	84 38.702	10.125	53694	53709
33 4.740	84 38.700	10.130	53722	53737
33 4.724	84 38.700	10.142	53609	53625
33 4.707	84 38.700	10.153	53622	53638
33 4.691	84 38.700	10.164	5351n	53526
33 4.675	84 38.700	10.176	53679	53695
33 4.658	84 38.700	10.187	53614	53630
33 4.642	84 38.700	10.199	53625	53641
33 4.626	84 38.700	10.210	5365A	53674
33 4.609	84 38.700	10.221	53681	53697
33 4.593	84 38.700	10.233	53761	53776
33 4.585	84 38.700	10.239	53644	53659
33 4.570	84 38.705	10.250	53593	53608
33 4.555	84 38.710	10.261	53526	53541
33 4.539	84 38.714	10.272	5363n	53645
33 4.524	84 38.719	10.283	53589	53604
33 4.509	84 38.724	10.294	53589	53604
33 4.494	84 38.729	10.306	53589	53604
33 4.479	84 38.734	10.317	53592	53608
33 4.464	84 38.739	10.328	53595	53611
33 4.448	84 38.743	10.339	53593	53610
33 4.433	84 38.748	10.350	5359n	53607
33 4.418	84 38.753	10.364	53597	53614
33 4.403	84 38.758	10.378	53582	53599
33 4.388	84 38.763	10.392	53579	53596
33 4.373	84 38.768	10.406	53559	53576
33 4.365	84 38.770	10.412	53806	53A23
33 4.357	84 38.769	10.419	53599	53616
33 4.342	84 38.768	10.433	53602	53619
33 4.327	84 38.766	10.467	53613	53630
33 4.312	84 38.765	10.500	53585	53602
33 4.296	84 38.763	10.533	53592	53609
33 4.281	84 38.762	10.567	53582	53600
33 4.266	84 38.760	10.600	53585	53603
33 4.251	84 38.759	10.633	53588	53606
33 4.235	84 38.757	10.667	5358n	53596
33 4.220	84 38.756	10.700	53577	53593
33 4.205	84 38.754	10.712	53591	53607
33 4.190	84 38.752	10.724	5358n	53596
33 4.174	84 38.751	10.736	53582	53598
33 4.159	84 38.749	10.748	53581	53597
33 4.144	84 38.748	10.761	53571	53588
33 4.129	84 38.746	10.773	5357A	53595
33 4.113	84 38.745	10.785	5358n	53597
33 4.098	84 38.743	10.797	53581	53598
33 4.083	84 38.742	10.809	53577	53594
33 4.068	84 38.740	10.821	53584	53601
33 4.052	84 38.739	10.833	53577	53594
33 4.037	84 38.737	10.852	53572	53589
33 4.022	84 38.736	10.870	53571	53590
33 4.007	84 38.734	10.889	5357n	53588
33 3.991	84 38.733	10.907	53569	53587
33 3.976	84 38.731	10.926	5357n	53587
33 3.961	84 38.730	10.944	5356A	53585
33 3.946	84 38.728	10.963	53562	53579
33 3.930	84 38.727	10.981	53564	53582
33 3.915	84 38.725	11.000	53566	53584
1234567890123456789012345678901234567890				

APPENDIX III

COMPUTER PROGRAMS FOR GRAVITY AND MAGNETICS MODELING

A computer program was developed for computing the vertical gravity anomaly caused by a hypothetical two-dimensioned structure using the method of Talwani, Worzel, and Landisman (1959). A listing of the main program and subroutines necessary for line printer plotting is given in Table 5.

A computer program was developed for computing horizontal, vertical, and total magnetic anomalies due to induction, NRM or mixed magnetization using the method of Talwani and Heirtzler (1965). A listing of the main program and all referenced subroutines is given in Table 6.

Table 5. Two-Dimensional Gravity Modeling Program

```

1234567890123456789012345678901234567890123456789012345678901234567890
C GRAVITY PROFILING FOR 2-DIMENSIONAL STRUCTURES
C GRAVITY FOR 2-DIMENSIONAL STRUCTURES(AFTER-TALWANI,WORTZEL,LANDIS,M,N)
C INPUT(2I10,3F10.3) CARD NO. ONE
C   LL=NO. OF POLYGONS, N=X=NO. OF GRAVITY VALUES, DX=SEPARATION OF
C   GRAVITY VALUES, XO=POSITION OF FIRST GRAVITY VALUE, SCALE=PLOT
C   SCALE-FOR DRAW
C IF SCALE=0, PROGRAM CALCULATES SCALE
C IF SCALE=1, NO GRAPH IS DRAWN
C INPUT(FREE FIELD) LL CARDS
C   NXZ=N+1 OF CORNERS OF POLYGOON TAKEN CLOCKWISE, DRHO=DENSITY
C   CONTRAST, X(I,J),Z(I,J)=COORDINATES OF CORNERS-JTH CORNER OF ITH
C   POLYGON
C REPEAT SEQUENCE FOR ADDITIONAL PROFILES
C HBLANK CARD AT END TO TERMINATE CALCULATION
C DIMENSION DRHO(50),X(50,20),Z(50,20),NN(50),XX(20),ZZ(20),GAL(500)
C DIMENSION A(80)
25 READ (5,900)A
900 FORMAT(80A)
  READ (5,500) LL,NDX,DX,XO  , SCALE
  WRITE(6,901)A
901 FORMAT(1H1,B0A1,/)
  WRITE(6,503) LL,NDX,DX,XO
503 FORMAT(1H,28HV,VERTICAL GRAVITY ANOMALY FOR IS, 9H POLYGONS/2X,
13HTHE,15H-GRAVITY VALUES,,F10.4*19H-KM.APART, BEGIN AT,F10.4)
  IF(LL) 26,20,27
27 DO 100 I=1,LL
500 FORMAT (2I10,3F10.5)
  READ(5,501) NXZ,DRHO(I),(X(I,J),Z(I,J),J=1,NXZ)
  WRITE(6,502) NXZ,DRHO(I), (X(I,J),Z(I,J),J=1,NXZ)
501 FORMAT( )
502 FORMAT(16H NO OF POINTS = .,110,22H DENSITY DIFFERENCE = /(1X*1,F10
(3,1))
100 NN(I) = NXZ
  DO 101 I=1,LL
    NN1 = NN(I)
    DO 101 J = 1,NN1
101 X(I,J) = X(I,J)-XO
  DO 102 I=1,NDX
    G=0.0
    DO 103 J=1,LL
      NNJ = NN(J)
      DO 104 K = 1,NNJ
        XX(K) = X(J,K)
104 ZZ(K)=Z(J,K)
      CALL TWLZ(NN(J),XX,ZZ,DRHO(J)+GA)
103 G= G+GA
  GAL(I) = G
  DO 110 M=1,LL
    NNM = NN(M)
    DO 110 N = 1,NNM
110 X(M,N) = X(N,N)-DX
102 CONTINUE
  WRITE(6,505) (GAL(I),I=1,NDX)
505 FORMAT(1X//24H GRAVITY ANOMALY IN MGAL,/(5F15.4))
  ISC=SCALE
  IF(ISC.EQ.13) GO TO 25
  IF(SCALE) 130,131,130
131 CALL MXSCL(NDX,GAL,SCALE)
130 CALL DRAW(NDX,1,GAL,SCALE)
  GO TO 25
26 STOP
END
1234567890123456789012345678901234567890123456789012345678901234567890

```

Table 5. (Concluded)

Table 6. Two-Dimensional Magnetics Modeling Program

```

1234567890123456789012345678901234567890123456789012345678901234567890
C COMPUTATION OF MAGNETIC ANOMALIES CAUSED BY THE MAGNETIZATION OF TWO
C DIMENSIONAL, (INFINITE EXTENT IN THIRD DIRECTION).
C THIS PROGRAM IS A MODIFICATION OF THE PROGRAM BY
C MANIK TALANI AND JAMES R. HEITZLER WHICH WAS PUBLISHED IN
C COMPUTERS IN THE MINERAL INDUSTRIES - PART 1, STANFORD UNIVERSITY
C PUBLICATION GEOL. SCI., VOL 9, NO. 1, PAGES 464-480.
C THIS PROGRAM BY GEORGE RUTH
C SCHOOL OF GEOPHYSICAL SCIENCES
C GEORGIA INSTITUTE OF TECHNOLOGY
C ATLANTA, GA 30332
C SEPTEMBER 20, 1974

DIMENSION FLOPT(200),PLUM(200),GUM(200),VANMLY(200,10,2),
* HANMLY(200,10,2),TANH(200,10,2),SUS(10),REMREC(10),REMDIP(10),
* REMMAG(10),VIND(200),VLEN(200),HIND(200),HKEM(200),
* TI,D(200),TREM(200),VTOT(200),HT,T(200),TTOT(200)
DIMENSION Y(10,20),Z(10,20),VNCRA(200),HWORK(200),TWORK(200)
DIMENSION WORK1(200),WORK2(200)

REAL MGTMN
INTEGER PRIND,PLINDV,PLINDH,PLINT,VCOMPI,VCOMPR,HCOMPI,
* HCOMPR,TCOMPI,TCOMPI,PRNTAL,PLVAL,PLHAL,PLTL
***** *****,***** *****,***** *****,***** *****,***** *****,***** C
***READ RUN DESCRIPTION CARD
1 READ (5,300) NPOLY,PRIND,PLINDV,PLINDH,PLINT,VCOMPI,VCOMPR,
* HCOMPI,HCOMPR,TCOMPI,TCOMPR,PRNTAL,PLVAL,PLHAL,PLTL
3000 FORMAT (15I2)
IF (NPOLY.EQ.0) GO TO 320
***** *****,***** *****,***** *****,***** *****,***** *****,***** *****,*****
***NPOLY = NUMBER OF POLYGONS
***THE FOLLOWING ARE OUTPUT OPTION VARIABLES
C IF VARIABLE = 0, OPTION NOT EXERCISED
C IF VARIABLE = 1, OPTION IS EXERCISED
***PRIND = LIST ANOMALIES FOR EACH POLYGON
***PLINDV = PLOT VERTICAL ANOMALY FOR EACH POLYGON
***PLINDH = PLOT HORIZONTAL ANOMALY FOR EACH POLYGON
***PLINT = PLOT TOTAL ANOMALY FOR EACH POLYGON
***VCOMPI = COMPOSITE PLOT OF VERTICAL ANOMALY DUE TO INDUCTION ONLY
***VCOMPR = COMPOSITE PLOT OF VERTICAL ANOMALY DUE TO REMANENCE ONLY
***HCOMPI = COMPOSITE PLOT OF HORIZONTAL ANOMALY DUE TO INDUCTION ONLY
***HCOMPR = COMPOSITE PLOT OF HORIZONTAL ANOMALY DUE TO REMANENCE ONLY
***TCOMPI = COMPOSITE PLOT OF TOTAL ANOMALY DUE TO INDUCTION ONLY
***TCOMPR = COMPOSITE PLOT OF TOTAL ANOMALY DUE TO REMANENCE ONLY
***PRNTAL = LINE PRINTER LISTING OF ANOMALIES DUE TO ALL POLYGONS
***PLVAL = PLOT VERTICAL ANOMALY DUE TO ALL POLYGONS - REMANENT + INDUCED
***PLHAL = PLOT HORIZONTAL ANOMALY DUE TO ALL POLYGONS - REMANENT + INDUCED
***PLTL = PLOT TOTAL ANOMALY DUE TO ALL POLYGONS - REMANENT + INDUCED
***** *****,***** *****,***** *****,***** *****,***** *****,***** *****,*****
***READ PROFILE DESCRIPTION CARD
***** *****,***** *****,***** *****,***** *****,***** *****,***** *****,*****
4 READ (5,100) NFPTS,FRSTX,DELX,DECPLX,OBSVHT,HATCHM
1000 FORMAT (13,PF8.3)
***** *****,***** *****,***** *****,***** *****,***** *****,***** *****,*****
***FRSTX = X COORDINATE OF THE FIELD POINT FARTHEST IN THE NEGATIVE
***   DIRECTION(LEFT).
***DELX = INTERVAL BETWEEN FIELD POINTS.
***NFPTS = NUMBER OF FIELD POINTS
***DECPLX = DECLINATION OF THE POSITIVE X AXIS OF THE PROFILE LINE,
***   MEASURED POSITIVE CLOCKWISE FROM GEOGRAPHIC NORTH IN DEGREES.
***OBSVHT = HEIGHT ABOVE PROFILE LINE AT WHICH ANOMALY WILL BE
***   CALCULATED, MEASURED POSITIVE UP(SEE FOLLOWING FIGURE).
***HATCHM = INTERVAL BETWEEN HATCHMARKS FOR PLOTS -- MUST BE AN
***   INTEGRAL MULTIPLE OF DELX
123456789012345678901234567890123456789012345678901234567890

```

Table 6. (Continued)

Table 6. (Continued)

```

1234567890123456789012345678901234567890123456789012345678901234567890
C*** FOR THIS POLYGON.
CALL POLYQ (NFPTS,NSI,ES,FLDPT,VBSVHT,PSUM,GSUM,I*X,Z,DELX)
C***CALCULATE ANOMALY DUE TO INDUCTION FOR THIS POLYGON AT EACH FIELD POINT.****
MGTION = SUS(I) + FLDPT
DO 40 J = 1,NFPTS
VA1MLY(J,I,1) = -2.*MGTION*((CDIPR*CDIFFR*QSUM(J))-(SDIPR*PSUM(.)))
HA1MLY(J,I,1) = -2.*MGTION*((CDIPR*CDIFFR*PSUM(J))+(SDIPR*QSUM(.)))
C***FOR ANOMALIES SMALL IN COMPARISON TO THE EARTH'S FIELD, THE INTENSITY OF THE
C*** TOTAL ANOMALY DUE TO INDUCTION IS THE SUM OF THE PROJECTIONS OF THE
C*** VERTICAL AND HORIZONTAL ANOMALIES DUE TO INDUCTION ALONG THE DIRECTION OF
C*** THE EARTH'S FIELD.
TA1MLY(J,I,1) = HA1MLY(J,I,1)*CDIPR*CDIFFR + VA1MLY(J,I,1)*SDIPR
40 CONTINUE
C***CALCULATE ANOMALY DUE TO REMANENT MAGNETIZATION FOR THIS POLYGON
444 4U &RM 81&-D POIHHH
CDIP = COS (.0174533*REMDIR(I))
SDIP = SIN (.0174533*REMDIR(I))
CDIFF = COS (.0174533*(DECPLX-RE*DEC(I)))
MGTION = REMMAG(I) + 1e0000*0
DO 50 J = 1,NFPTS
VA1MLY(J,I,2) = 2.0*MGTION*((CDIP*CDIFF*QSUM(J))-(SDIP*PSUM(J)))
HA1MLY(J,I,2) = 2.0*MGTION*((CDIP*CDIFF*PSUM(J))+(SDIP*QSUM(J)))
C***FOR ANOMALIES SMALL IN COMPARISON TO THE EARTH'S FIELD, THE INTENSITY OF THE
C*** TOTAL ANOMALY DUE TO REMANENT MAGNETIZATION IS THE SUM OF THE
C*** PROJECTIONS OF THE VERTICAL AND HORIZONTAL ANOMALIES DUE TO REMANENT
C*** MAGNETIZATION ALONG THE DIRECTION OF THE EARTH'S FIELD.
TANMLY(J,I,2) = HA1MLY(J,I,2)*CDIPR*CDIFFR + VA1MLY(J,I,2)*SDIPR
50 CONTINUE
C********END OF ANOMALY CALCULATIONS***** ****
C********BEGIN INDIVIDUAL POLYGON OUTPUT SECTION***** ****
C***PRINT ANOMALIES FOR THIS POLYGON AND PLOT.
DO 130 I = 1,NPOLY
C ADD REMANENT + INDUCED FOR INDIVIDUAL POLYGONS
DO 60 J = 1,NFPTS
VWORK(J) = VA1MLY(J,I,1) + VA1MLY(J,I,2)
HWORK(J) = HA1MLY(J,I,1) + HA1MLY(J,I,2)
60 TWORK(J) = TANMLY(J,I,1) + TANMLY(J,I,2)
C***PRINT ANOMALIES FOR INDIVIDUAL POLYGONS*****
IF (PRIND) 70,120,70
70 WRITE (6,6000) I,SUS(I)
6000 FORMAT(1H1,'POLYGON NUMBER ',I2,'/' SUSCEPTIBILITY IS'
1F10.6,' EMU',/, ' CORNERS ARE ( X , Z ) '
DO 80 J = 1,NSIDES
80 WRITE (6,7000) X(I,J), Z(I,J)
7000 FORMAT(1H ,( 'F8.3', 'F8.3' ) )
M = IFIX (1000.0 * REMMAG(I))
IF (M) 100,90,100
90 WRITE (6,8000)
8000 FORMAT (1H0,'MAGNETIZATION IS INDUCED ONLY.')
GO TO 110
100 WRITE (6,9000) REMDEC(I),RE*DIP(I),REMMAG(I)
9000 FORMAT(1H0,'MAGNETIZATION IS MIXED.',/, ' REMANENT '
1'MAGNETIZATION VECTOR IS DEFINED BY',/, ' DEC =',F8.3', ' INC =',
2F8.3,' MAGNITUDE =',F10.6,' EMU')
110 WRITE (6,9001)
9001 FORMAT(1H0,'ANOMALIES IN GRAMAS',/, '1X',24('****'),/, ' FIELD POINT'
1 '12X', 'INCIDED', '29X', 'R.FANNT', '29X', 'TOTAL', '17X'
2 '3(V', '9X', 'H', '9X', 'T', '15X', '24('****'), '***')
DO 118 J=1,NFPTS
11A WRITE (6,9002) FLDPT(J),VA1MLY(J,I,1),HA1MLY(J,I,1),TANMLY(J,I,1),
1*VANMLY(J,I,2),HA1MLY(J,I,2),TANMLY(J,I,2),VWORK(J),HWORK(J),
2TWORK(J)
9002 FORMAT (1H 'F9.3', '3(F10.3,X))
C***PLOT VERTICAL ANOMALY FOR THIS POLYGON -- REMANENT + INDUCED
120 IF (PLINUV) 121,123,121
121 FSCALE = 0.0
CALL CONARY(VANMLY,I,1,WUR,1,NFPTS)
CALL CONARY(VANMLY,I,2,WUR,2,NFPTS)
CALL GRSCL(NFPTS,WORK1,FSCALE,1,EXP0+MAX)
CALL GNSCL(NFPTS,WORK2,FSCALE,1,EXP0+MAX)
CALL GRSCL(NFPTS,VWUR,FSCALE,1,EXP0+MAX)
WRITE (6,9004)
9004 FORMAT (1H1/40X,'VERTICAL ANOMALY FOR POLYGON NUMBER ',I2)
123456789012345678901234567890123456789012345678901234567890

```

Table 6. (Continued)

```

1234567890123456789012345678901234567890123456789012345678901234567890
    CALL SPL0T(NFPTS+FLDPT,W0R1,W0R2,V0RK,FSCAL,REMMAG(I),
    * MAX,IEXPO,ITICKS)
C***PLOT HORIZONTAL ANOMALY FOR THIS POLYGON -- REMANENT + INDUCED
123 IF (PLINH) 124,125,124
124 FSCALE = 0.0
    CALL CONARY(HANMLY,I+1,W0R1,NFPTS)
    CALL CONARY(HANMLY,I+2,W0R2,NFPTS)
    CALL GRSCAL(,NFPTS,W0RK1,FSCALE,IEXPO,MAX)
    CALL GRSCAL(,NFPTS,W0RK2,FSCALE,IEXPO,MAX)
    CALL GRSCAL(,NFPTS,W0RK,FSCALE,IEXPO,MAX)
    WRITE (6,9008) I
9008 FORMAT (1H1,59X,'HORIZONTAL ANOMALY FOR POLYGON NUMBER ',I2)
    CALL SPL0T(NFPTS+FLDPT,W0R1,W0R2,W0RK,FSCAL,REMMAG(I),
    * MAX,IEXPO,ITICKS)
C***PLOT TOTAL ANOMALY FOR THIS POLYGON -- REMANENT + INDUCED
125 IF (PLINT) 126,130,126
126 FSCALE = 0.0
    CALL CONARY(TANMLY,I+1,W0R1,NFPTS)
    CALL CONARY(TANMLY,I+2,W0R2,NFPTS)
    CALL GRSCAL(NFPTS,W0RK1,FSCALE,IEXPO,MAX)
    CALL GRSCAL(NFPTS,W0RK2,FSCALE,IEXPO,MAX)
    CALL GRSCAL(NFPTS,TW0RK,FSCALE,IEXPO,MAX)
    WRITE (6,9009) I
9009 FORMAT (1H1,44X,'TOTAL ANOMALY FOR POLYGON NUMBER ',I2)
    CALL SPL0T(NFPTS+FLDPT,W0R1,W0R2,TW0RK,FSCAL,REMMAG(I),
    * MAX,IEXPO,ITICKS)
130 CONTINUE
C********END OF INDIVIDUAL POLYGON OUTPUT SECTION*****,
C********BEGIN FIELD POINT SUMMATION SECTION*****,
C***ZERO ALL FIELD POINT SUMMING ARRAYS.
DO 135 I = 1,NFPTS
    VIND(I) = 0.0
    VREM(I) = 0.0
    HIND(I) = 0.0
    HREM(I) = 0.0
    TIND(I) = 0.0
    TREM(I) = 0.0
135 CONTINUE
DO 140 I = 1,NFOLY
    DO 137 J = 1,NFOLY
        VIND(I) = VIND(I) + VA1MLY(I,J,1)
        HIND(I) = HIND(I) + HA1MLY(I,J,1)
        TIND(I) = TIND(I) + TA1MLY(I,J,1)
        VREM(I) = VREM(I) + VR1MLY(I,J,2)
        HREM(I) = HREM(I) + HR1MLY(I,J,2)
        TREM(I) = TREM(I) + TR1MLY(I,J,2)
    137 VTOT(I) = VIND(I) + VREM(I)
    HTOT(I) = HIND(I) + HREM(I)
    TTOT(I) = TIND(I) + TREM(I)
140 CONTINUE
C********END FIELD POINT SUMMATION SECTION*****,
C********BEGIN COMPOSITE OUTPUT SECTION*****,
C***PLOT COMPOSITION FOR VERTICAL ANOMALY DUE TO INDUCTION ONLY
IF (VCMP) 145,145
145 FSCALE = 0.0
DO 150 I = 1,NPOLY
    CALL CONARY(VANMLY,I+1,W0R1,NFPTS)
150 CALL GRSCAL(,NFPTS,W0RK1,FSCALE,IEXPO,MAX)
    CALL GRSCAL(,NFPTS,VIND,FSCALE,IEXPO,MAX)
    WRITE (6,9010)
9010 FORMAT (1H1,40X,'VERTICAL ANOMALY DUE TO INDUCTION ONLY.')
    CALL CPLOT(NPOLY,NFPTS,FLDPT,VANMLY,I,VIND,FSCALE,1,MAX,IEXPO,
    * ITICKS)
C***PLOT COMPOSITION FOR VERTICAL ANOMALY DUE TO REMANENCE ONLY.
155 IF (VCMPR) 155,153,155
155 FSCALE = 0.0
DO 160 I = 1,NPOLY
    CALL CONARY(VANMLY,I+2,W0R1,NFPTS)
160 CALL GRSCAL(,NFPTS,W0RK1,FSCALE,IEXPO,MAX)
    CALL GRSCAL(,NFPTS,VREM,FSCALE,IEXPO,MAX)
    WRITE (6,9011)
9011 FORMAT (1H1,40X,'VERTICAL ANOMALY DUE TO REMANENCE ONLY.')
    CALL CPLOT(NPOLY,NFPTS,FLDPT,VANMLY,I,VREM,FSCALE,1,MAX,IEXPO,
1234567890123456789012345678901234567890123456789012345678901234567890

```

Table 6. (Continued)

```

123456789012345678901234567890123456789012345678901234567890123456789012345678901234567890
* ITICKS)
C***PLOT COMPOSITION FOR HORIZONTAL ANOMALY DUE TO INDUCTION ONLY
163 IF (INCOMPI) 165,173,165
165 FSCALE = 0.0
DO 170 I = 1,NPOLY
CALL CONARY(HANMLY,I,1,WOR,1,NFPTS)
170 CALL GRSCAL(.NFPTS,WORK1,FSCALE,IEXP0+MAX)
CALL GRSCAL(.NFPTS,HIND,FSCALE,IEXP0+MAX)
WRITE (6,9012)
9012 FORMAT (1H1,40X,'HORIZONTAL ANOMALY DUE TO INDUCTION ONLY')
CALL CPLOT(NPOLY,NFPTS,FLDPT,HANLY,I,HIND,FSCALE,2,MAX,IEXP0,
* ITICKS)
C***PLOT COMPOSITION FOR HORIZONTAL ANOMALY DUE TO REMANENCE ONLY
173 IF (HCGMPRI) 175,183,175
175 FSCALE = 0.0
DO 180 I = 1,NPOLY
CALL CONARY(HANMLY,I,2,WOR,1,NFPTS)
180 CALL GRSCAL(.NFPTS,WORK1,FSCALE,IEXP0+MAX)
CALL GRSCAL(.NFPTS,HREM,FSCALE,IEXP0+MAX)
WRITE (6,9013)
9013 FORMAT (1H1,40X,'HORIZONTAL ANOMALY DUE TO REMANENCE ONLY')
CALL CPLOT(NPOLY,NFPTS,FLDPT,HANLY,I,HREM,FSCALE,2,MAX,IEXP0,
* ITICKS)
C***PLOT COMPOSITION FOR TOTAL ANOMALY DUE TO INDUCTION ONLY
183 IF (TCMPI) 185,193,185
185 FSCALE = 0.0
DO 190 I = 1,NPOLY
CALL CONARY(TANMLY,I,1,WOR,1,NFPTS)
190 CALL GRSCAL(.NFPTS,WORK1,FSCALE,IEXP0+MAX)
CALL GRSCAL(.NFPTS,TIND,FSCALE,IEXP0+MAX)
WRITE (6,9014)
9014 FORMAT (1H1,40X,'TOTAL ANOMALY DUE TO INDUCTION ONLY')
CALL CPLOT(NPOLY,NFPTS,FLDPT,TANMLY,I,TIND,FSCALE,3,MAX,IEXP0,
* ITICKS)
C***PLOT COMPOSITION FOR TOTAL ANOMALY DUE TO REMANENCE ONLY
193 IF (TCQMPRI) 195,205,195
195 FSCALE = 0.0
DO 200 I = 1,NPOLY
CALL CONARY(TANMLY,I,2,WOR,1,NFPTS)
200 CALL GRSCAL(.NFPTS,WORK1,FSCALE,IEXP0+MAX)
CALL GRSCAL(.NFPTS,TREM,FSCALE,IEXP0+MAX)
WRITE (6,9015)
9015 FORMAT (1H1,40X,'TOTAL ANOMALY DUE TO REMANENCE ONLY')
CALL CPLOT(NPOLY,NFPTS,FLDPT,TANMLY,I,TREM,FSCALE,3,MAX,IEXP0,
* ITICKS)
205 CONTINUE
C*****END COMPOSITE OUTPUT SECTION*****
C*****REGIN ANOMALIES DUE TO ALL POLYGONS OUTPUT SECTION*****
C***PRINT OUT ANOMALIES DUE TO ALL POLYGONS
IF (PRINTAL) 206,260,206
206 REMFLG = 0.0
DO 210 I = 1,NPOLY
210 REMFLG = REMFLG + REMMAG(I)
WRITE (6,9016) NPOLY
9016 FORMAT (1H1,'ANOMALIES DUE TO ALL ',I2,' POLYGON(S)')
IF (IREMFLG) 230,220,230
220 WRITE (6,8000)
GO TO 240
230 WRITE (6,9017)
9017 FORMAT (1H0,'MAGNETIZATION IS MIXED.')
240 WRITE (6,9001)
DO 250 I = 1,NFPTS
250 WRITE (6,9002) FLDPT(I),VIRL(I),HIND(I),TIND(I),VREM(I),HREM(I),
1 TREM(I),VTOT(I),HTOT(I),TTOT(I)
C***PLOT VERTICAL ANOMALY DUE TO ALL POLYGONS -- REMANENT + INDUCED
260 IF (PLVAL) 270,280,270
270 FSCALE = 0.0
CALL GRSCAL(.NFPTS,VIND,FSCALE,IEXP0+MAX)
CALL GRSCAL(.NFPTS,VREM,FSCALE,IEXP0+MAX)
CALL GRSCAL(.NFPTS,VTOT,FSCALE,IEXP0+MAX)
WRITE (6,9018)
9018 FORMAT (1H1,41X,'VERTICAL ANOMALY DUE TO ALL POLYGONS')
CALL SPLOT (.NFPTS,FLDPT,VIRL,D,VREM,VTOT,FSCALE,REMFLG,MAX,IEXP0,
123456789012345678901234567890123456789012345678901234567890123456789012345678901234567890

```

Table 6. (Continued)

```

1234567890123456789012345678901234567890123456789012345678901234567890
* ITICKS
C***,*****PLOT HORIZONTAL ANOMALY DUE TO ALL POLYGONS - REMANENT + INDUCED
28n IF (PLHAL) 290+300,290
290 FSCALE = 0.0
    CALL GRSCAL(NFPTS,HIND,FSCALE,IEXP0,MAX)
    CALL GRSCAL(NFPTS,HREM,FSCALE,IEXP0,MAX)
    CALL GRSCAL(NFPTS,HTOT,FSCALE,IEXP0,MAX)
    WRITE (6,9019)
9019 FORMAT (1H1,41X,'HORIZONTAL ANOMALY DUE TO ALL POLYGONS')
    CALL SPLUT (NFPTS,FLOPT,H1,D,HRE,HTOT,FSCALE,REMFLG,MAX,IEXP0,
* ITICKS)
C***,*****PLOT TOTAL ANOMALY DUE TO ALL POLYGONS- REMANENT + INDUCED
30n IF (PLTAL) 310+315,310
310 FSCALE = 0.0
    CALL GRSCAL(NFPTS,TIND,FSCALE,IEXP0,MAX)
    CALL GRSCAL(NFPTS,TREM,FSCALE,IEXP0,MAX)
    CALL GRSCAL(NFPTS,TTOT,FSCALE,IEXP0,MAX)
    WRITE (6,9020)
9020 FORMAT (1H1,45X,'TOTAL ANOMALY DUE TO ALL POLYGONS')
    CALL SPLUT (NFPTS,FLOPT,TIND,TREM,TTOT,FSCALE,REMFLG,MAX,IEXP0,
* ITICKS)
315 GO TO 1
320 CALL EXIT
END
1234567890123456789012345678901234567890123456789012345678901234567890

```

```

1234567890123456789012345678901234567890123456789012345678901234567890
SUBROUTINE GRSCAL(NFPTS,A,FSCALE,IEXP0,MAX)
DIMENSION A(200)
C***,*****THIS SUBROUTINE FINDS THE VARIABLE WITH THE GREATEST ABSOLUTE VALUE IN THE
C ARRAY A WHICH HAS NFPTS ELEMENTS.
C FSCALE IS THEN SET EQUAL TO THE SMALLEST VALUE FOR FULL SCALE WHICH WILL
C BEST PRESENT THE ELEMENTS OF A.
C IEXP0 AND MAX ARE SUCH THAT FSCALE = MAX * 10 ** IEXP0 .
C***,*****DO 15 I = 1,NFPTS
15 I = 1,NFPTS
5 IF (ABS(A(I))-FSCALE) 15+15+10
10 FSCALE = ABS(A(I))
15 CONTINUE
C** IF ALL VALUES OF THE ARRAY ARE ZERO, SET FSCALE = 1.0 ARBITRARILY.
    IF (FSCALE) 20+20+25
20 FSCALE = 1.0
25 EXP0 = LOG10 (FSCALE)
    IF (EXP0) 30,35+40
30 IEXP0 = EXP0 + 1
    GO TO 45
35 MAX = 1
    RETURN
40 IEXP0 = EXP0
45 J = FSCALE/(10.0**IEXP0)
    IF (J.LT.2) GO TO 50
    IF (J.LT.5) GO TO 55
    FSCALE = 10.0 * (10.0**IEXP0)
    MAX = 30
    RETURN
50 FSCALE = 2.0 * (10.0**IEXP0)
    MAX = 2
    RETURN
55 FSCALE = 5.0 * (10.0**IEXP0)
    MAX = 5
    RETURN
END
1234567890123456789012345678901234567890123456789012345678901234567890

```

Table 6. (Continued)

```

1234567890123456789012345678901234567890123456789012345678901234567890
SUBROUTINE POLYPY (NFPTS, NSIDES, FLOPT, OBSVHT, PSUM, QSUM)
* INDEX,X,Z,DELX)
DIMENSION EXX(21),ZEE(21),FLOPT(200),PSUM(200),QSUM(200)
DIMENSION X(10*20),Z(10*20)
***** READ COORDINATE CARDS FOR POLYGON CORNERS
***** ONE COORDINATE CARD FOR EACH CORNER OF THE POLYGON--CLOCKWISE ORDER.
***** EXX(I) = X COORDINATE OF THE ITH CORNER OF POLYGON
***** ZEE(I) = Z COORDINATE OF THE ITH CORNER OF POLYGON. POSITIVE DOWN.
***** DO 10 I = 1,NSIDES
READ (1,1000) EXX(I),ZEE(I)
1000 FORMAT(1)
***** SAVE CORNER COORDINATES FOR PRINTOUT.
  X(INDEX,I) = EXX(I)
  10 Z(INDEX,I) = ZEE(I)
  NSIDUP1 = NSIDES + 1
  EXX(NSIDUP1) = EXX(1)
  ZEE(NSIDUP1) = ZEE(1)
  DO 150 I = 1,NFPTS
  PSUM(I) = 0.0
  QSUM(I) = 0.0
  X1 = EXX(I) - FLOPT(I)
  Z1 = ZEE(I) + OBSVHT
  15 RS1,I = (X1*X1+Z1*Z1)
***** IF X AND Z ARE BOTH ZERO, ATAN2 GIVES ERROR. SO CHANGE Z SLIGHTLY
  IF (RS1.NE.0.0) GO TO 17
  Z1 = .0001 * DELX
  THETD = 0.0
  GL = ALOG (.0001 * DELX * DELX)
  GO TO 15
  17 THETA = ATAN2(Z1,X1)
  J = 2
  20 X2 = EXX(J) - FLOPT(I)
  Z2 = ZEE(J) + OBSVHT
  25 RSG2 = (X2*X2+Z2*Z2)
  IF (RSG2.NE.0.0) GO TO 27
  Z2 = .0001 * DELX
  THETD = 0.0
  GL = ALOG (.0001 * DELX * DELX)
  GO TO 25
  27 THETB = ATAN2(Z2,X2)
  IF (Z1-Z2) 40,30,40
  30 P = 0.0
  Q = 0.0
  GO TO 120
  40 OMEGA = THETA - THETB
  IF (OMEGA) 60,50,50
  50 IF(OMEGA-3.1415927) 70,70,40
  60 IF(OMEGA+3.1415927) 30,70,70
  70 THETU = OMEGA
  GO TO 110
  80 IF(OMEGA) 90,100,100
  90 THETU = OMEGA - 6.283153
  GO TO 110
  100 THETO = OMEGA + 6.283153
  110 GL = 0.5 * ALOG(RSG2/RSQ1)
  115 X12 = X1 - X2
  Z21 = Z2 - Z1
  XSQ = X12 * X12
  ZSQ = Z21 * Z21
  XZ = Z21 * X12
  P = -(1/RSQ1*(XSQ+ZSQ))+THETD + ((XZ/(XSQ+ZSQ))*GL)
  Q = -(THETD*(XZ/(XSQ+ZSQ))) - (GL*(ZSQ/(XSQ+ZSQ)))
  120 PSUM(I) = PSUM(I) + P
  QSUM(I) = QSUM(I) + Q
***** RELEASE ALL VARIABLES INVOLVING ONLY THE SECOND POLYGON CORNER AS THE
***** VARIABLES INVOLVING ONLY THE FIRST POLYGON CORNER SO THEY DON'T
***** HAVE TO BE CALCULATED AGAIN.
  140 X1 = X2
  Z1 = Z2
  RSQ1 = RSQ2
  THETA = THETU
1234567890123456789012345678901234567890123456789012345678901234567890

```

Table 6. (Continued)

```

1234567890123456789012345678 01234567890123456789012345678901234567890
C***CHECK TO SEE IF ALL SIDES HAVE BEEN DONE.
      J = J + 1
      JR = J - 1
      IF(JR-.NSIDP1) 20+150+150
150 CONTINUE
      RETURN
      EN,
1234567890123456789012345678901234567890123456789012345678901234567890

```

```

1234567890123456789012345678901234567890123456789012345678901234567890
      SUBROUTINE CONARY (ARRAY1,I,J,ARRAY2,NFPTS)
      DIMENSION ARRAY1(200,10,2),ARRAY2(200)
C***,*****,*-*-*-*-*-*-*-*-*-*-*-*-*-*-*-*-*-*-*-*-*-*-*-*-*-*-*-*-*-*-*-*-*-*-
C   THIS SUBROUTINE SELECTS THE DESIGNATED ELEMENTS OF THE THREE DIMENSIONAL
C   ARRAY, ARRAY1 AND PUTS THEM INTO A ONE DIMENSIONAL ARRAY, ARRAY2)
C   THAT IS, ARRAY2(1) = ARRAY1(1,I,J) THRU TO
C   ARRAY2(NFPTS) = ARRAY1(NFPTS,I,J) ARE PERFORMED.
C***,*****,*-*-*-*-*-*-*-*-*-*-*-*-*-*-*-*-*-*-*-*-*-*-*-*-*-*-*-*-*-*-*-*-*-
      DO 10 K = 1,NFPTS
10  ARRAY2(K) = ARRAY1(K,I,J)
      RETURN
      END
1234567890123456789012345678901234567890123456789012345678901234567890

```

Table 6. (Continued)

```

1234567890123456789012345678901234567890123456789012345678901234567890
      SU,ROUTINE SPLIT (NFPTS,FLOPT,A*,C,FSCALE,REMFLG,MAX,IEXPO,
      * ITICKS)
      DIMENSION A(200),B(200),C(200),FLOPT(200),ALINE(101)
      REAL II
      DATA BLNK/1H//,AST/1H//,DOT/1H//,RR/1H//,II/1H//,DASH/1H//,PLS/1H//
***** THIS SUBROUTINE GENERATES A LINE PRINTER PLOT OF THE ELEMENTS OF THE ARRAYS
C   A + d AND C VS. THE FIELD P(I).TS. FLOPT .
C   FLOPT ELEMENTS ARE LISTED ALONG THE ABSISSA AND THE ARRAY ELEMENTS
C   PLOTTED ALONG THE ODUINTE. HATCH MARKS ARE PLACED ALONG THE ABSISSA
C   EVERY ITICKS TH POINT.
C   FSCALE IS THE FULL SCALE LIMIT OF THE PLOT.
C   FSCALE = MAX * 10 ** IEXPO
C   REMFLAG PERMITS CHOICE OF PLOTTING SYMBOLS DEPENDING ON WHETHER THE MAG-
C   NETIZATION IS MIXED OR NOT.
C   REMFLAG = 0 , USE SYMBOLS FOR INDUCTION ONLY
C   = 1 , USE SYMBOLS FOR MIXED MAGNETIZATION
***** N = ITICKS
      WRITE (6,500) IEXPO,IE,PO,AX,MAX
 500 FORMAT (1H+17X,I1,99X,I1,/,12Y1-1,I2,1X10',47X,'0',46X,'+',0
     1 I2,1X10',/,1 FIELD POINT,3X,21(' ', ' '),/15X,21('SH' ))
      WRITE (6,600)
 600 FORMAT (1H+14X,20('+' , . . . ),'+')
      DO 10 I = 1:101
 10 ALINE(i) = BLNK
      ALINE( 1) = DOT
      ALINE( 51) = DOT
      ALINE(101) = DOT
      DO 30 J = 1,N,FPTS
      IF (ITICKS-N) 13,12,13
 12 N = 1
      ALINE( 1) = PLS
      ALINE( 2) = DASH
      ALINE( 50) = DASH
      ALINE( 51) = PLS
      ALINE( 52) = DASH
      ALINE(100) = DASH
      ALINE(101) = PLS
      GO TO 14
 13 N = N + 1
 14 J = 51.500001 + (A(I)/FSCALE)*50
      M = IFIX (1000.0 * REMFLG)
      IF (M) 16,15,16
 15 ALINE(J) = AST
      L = J
      K = J
      GO TO 18
 16 ALINE(J) = II
      K = 51.500001 + (B(I)/FSCALE) * 50.0
      ALINE(K) = RR
      L = 51.500001 + (C(I)/FSCALE) * 50.0
      ALINE(L) = AST
 18 WRITE (6,1000) FLOPT(I),ALINE
 1000 FORMAT (1H ,F10.2,4X,101A1)
      WRITE (6,2000)
 2000 FORMAT (1H+14X,1H+,99X,1H+)
      IF (N-1) 25,20,25
 20 ALINE( 2) = BLNK
      ALINE( 50) = BLNK
      ALINE( 52) = BLNK
      ALINE(100) = BLNK
 25 ALINE(L) = BLNK
      ALINE(K) = BLNK
      ALINE(J) = BLNK
      ALINE( 1) = DOT
      ALINE( 51) = DOT
      ALINE(101) = DOT
 30 CONTINUE
      WRITE (6,3000)
 3000 FORMAT (1H+14X,20('+' , . . . ),'+')
      RETURN
      END
1234567890123456789012345678901234567890123456789012345678901234567890

```

Table 6. (Concluded)

```

1234567890123456789012345678901234567890123456789012345678901234567890
SUBROUTINE CPLOT(NPOLY,NFPTS,FLDPT,A,K,B,FSCALE,INDEX,MAX,IEXPO,
* ITICKS)
DIMENSION FLDPT(200),A(200,10,2),B(200),ALINE(101),SUM(3),LINE(11)
REAL NUM(10)
DATA BLNK/1H //,DOT/1H./,(NUM(I),I=1,10)/1H1,1H2,1H3,1H4,1H5,1H6,
* 1H7,1H8,1H9,1H0/,(SU(I),I=1,3)/1HV,1HH,1HT//,DASH/1H-/,PLS/1H+/
C THIS SUBROUTINE GENERATES A COMPOSITE LINE PRINTER PLOT OF THE ELEMENTS OF
C THE ARRAY A AS FOLLOWS. NOTE A IS DIMENSIONED AS A(200,10,2).
C THIS SUBROUTINE WILL PLOT THE POINTS A(ALPHA,BETA,1) OR
C A(ALPHA,BETA,2) AS DESCRIBED BY THE FOLLOWING. NPOLY PLOTTING SYMBOLS
C ARE PLOTTED FOR EACH VALUE OF THE ABSISSA. FOR NFPTS FIELD POINTS. ALSO
C FOR EACH VALUE OF THE A,SCISSA A PLOTTING SYMBOL REPRESENTING THE CORRESPOND-
C ING ELEMENT OF THE ARRAY B WHICH IN THIS CASE REPRESENTS THE ALGEBRAIC
C SUM OF THE NPOLY VALUES FOR ARRAY A IS ALSO PLOTTED.
C FLDPT ELEMENTS ARE LISTED ALONG THE ABSISSA AND THE ARRAY ELEMENTS OF
C A AND B ARE PLOTTED ALONG THE ORDINATE. HATCH MARKS ARE PLACED ALONG
C THE ABSISSA EVERY ITICKS TH POINT. FSCALE IS THE FULL SCALE LIMIT OF
C THE PLOT. FSCALE = MAX * 10 ** IEXPO .
N = ITICKS
WRITE (6,500) IEXPO,IE,PD,AX,MAX
500 FORMAT (1H ,17X,I1,99X,I1,/,12,'-',I2,,X10',47X,'0',46X,'+',1
 1 I2,'X10',/,' FIELD POINT',3X,P1('      '),15X,P1('5H' ))
WRITE (6,600)
600 FORMAT (1H+14X,20('+'..,..'),+'++)
DO 10 I = 1,101
10 ALINE(I) = BLNK
ALINE( 1) = DOT
ALINE( 51) = DOT
ALINE(101) = DOT
DO 40 I = 1,NFPTS
IF (ITICKS-N) 13,12,13
12 N = 1
ALINE( 1) = PLS
ALINE( 2) = DASH
ALINE( 50) = DASH
ALINE( 51) = PLS
ALINE( 52) = DASH
ALINE(100) = DASH
ALINE(101) = PLS
GO TO 14
13 N = N + 1
14 DO 20 J = 1,NPOLY
L = 51.500001 + (A(I,J,K)/FSCALE) * 50.0
***SAVE NUMBER OF THE ELEMENT WHICH WAS CHANGED FROM BLANK
LINE(J) = L
***REPLACE BLANK LINE ELEMENT BY CHARACTER FOR DATA POINT.
20 ALINE(L) = NUM(J)
L = 51.500001 + (B(I)/FSCALE) * 50.0
ALINE(L) = SUM(INDEX)
***J IS NOW = NPOLY + 1
LINE(J) = L
WRITE(6,1000) FLDPT(I),ALINE
1000 FORMAT(1H ,F10.2,4X,101A1)
WRITE (6,2000)
2000 FORMAT (1H+14X,1H*,99X,1H*)
***RESTORE BLANKS TO THOSE LINE ELEMENTS WHICH WERE CHANGED
DO 30 L = 1,J
M = LINE(L)
30 ALINE(M) = BLNK
***RESTORE DOTS TO THOSE LINE ELEMENTS WHICH MAKE UP THE AXIS AND X,Y HAVE
*** BEEN CHANGED.
IF (N-1) 38,35,38
35 ALINE( 2) = BLNK
ALINE( 50) = BLNK
ALINE( 52) = BLNK
ALINE(100) = BLNK
38 ALINE( 1) = DOT
ALINE( 51) = DOT
ALINE(101) = DOT
40 CONTINUE
WRITE (6,300)
3000 FORMAT (1H+14X,20('+'..,..'),+'++)
RETURN
END
1234567890123456789012345678901234567890123456789012345678901234567890

```

APPENDIX IV

PALEOMAGNETIC DATA COLLECTION AND REDUCTION

Samples from the Meriwether dike were collected and analyzed for NRM (Natural Remanent Magnetization) by Doyle Watts of the Ohio State University. Thirteen cores were obtained from a single outcrop of the Meriwether dike 5.5 miles northeast of Greenville on Georgia State Highway 362. In all, 26 one inch cylinders were cut from the cores. The samples were analyzed for Natural Remanent Moment (no magnetic cleaning) using a Schonstedt SSM1 Spinner Magnetometer. Direction and magnitude of the NRM are given for each sample in Table 7. Sample numbers are those used by Watts (personal communication) and the letter A, B, or C following the number indicates the first, second, or third cylinder cut from a core. Cores NW73174 through NW73182 were taken from the center portion of the dike and the remaining cores from the chilled edges of the dike.

Table 7. Natural Remanent Moments of Cores Taken From
The Meriwether Dike (Watts, Personal Communication)

Ohio State University Sample Number	Remanent Moment		
	Magnitude	Declination	Inclination
NW73174B	0.00144	7.82	26.26
NW73175A	0.00144	2.98	28.54
NW73175B	0.00156	8.86	35.49
NW73176B	0.00150	1.03	35.39
NW73177B	0.00150	21.69	27.86
NW73177C	0.00151	18.31	35.96
NW73178B	0.00174	12.42	25.20
NW73178C	0.00168	13.94	26.29
NW73179B	0.00152	18.10	22.61
NW73179C	0.00149	22.29	21.84
NW73180B	0.00173	10.08	26.39
NW73180C	0.00175	14.89	25.46
NW73180D	0.00170	12.01	27.20
NW73181B	0.00166	14.77	29.96
NW73182B	0.00162	16.20	23.21
NW73182C	0.00153	19.51	25.58
NW73183B	0.00215	36.16	27.72
NW73183C	0.00220	36.84	31.15
NW73184B	0.00211	33.78	23.38
NW73184C	0.00173	30.42	16.23
NW73185B	0.00201	42.87	27.96
NW73185C	0.00193	46.15	27.09
NW73186B	0.00220	42.11	32.70
NW73186C	0.00210	46.66	31.44
NW73187B	0.00212	49.75	30.89
NW73187C	0.00216	42.37	30.95

BIBLIOGRAPHY

BIBLIOGRAPHY

Armstrong, R.L., and J. Besancon. A triassic time scale dilemma: K-Ar dating of Upper Triassic mafic igneous rocks of eastern U.S.A. and Canada and Post-Upper Triassic plutons, western Idaho, U.S.A. *Eclogae geol. Helv.*, 63(1), 15-38, 1970.

Balsley, J.R., and A.F. Buddington. Iron-Titanium Oxide minerals, rocks, and aeromagnetic anomalies of the Adirondack Area, New York. *Economic Geology*, 53, 777-805, 1958.

Bentley, R.D., and T.L. Neathery. Geology of the Brevard zone and related rocks of the inner Piedmont of Alabama. *Alabama Geol. Survey, 8th Annual Field Trip Guidebook*, Dec. 4-5, 1970.

Cohee, C.V., Chairman. Tectonic Map of the United States excluding Alaska and Hawaii. *U.S. Geological Survey and American Association of Petroleum Geologists*, scale 1:2,500,000, 1962.

de Boer, Jelle. Paleomagnetic-tectonic study of Mesozoic dike swarms in the Appalachians. *J. Geophys. Res.*, 72(8), 2237-2250, 1967.

Dobrin, M.B. Introduction to Geophysical Prospecting. Second edition, McGraw-Hill, 446 pages, 1960.

Dorman, Leroy M., and Robert E. Ziegler. Gravimetric reference base net, State of Georgia. *Georgia Geological Survey*, in preparation.

Garland, George D. Introduction to Geophysics - Mantle, Core, and Crust. Saunders, 420 pages, 1971.

Georgia Department of Mines, Mining, and Geology. *Geologic Map of Georgia*, scale 1:500,000, 1939.

Green, R. Remanent magnetization and the interpretation of magnetic anomalies. *Geophysical Prospecting*, 8, 98-110, 1960.

Hood, Peter. Remanent magnetism - a neglected factor in aeromagnetic interpretation. *Canadian Mining Journal*, 84(4), 76-79, 1963.

Johnson, Robert W., and Joel S. Watkins, Aeromagnetic map of Staunton and vicinity, Virginia. *U.S. Geological Survey, Geophysical Investigations Map GP-414*, scale 1:62,500, 1963.

King, P.B. Systematic pattern of Triassic dikes in the Appalachian region. *Geological Survey Research 1961*, U.S. Geol. Survey Prof. Paper 424-B, B93-B95, 1961.

Lee, Doyce L. A diabase dike in Meriwether County, Georgia (abstr.) Bull. of the Ga. Acad. of Sci., 29(2), 127, 1971.

Lester, J.G., and A.T. Allen. Diabase of the Georgia Piedmont. Bull. of the Geol. Soc. of Amer., 61, 1217-1224, 1950.

Matshusita, S., and Wallace H. Campbell, editors. Physics of Geomagnetic Phenomena, Vol 1. Academic Press, 1967.

May, P.R. Pattern of Triassic-Jurassic diabase dikes around the North Atlantic in the context of predrift position of the continents. Geol. Soc. of Amer. Bull., 82, 1285-1292, 1971.

National Aeronautics and Space Administration. Earth Resources Aircraft Program, Screening and Indexing Report, Mission 131. Manned Spacecraft Center; Houston, Texas; September 1970. Film: Mission 131, site 217, roll 3, Color infrared Zeiss camera, frames 43, 44, and 45, 1970.

Petty, A.J., F.A. Petrafeso, and F.C. Moore, Jr. Aeromagnetic Map of the Savannah River Plant Area South Carolina and Georgia. U.S. Geological Survey, Geophysical Investigations Map GP-489, scale 1:250,000, 1965.

Philbin, P.W., F.A. Petrafeso, and C.L. Long. Aeromagnetic Map of the Georgia Nuclear Laboratory Area, Georgia. U.S. Geological Survey Geophysical Investigations Map GP-488, scale 1:250,000, 1964.

Privett, Donald R. Structure and petrography of some diabase dikes in central South Carolina (abstr.). Geol. Soc. Amer. Spec. Paper 87, p. 260, 1966.

Stockwell, C.H., Chairman. Tectonic Map of Canada. Canada Geological Survey, Map 1251A, scale 1:5,000,000, 1969.

Strangway, D.W. Interpretation of the magnetic anomalies over some Precambrian dikes. Geophysics, XXX(5), 783-796, 1965.

Talwani, Manik, J.L. Worzel, and Mark Landisman. Rapid gravity computations for two-dimensional bodies with application to the Mendocino submarine fracture zone. J. Geophys. Res., 64(1), 49-59, 1959.

Talwani, Manik, and James R. Heirtzler. Computation of magnetic anomalies caused by two-dimensional structures of arbitrary shape. Computers in the Mineral Industries, Part I, Stanford University Publications, Geol. Sci., 9(1), 464-480, 1965.

U.S. Geological Survey. North-Central Georgia Aeromagnetic Map. Georgia Geological Survey, in preparation.

Watson, Thomas L. Granites and gneisses of Georgia. Geological Survey of Georgia Bull. 9A, 1902.

Weigand, Peter W., and Paul C. Ragland, Geochemistry of Mesozoic dolerite dikes from eastern North America. Contr. Mineral and Petrol., 29, 195-214, 1970.

C-35-608

EFFECTS OF CRUSTAL FEATURES ON THE
GRAVITY FIELD AND ISOSTATIC COMPENSATION

FINAL REPORT

Leland Timothy Long

December, 1974

U.S. ARMY RESEARCH OFFICE - DURHAM

GRANT NO. DA-ARO-D-31-124-71-G117

GEORGIA INSTITUTE OF TECHNOLOGY
ATLANTA, GEORGIA 30332

APPROVED FOR PUBLIC RELEASE;

DISTRIBUTION UNLIMITED

The findings in this report are not to be construed as an official department of the army position, unless so designated by other authorized documents.

Unclassified

Security Classification

DOCUMENT CONTROL DATA - R & D

(Security classification of title, body of abstract and indexing annotation must be entered when the overall report is classified)

1. ORIGINATING ACTIVITY (Corporate author)	2a. REPORT SECURITY CLASSIFICATION
School of Geophysical Sciences Georgia Institute of Technology Atlanta, Georgia 30332	Unclassified
	2b. GROUP
	NA

3. REPORT TITLE

EFFECTS OF CRUSTAL FEATURES ON THE GRAVITY FIELD AND ISOSTATIC COMPENSATION

4. DESCRIPTIVE NOTES (Type of report and inclusive dates)

Final Report 4/1/72 - 6/30/74

5. AUTHOR(S) (First name, middle initial, last name)

Leland T. Long

6. REPORT DATE	7a. TOTAL NO. OF PAGES	7b. NO. OF REFS
December, 1974	7	11
8a. CONTRACT OR GRANT NO.	8b. ORIGINATOR'S REPORT NUMBER(S)	
DAHCO4-74-G-0003	None	
9. PROJECT NO.	9b. OTHER REPORT NO(S) (Any other numbers that may be used in this report)	
ARO-D Project Number RDRD-EVS-9110	None	
10. DISTRIBUTION STATEMENT	Approved for public release; distribution unlimited.	

11. SUPPLEMENTARY NOTES	12. SPONSORING MILITARY ACTIVITY
None	U. S. Army Research Office-Durham Box CM, Duke Station Durham, North Carolina 27706

13. ABSTRACT

The main purpose of the gravity analysis was to investigate the effects of crustal features and major geologic units on gravity anomalies and on isostatic compensation. The study of isostatic compensation utilized the theory of Dorman and Lewis in which topographic features were assumed to be related linearly to compensation and its corresponding Bouguer anomaly. An isostatic response function was derived directly from the relation between topography and Bouguer anomalies in the southeastern United States. The results of the analysis indicate over compensation with either undercompensation at 150 km depths or lateral compensation. Another possibility is lateral crustal inhomogeneity. Interpretations with lateral inhomogeneities are preferred because detailed gravity data have revealed numerous anomalously shallow high-density crustal structures in the southeastern United States.

In general in the southeastern United States lateral inhomogeneities in the crust are significant and must be considered in any analysis of the crustal response to applied stresses. This fact was particularly evident in attempting to compute an isostatic response function. The analysis also strongly supports vertical movement of crustal blocks as a major tectonic mechanism in the southeastern United States.

Unclassified
Security Classification

14. KEY WORDS	LINK A		LINK B		LINK C	
	ROLE	WT	ROLE	WT	ROLE	WT
isostasy						
gravity analysis						
isostatic response function						
crustal structure						
southeastern United States						
Georgia						
South Carolina						

EFFECTS OF CRUSTAL FEATURES ON THE GRAVITY FIELD AND ISOSTATIC COMPENSATION

Statement of Problem Studied

The main purpose of the gravity analysis was to investigate the effects of crustal features and major geologic units on the gravity field and isostatic compensation.

Crustal features and major geologic units have been examined by obtaining detailed field data near known structures or by obtaining detailed gravity data in lines across structures. Conventional analysis methods have been used to relate the observed gravity anomalies to the interpreted shape of these structures. Conventional analysis methods have also been applied to gridded regional gravity data in the southeastern United States. The analysis in these investigations was directed toward accumulating evidence implicating recent crustal movement in response to isostatic stresses as a major tectonic mechanism of the southeastern United States.

The study of isostatic compensation utilized the theory presented by Dorman and Lewis (1970) and Lewis and Dorman (1970). In application of the theory, topographic features were assumed to be related linearly to compensating masses. The object was then to derive the functional relation between the topography and the Bouguer anomalies derived from the compensating masses. Similarly density anomalies in the crust should be functionally related to Bouguer anomalies. Attempts were made to include surface densities and short wavelength anomalies in the derivation of the response function. Attempts were also made to interpret the response function in terms of isostatic mechanisms or crustal structure.

Results and Conclusions Reached

The research covered by this grant proceeded in two stages. The first stage was a preliminary analysis based on incomplete data. As a result of the preliminary analysis tentative conclusions were derived and utilized to establish more specific goals for the second stage of research. The second stage in the analysis in most cases supported the conclusions of the first stage of analysis.

Preliminary results

An isostatic response function can be derived for an area as small as the southeastern United States. However, the truncation of structures at the edge of the 512 x 512 km square area requires that the derivation of Dorman and Lewis (1970) be modified to utilize the first derivatives in the computation of the isostatic response function. Also, the numerical precision of the data must be carefully evaluated to

prevent these errors from dominating the results. At wavelengths less than 30 km the Bouguer anomalies and elevation were virtually random functions and uncorrelated in the southeastern United States.

The response function derived for the southeastern United States showed a significant oscillatory character. The response function for a linear impulse in topography according to the derived function would be positive from 50 to 125 km and slightly negative from 125 to 250 km. The positives in the response function effectively balance an anomalously high ratio of Bouguer anomalies to elevation of -0.14 mgals/meter. This anomalously high value at long wavelengths implies that mountains in the southeastern United States are over compensated and should be experiencing isostatic forces compatible with uplift. Contemporary uplift is supported by releveling data (Leade, 1971). The response function for the southeastern United States also showed significant asymmetry which is probably related to the asymmetry of the continental margin.

The existence of oscillations in the response function as opposed to the nearly uniform decay such as observed by Dorman and Lewis (1970) has significant tectonic implications. Primarily, the response function observed contains wavelengths much shorter than typically observed in crustal loading or unloading such as caused by glacial rebound. The significance of this difference is perhaps that two independent mechanisms are involved. The mechanism for glacial rebound is a short-term elastic deformation of the crust, in which the rate of deformation is controlled primarily by the viscosity of the upper mantle. The mechanism for the observed isostatic response function is perhaps a non-linear deformation of the crust. The causitive stresses would be long-term stresses related to the inherent isostatic inequilibrium of crustal structures (Artyukov, 1974). For the longer durations involved the mantle is virtually a perfect fluid.

Inversion of the isostatic response function requires that constraints be applied to obtain a solution because potential data are inherently non-unique. The most common restraint for isostasy is to assume local compensation (Dorman and Lewis, 1972). For the southeastern United States a solution constrained by local compensation would require significant negative compensation below 150 km. A physical mechanism which can explain the existence of negative compensation at depths of 150-200 kilometers can be derived from recent movement of the North American plate. This mechanism requires that the roots of the mountainous regions displace the upper mantle downward. Because the downward displaced material is cooler, the equilibrium depths of phase changes in the crystalline structure shifts upward causing increased density of the material and consequently negative compensation. This mechanism introduces a momentary density instability in the mantle which has been utilized as a driving mechanism for a model of mantle convection (Lowell and Bodvarsson, 1973). However, significant phase transformations are currently unknown in

the depth range of 150 to 250 km. This physical model could have also explained the existence of asymmetry in the response function.

While the physical model for negative compensation at depth is plausible, the model is not supported by gravity data which indicate that many of the geologic structures which undoubtedly contribute to the oscillation of the response function are within the crust. The oscillation wavelength of the isostatic response function indicates that a block width of 50 to 100 km would be appropriate for lateral compensation. At least three physical models can explain the existence of the lateral inhomogeneity of the crust. The first is an isostatic reaction of crustal blocks to erosion or depositional loading such as has occurred in the coastal plain regions of the southeastern United States. The second is an attachment of island arcs or crustal fragments onto the southeast edge of the North American Plate during the closing of a proto-Atlantic ocean. Evidence for island arc configurations exist in the Piedmont Province of Georgia and South Carolina (Denman, 1974). The third is the intrusion of basic rocks during the early development stage of the Atlantic ocean. (See Long and Lowell, 1973).

Revised objectives

The main objective for the second stage of the gravity analysis was, as in the first stage, to investigate the effects of crustal features and major geologic units on the gravity field and isostatic compensation. As a consequence of the preliminary results from the first stage the following six more specific objectives were developed.

1. Compute and invert the response function with a revised and expanded data set.
2. Evaluate the significance in the difference between the isostatic response function and observed deformation of glacial rebound.
3. Evaluate the significance and influence of an intermediate crustal layer.
4. Compare classical models for computing isostatic anomalies to the observed response functions.
5. Model the isostatic response of the crust by use of numerical methods and include in the model the effects of temperature changes, viscosity, erosion, deposition and other parameters which might influence the isostatic response function.
6. Support detailed gravity field work.

Conclusions

The complete data set did not change the preliminary isostatic response function significantly. Consequently most of the preliminary

results remain unchanged. Evaluation of the revised objectives indicate the following conclusions.

1. The isostatic response function obtained with the more complete data set was virtually the same as was obtained previously. Inversion techniques have been investigated by Dorman and Lewis (1972). However, for the southeastern United States data inversions with local compensation do not give realistic solutions for density distributions with depth. The conclusions with respect to lateral compensation are the same as given above.

2. The best explanation for the difference between the crustal response to glacial unloading and the observed isostatic response function perhaps relates to the manner in which the isostatic stresses are distributed and the character of material flow in the upper mantle. Glacial unloading at the earth's surface creates a regional or smooth stress at the crust-mantle contact which remains within the elastic limit of the crust and which excites viscous flow in the mantle. In contrast the stresses for the long-term non-elastic, non-linear deformation of the crust are localized stresses related to local topography or anomalous density structures in the crust. The mantle is a virtual fluid for the longer time periods involved.

3. A detailed gravity data line across north Georgia (Long, 1974) indicates that intermediate layer undulates with the topography. In the Coastal Plain an intermediate layer may not exist as a discrete layer since in places crustal material with perhaps composition similar to that expected for the intermediate layer approaches the surface. Explanations for the correlation of density anomalies at depth with topography could include the influence of vertical uplift of discrete crustal blocks and lateral variations in crustal structure generated by some currently inactive tectonic mechanism.

4. None of the classical models for computing isostatic anomalies are compatible with the strong negative compensation at greater depths or the effects of lateral variations in crustal structure like those observed in the isostatic response function for the southeastern United States. Smoothed free air anomalies were utilized almost entirely for the evaluation of isostatic equilibrium.

5. The utilization of numerical methods to generalize the crustal response was not attempted beyond the evaluation of elevation versus heat flow (Long and Lowell, 1973). Such an analysis would require computations which are significantly more involved than allowed by the available time or resources on this grant. Preliminary analysis indicates that there exists a significant potential for results through application of numerical techniques to problems of the crustal response to stress.

6. The support for detailed gravity studies in the field has made possible a number of gravity anomaly maps of significant

structures in the southeastern United States (see Long, 1974). Additional data were obtained with the objective of obtaining evidence of vertical crustal movement. In general the data support the existence of recent vertical movements.

Some of the detailed gravity studies were in conjunction with seismic monitoring in the epicentral regions of recent earthquakes. Partially as a result of the detailed gravity data a relation has been shown to exist between interpreted structures and the locations of aftershocks. In the case of Bowman and Summerville, South Carolina, high-density and high-velocity geologic units in the crust are spatially associated with earthquakes. These units have higher rigidity than the surrounding crustal material and the rigidity contrast allows amplification of low-level regional stresses. Earthquakes occur where the geometry would predict the greatest amplification of regional stress.

Recommendations

This research has shown that the lateral inhomogeneity of the crust in the southeastern United States prohibits the application of techniques which are based on uniform layers. Therefore, it is recommended that the study of tectonics or crustal deformation be investigated by numerical methods as suggested in objective 5 above.

Continued support for detailed studies are recommended so that more areas may be mapped with the one kilometer spacing required for resolution of structures in the upper crust.

Although direct computation of the isostatic response function does not always yield results directly related to isostasy, similar analyses are recommended for other areas so that the variation in the influence of lateral variations may be evaluated.

Bibliography

Artyushkov, E. V. (1974). Can the earth's crust be in a state of isostasy, J. Geophys. Res., 79, pp. 741-752.

Dorman, H. L. (1974). Implications of seismic activity at the Clark Hill Reservoir. Masters Thesis, Georgia Institute of Technology. 103 pp.

Dorman, L. M., and B. T. R. Lewis (1970). Experimental isostasy, 1, Theory of the determination of the earth's isostatic response to a concentrated load, J. Geophys. Res., 75, pp. 3357-3365.

Dorman, L. M., and B. T. R. Lewis (1972). Experimental isostasy, 3, Inversion of the isostatic Green function and lateral density changes, J. Geophys. Res., 77, pp. 3063-3077.

Lewis, B. T. R., and L. H. Dorman (1970). Experimental isostasy, 2, An isostatic model for the U.S.A. derived from gravity and topographic data, J. Geophys. Res., 75, pp. 3367-3386.

Lowell, R. P., and G. Bodvarsson (1973). A one-dimensional convection model: Application to an internally heated two-phase mantle. Jokull, 23, pp. 19-36.

Meade, B. K. (1971). Report of the sub-commission on recent crustal movement in North America, Paper presented at XV Gen. Assembly of IUGG - International Association of Geodesy, Moscow, USSR. Aug. 2-14, NOS, NOAA.

Publications Supported by Grant

Long, L. T., S. R. Bridges and Leroy Dorman (1972). Simple Bouguer gravity map of Georgia, Georgia Geological Survey, 8.5 x 11 inches 2 pp explanation.

Long, L. T., and R. P. Lowell (1973). Thermal model for some continental margin sedimentary basins and uplift zones, Geology, Vol. 1, No. 2, pp 87-88.

Long, Leland Timothy (1974). Bouguer gravity anomalies of Georgia, Bulletin 87, Georgia Geological Survey, Symposium on the Petroleum Geology of the Georgia Coastal Plain, pp 141-166.

Long, Leland Timothy, Pradeep Talwani, and S. R. Bridges (1975). Simple Bouguer Gravity of South Carolina, South Carolina Division of Geology, Map with explanation (in preparation).

Thesis

Kotne, George H., III (1973). Geophysical Investigation of a diabase dike, Masters Thesis, Georgia Institute of Technology, Atlanta, Georgia.

Presentations at Scientific Meetings

Bridges, S. R., Study of a positive Bouguer gravity anomaly in Tift County, Georgia. Presented at Georgia Academy of Science, April, 1973.

Long, L. T., S. R. Bridges, and Leroy Dorman, Bouguer anomaly map of Georgia, Presented at Southeastern Section meeting of the Geological Society of America, March, 1972.

Talwani, Pradeep, Leland T. Long and Samuel R. Bridges, Regional gravity anomalies and crustal structure in South Carolina. Presented at Annual meeting of the Geological Society of America, November, 1974.

Participating Personnel

The research has provided an opportunity to exchange ideas with researchers in southeastern universities and government agencies. At Georgia Tech the research has contributed to the education of many graduate and undergraduate students. The following students worked full time for at least one term on the research.

S. K. Bridges (undergraduate and graduate assistant) B.S. in Physics with Geophysics minor.

G. M. Rothe (undergraduate and graduate assistant) B.S. in Physics with Geophysics minor, M.S. in Geophysics. Mr. Rothe is continuing work toward a Ph.D. in Geophysics at University of Washington.

J. A. Champion (graduate assistant)

L. Evans (graduate assistant)

The following assisted the research in field measurements or computer programming.

J. H. McKee (graduate assistant) M.S. in Geophysics

H. E. Dernian (graduate assistant) M.S. in Geophysics

J. Butler (graduate assistant)

W. W. Patzeltitsch (graduate assistant)

H. B. Clark (undergraduate assistant)

J. C. Weisenhorn (undergraduate assistant)

A. P. Barke (undergraduate assistant)

H. W. Bruce (computer programmer)

C. Sparrow (computer programmer)

S. R. Wheeler (computer programmer)